

# TECHNISCHE UNIVERSITÄT MÜNCHEN

Fakultät für Medizin

Institut für Experimentelle Hämatologie

## A Novel *In Vivo* Model to Investigate Regulators of GCB Cells and GC Derived Lymphomas

Seren Baygün

Vollständiger Abdruck der von der Fakultät für Medizin der Technischen Universität München zur Erlangung des akademischen Grades eines

**Doctor of Philosophy (Ph.D.)**

genehmigten Dissertation.

Vorsitzender: Prof. Dr. Roland M. Schmid

Betreuer: Prof. Dr. Marc Schmidt-Supprian

**Prüfer der Dissertation:**

1. Prof. Dr. Florian Bassermann

2. Prof. Dr. Radu Roland Rad

Die Dissertation wurde am 22.12.2021 bei der Fakultät für Medizin der Technischen Universität München eingereicht und durch die Fakultät für Medizin am 28.02.2022 angenommen.

## ABSTRACT

Germinal centers (GCs) are transient and dynamic anatomical regions formed by immune and stromal cells upon antigenic challenges, in which diversification and selection of B cells bearing specific immunoglobulins (B cell receptors) take place for the establishment of antibody-mediated immunity. GCs are also the origin of most B cell neoplasms, including follicular lymphoma (FL), diffuse large B cell lymphoma (DLBCL), and Burkitt lymphoma (BL). Somatic mutations and chromosomal lesions orchestrate the transformation of GCB cells by altering their gene expression, epigenome, immune signaling pathways, and metabolism, which facilitate the acquisition of malignant traits such as uncontrolled cell growth, clonal expansion, disruption of terminal differentiation, and evasion of immune surveillance. Microarray-based genomic profiling and high throughput sequencing studies revealed the multi-hit nature of these lymphomas and identified many recurrent genetic alterations associated with lymphomagenesis. However, the challenge remains to characterize the (mal) functions and molecular networks of these alterations in disease pathogenesis. In this regard, developing approaches utilizing functional genomics is a critical objective, as it can allow for the distinction of passenger mutations from drivers, reveal epigenetically or (post-) transcriptionally dysregulated non-mutated genes, and permit investigation of clonal evolution in lymphomas. As an alternative to classical model systems employing lymphoma cell lines or autochthonous mouse models, here I describe a novel *in vivo* model that allows for functional interrogations to identify critical players of GCB cells and GC derived lymphomas. In my model, conditionally immortalized hematopoietic progenitor (Hoxb8-FL) cells generated from compound-mutant mice carrying the *VavP-Bcl2* transgene (a driver for spontaneous germinal center hyperplasia and FL in mice) along with transgenes allowing conditional gene targeting (Cre-LoxP) and gene editing (CRISPR/Cas9), provided primary cell pools to introduce lymphoma-associated genetic alterations for testing *in vivo*. Upon adoptive transfer into recipient mice, *VavP-Bcl2* Hoxb8-FL progenitor cells successfully produced mature myeloid and lymphoid cells *in vivo* as a result of a transient differentiation wave. Characterization of secondary lymphoid organs revealed that this adoptive transfer model generated all mature B cell compartments and, most importantly, provided large numbers of long-lasting GCB cells and plasma cells in the absence of immunization similar to *VavP-Bcl2* transgenic control animals. Moreover, the transfer of *Cy1cre-*

carrying VavP-*Bcl2* Hoxb8-FL cell pools resulted in successful conditional gene activation in GCB cells and plasma cells *in vivo* demonstrating that studying the function of genes specifically in GCB and plasma cells is achievable in this model. To introduce genetic perturbations in Hoxb8-FL cells, I optimized gene-modification strategies involving viral delivery, electroporation, and protein transduction methods. By utilizing these established techniques, I achieved highly efficient CRISPR/Cas9 mediated gene knock-out and gene knock-in in Hoxb8-FL cells, and I generated progenitor cells carrying the most recurrent genetic alterations of GC-lymphomas, including inactivation of histone-lysine N-methyltransferase 2D (KMT2D) and Herpes Virus Entry Mediator (HVEM). Adoptive transfer of retrovirally transduced VavP-*Bcl2* Hoxb8-FL cells confirmed that this model system can enable tracking the impact of the induced genetic changes on the evolution of targeted B cells *in vivo*. Finally, I showed that integrated provirus-mediated expression of a potent proto-oncogene, c-MYC, in BCL2-expressing B cells drove mature B cell lymphomas, indicating that my adoptive transfer model can contribute to the functional understanding of BCL2-collaborating alterations in B cell lymphomas.

Overall, I believe this versatile model constitutes a valuable *in vivo* approach for monitoring clonal competition in GCB cells and GC derived B cell lymphomas as well as for dissecting the role of the microenvironment in disease pathogenesis.

## ZUSAMMENFASSUNG

Keimzentren (GCs) sind kurzlebige und dynamische anatomische Regionen, die während Antigen-getriebenen Immunreaktionen durch Immun- und Stromazellen gebildet werden und in denen die Diversifizierung und Selektion von B-Zellen, die bestimmte Immunglobuline (B Zellrezeptoren) auf ihrer Oberfläche tragen, für die Etablierung der Antikörper-vermittelten Immunität stattfindet. GCs sind auch der Ursprung der meisten B-Zell-Neoplasien, darunter das folliculäre Lymphom (FL), das diffus großzellige B-Zell-Lymphom (DLBCL) und das Burkitt-Lymphom (BL). Somatische Mutationen und chromosomale Läsionen bewirken die maligne Transformation von GCB-Zellen, indem sie ihr Transkription, ihr Epigenom, ihre Immunsignalwege und ihren Stoffwechsel verändern, was den Erwerb bösartiger Eigenschaften wie unkontrolliertes Zellwachstum, klonale Expansion, Störung der terminalen Differenzierung und Umgehung der Immunüberwachung erleichtert. Microarray-basierte genomische Charakterisierungen und Hochdurchsatz-Sequenzierungsstudien haben den Multi-Hit-Charakter dieser Lymphome aufgedeckt und einen wesentlichen Beitrag zur Identifizierung der häufigsten genetischen Veränderungen geleistet, die an der Lymphomgenese beteiligt sind. Die Charakterisierung und Erforschung der Funktionen und molekularen Netzwerke dieser Veränderungen bei der Krankheitsentstehung bleibt jedoch eine signifikante Herausforderung. In dieser Hinsicht ist die Entwicklung von experimentellen Ansätzen der funktionelle Genomik ein wichtiges Ziel, da sie die Unterscheidung zwischen Passagier- und Treibermutationen ermöglichen, epigenetisch oder (post-) transkriptionell dysregulierte nicht-mutierte Gene identifizieren können und die Untersuchung der klonalen Evolution in Lymphomen erlauben. Als Alternative zu klassischen Modellsystemen, die Lymphomzelllinien oder autochthone Mausmodelle verwenden, beschreibe ich hier ein neuartiges In-vivo-Modell, das funktionelle Untersuchungen zur Identifizierung und Beschreibung kritischer Akteure in der Evolution von GCB-Zellen und GC-abgeleiteten Lymphomen ermöglicht. Mein Modell basiert auf konditional immortalisierten hämatopoetischen Vorläuferzellen (Hoxb8-FL), die aus Mäusen die das VavP-Bcl2-Transgen (ein Treiber von spontaner Keimzentrumshyperplasie und FL bei Mäusen) zusammen mit Transgenen für konditionales Gen-Targeting (Cre-LoxP) und Gen-Editierung (CRISPR/Cas9) tragen, generiert wurden. In diese primäre Hoxb8FL Zellpools können dann weitere Lymphom-assoziierte genetische Veränderungen für Tests *in vivo* eingeführt werden.

Nach dem adoptiven Transfer in Empfängermäuse entwickelten sich aus den VavP-Bcl2 Hoxb8-FL Vorläuferzellen reife myeloische und lymphoide Zellen *in vivo* als Ergebnis einer transienten Differenzierungswelle. Die Charakterisierung sekundärer lymphatischer Organe zeigte, dass dieses adoptive Transfermodell alle reifen B-Zell-Kompartimente erzeugen konnte und, von größter Wichtigkeit, eine große Anzahl langlebiger GCB-Zellen und Plasmazellen ohne vorherige Immunisierung. Die B-Zelldifferenzierung meines adoptiven Transfermodells glich in allen untersuchten Aspekten den VavP-Bcl2-transgenen Kontrolltieren. Darüber hinaus führte der Transfer von Cy1cre-tragenden VavP-Bcl2-Hoxb8-FL-Zellpools zu einer erfolgreichen konditionalen Genaktivierung in GCB-Zellen und Plasmazellen *in vivo*. Dies zeigt, dass die Untersuchung der Funktion von Genen speziell in GCB- und Plasmazellen in meinem Modell möglich ist. Um genetische Veränderungen in Hoxb8-FL-Zellen einzubringen optimierte ich die Geneditierungs-Strategien, welche auf viraler Transduktion, Elektroporation und Proteintransduktionsmethoden beruhen. Durch die Etablierung dieser Techniken gelang es mir, hocheffiziente CRISPR/Cas9-vermittelte Gen-Knock-outs und Gen-Knock-ins in Hoxb8-FL-Zellen einzubringen. Somit konnte ich Vorläuferzellen generieren, welche die häufigsten genetischen Veränderungen von GC-Lymphomen tragen, einschließlich der Inaktivierung der Histon-Lysin-N-Methyltransferase 2D (KMT2D) und des Herpes-Virus-Entry-Mediators (HVEM). Der adoptive Transfer von retroviral transduzierten VavP-Bcl2-Hoxb8-FL-Zellen bewies, dass dieses Modellsystem es ermöglicht die Auswirkungen von induzierten genetischen Veränderungen auf die Evolution der B-Zellen *in vivo* zu verfolgen. Abschließend konnte ich zeigen, dass die integrierte Provirus-vermittelte Expression von c-MYC, eines potenten Proto-Onkogens, in BCL2-exprimierenden B-Zellen zu reifen B-Zell-Lymphomen führt. Dies deutet darauf hin, dass mein Adoptivtransfer-Modell zum funktionellen Verständnis von mit BCL2 zusammenwirkenden Veränderungen in B-Zell-Lymphomen beitragen kann.

Insgesamt glaube ich, dass dieses vielseitige Modell einen wertvollen In-vivo-Ansatz für die Erforschung der klonalen Evolution in GCB-Zellen und GC-abgeleiteten B-Zell-Lymphomen darstellt und dazu beitragen kann die Rolle der Mikroumgebung in der Krankheitspathogenese aufzuklären.

|   |    |
|---|----|
| 1. INTRODUCTION .....   | 1  |
| 1.1. B Cell Biology and Germinal Center Derived B-Cell Lymphomas.....               | 1  |
| 1.1.1. B Cell Biology .....   | 1  |
| 1.1.2. Germinal Center Derived Mature B-Cell Lymphomas.....                         | 3  |
| 1.1.3. Pathogenesis of Germinal Center Derived Mature B-Cell Lymphomas .....        | 4  |
| 1.1.4. KMT2D in B cell Lymphomagenesis .....  | 6  |
| 1.1.5. HVEM in B cell Lymphomagenesis .....   | 7  |
| 1.1.6. MYC and BCL6 in B Cell Lymphomagenesis .....                                 | 8  |
| 1.2. Conditionally Immortalized Hematopoietic Progenitor Cells .....                | 10 |
| 1.3. CRISPR/Cas9 Based Gene Editing and <i>PiggyBac</i> Transposon Mutagenesis..... | 11 |
| 1.3.1. CRISPR/Cas9 Based Gene Editing.....  | 11 |
| 1.3.2. <i>PiggyBac</i> Transposon Mutagenesis .....                                 | 14 |
| 1.4. Aim of the Study.....  | 17 |
| 2. MATERIALS AND METHODS .....  | 20 |
| 2.1. Materials .....  | 20 |
| 2.1.1. Equipment .....  | 20 |
| 2.1.2. Consumables .....  | 20 |
| 2.1.3. Antibodies.....  | 21 |
| 2.1.4. Plasmids.....  | 23 |
| 2.1.5. Oligos .....   | 23 |
| 2.2. Methods .....  | 25 |
| 2.2.1. Genetically Modified Mouse Strains.....                                      | 25 |
| 2.2.2. Adoptive Transfer of Hoxb8-FL Cells into Recipient Mice.....                 | 28 |

|   |    |
|---|----|
| 2.2.3. Organ Collection and Processing .....  | 29 |
| 2.2.4. DNA and RNA Preservation in RNAlater .....   | 29 |
| 2.2.5. Flow Cytometry .....   | 29 |
| 2.2.6. Cell Culture .....   | 30 |
| 2.2.7. HEK293T Transfection and Virus Production .....  | 31 |
| 2.2.8. Hoxb8-FL Generation.....   | 32 |
| 2.2.9. Generation of Single Cell-Derived Clones.....  | 32 |
| 2.2.10. Magnetic Activated Cell Sorting (MACS).....   | 32 |
| 2.2.11. Molecular Cloning.....  | 33 |
| 2.2.12. Gene Editing Assessment at DNA Level .....  | 34 |
| 2.2.13. Gene Editing by Electroporation.....  | 35 |
| 2.2.14. His-TAT-NLS-Cre Transduction.....   | 36 |
| 2.2.15. Statistical Analysis and Software .....   | 36 |
| 3. RESULTS .....  | 37 |
| 3.1. Generation of Hoxb8-FL Lines and Establishment of Gene Editing Protocols in Hoxb8-FL Cells .....           | 37 |
| 3.1.1. Generation of Hoxb8-FL Lines .....   | 37 |
| 3.1.2. Establishment of Gene Editing Protocols in Hoxb8-FL Cells .....  | 38 |
| 3.2. Targeting GC Derived Lymphoma-Associated Tumor Suppressor Genes in Hoxb8-FL Cells .....                    | 51 |
| 3.2.1. Targeting Histone-lysine N-methyltransferase 2D (KMT2D).....   | 51 |
| 3.2.2. Targeting Herpes Virus Entry Mediator (HVEM).....  | 53 |
| 3.2.2. Combining KMT2D and HVEM Targeting with Insertional Mutagenesis for Hoxb8-FL Based Genetic Screens ..... | 54 |

|  |     |
|--|-----|
| 3.3. <i>In vivo</i> Use of VavP-Bcl2 Hoxb8-FL Cells for the Investigation of Regulators of GCB cells and GC derived lymphomas .....    | 56  |
| 3.3.1. Establishment of VavP-Bcl2 Hoxb8-FL Adoptive Transfer System to Study Regulators of GCB cells .....                             | 56  |
| 3.3.2. Adoptive Transfer of Retrovirally Transduced VavP-Bcl2 Hoxb8-FL Cells .....   | 63  |
| 3.3.3. <i>In vivo</i> Conditional Gene Targeting in VavP-Bcl2 Hoxb8-FL Derived GCB cells .....   | 65  |
| 3.3.4. Generation of Lymphoma Mouse Models via VavP-Bcl2 Hoxb8-FL Adoptive Transfer System .....                                       | 66  |
| 4. DISCUSSION.....   | 69  |
| 4.1. The VavP- <i>Bcl2</i> Hoxb8-FL System to Investigate Regulators of GCB cells and GC Derived B-Cell Lymphomas <i>In vivo</i> ..... | 69  |
| 4.2. Gene Editing in Hoxb8-FL Cells.....   | 72  |
| 4.3. Introduction of Lymphoma-Predisposing Genetic Alterations in VavP-Bcl2 Hoxb8-FL cells by CRISPR/Cas9 .....                        | 78  |
| 4.4. The VavP-Bcl2 Hoxb8-FL Adoptive Transfer Model: A Novel System for Studying GCB Cells and GC derived B-Cell Lymphomas .....       | 80  |
| 4.5. Contribution of the Established Model System and Potential Pitfalls with Alternative Solutions.....                               | 85  |
| 5. SUPPLEMENTARY MATERIAL.....   | 89  |
| 6. REFERENCES.....   | 96  |
| ACKNOWLEDGMENT.....  | 115 |

## 1. INTRODUCTION

### 1.1. B Cell Biology and Germinal Center Derived B-Cell Lymphomas

#### 1.1.1. B Cell Biology

The immune system protects organisms from infectious agents, harmful substances, and diseases through immunogenic recognition, launching effector mechanisms and ultimately generating durable immune memory. Innate and adaptive immune responses orchestrate the two main phases of the immune response; the former composes the first lines of the defense by generating immediate, fast, and nonspecific responses whereas the latter establishes a protective immune repertoire in part by generating high-affinity antibodies against specific antigens and providing immunological memory for long-lasting immunity.

B cells are one of the key players of the adaptive immune system as they generate a wide range of antibody repertoires, establish immune memory, and regulate T cell responses. Moreover, they also function in innate immune responses during the first line of defense (Viau & Zouali, 2005). Throughout adult life, B cells are produced from hematopoietic stem cells (HSC) in the bone marrow, migrate to peripheral lymphoid organs, and mature into several subtypes that locate at sub anatomical structures. Importantly, all these steps are strictly controlled by distinct checkpoints. Given the central role of B cells in the immune system, abnormalities occurring in B-cell development, selection, activation, or regulation can lead to severe pathological outcomes including immunodeficiency, autoimmunity, and lymphoma development (LeBien & Tedder, 2008).

B cell development is dominated by the production of their B cell receptor (BCR) composed of two immunoglobulin chains, that recognizes a specific antigen. The developmental checkpoints ensure that a functional BCR is produced that does not recognize self-structures. At the end of their developmental journey, B cells differentiate to plasma cells and secrete their BCR, which is then termed antibody. During B cell development in the bone marrow, immunoglobulin (*I*G) genes are rearranged in a process called V(D)J recombination by somatic recombination of V, D

and J gene segments for functional antigen receptor repertoire generation. Positively selected cells with successful rearrangements are exposed to clonal deletion against self-reactivity, then surviving immature B cells migrate to the secondary lymphoid organs and mature into follicular B (FOB) cells or marginal zone B (MZB) cells (Melchers, 2015). Mature FOB cells search for antigen and can circulate between secondary lymphoid organs (Viau & Zouali, 2005) (Dorshkind & Rawlings, 2018) . Upon antigen encounter, activated B cells either become short-lived plasmablasts that secrete moderate affinity antibodies to support an immediate extrafollicular response or enter the germinal center reaction for a more persistent response. In the germinal center (GC), B cells introduce random mutations into their B cell receptor genes followed by selection of B cells with increased affinity for specific antigens to ultimately generate high affinity antibodies (Eisen, 2014). GCs are transient anatomical structures established after antigenic challenges. They are composed of dark and light zones which were defined based on the differential macroscopic appearance resulting from B cells' compactness levels in these two areas (Mesin et al., 2016). Some of the antigen activated B cells engage with activated T helper (Th) cells for a complete activation and start to proliferate enormously by giving rise to the histologically "dark" zone in germinal centers. In parallel, a mutational biological process termed somatic hypermutation (SHM) is induced in these proliferating germinal center B (GCB) cells for the diversification of their BCRs by targeting the variable regions of immunoglobulin genes with an induced mutator, the activation-induced cytidine deaminase (AID) enzyme (Jacob et al., 1991) (Maul & Gearhart, 2010). In the light zone, antigens, which are soluble or trapped & presented by follicular dendritic cells, are captured by the diversified BCRs of individual B cells with different efficiencies based on the affinity of the respective BCR for the antigen. The captured antigens are later presented to T follicular helper cells (Tfh) residing in the germinal centers. GCB cells receiving efficient cytokine and coreceptor signals from cognate Tfh cells (Tfh cells whose TCR can recognize the antigen presented by the GCB cell) are positively selected (clonal selection) to survive, expand and become memory B cells and long-lived antibody secreting plasma cells (PC). Alternatively, GCB cells can re-enter the germinal center reaction for additional rounds of mutation and selection resulting in further improvements of their BCR affinities. On the other hand, cells which do not get adequate signals are eliminated by apoptosis (De Silva & Klein, 2015). Moreover, class-switch recombination (CSR), which was recently shown

to occur mostly prior to germinal center reaction in B cells when the initial activation occurs, enables the change of the effector functions of the immunoglobulins. This occurs via isotype switching of their immunoglobulin constant region gene segments through AID-induced DNA double strand breaks and adapts the immune system according to the needs required for the efficient defense (Roco et al., 2019).

### **1.1.2. Germinal Center Derived Mature B-Cell Lymphomas**

Lymphomas are hematological neoplasms that arise from the malignant transformation of white blood cells of the immune system such as B cells, T cells, or natural killer (NK) cells. Based on the histopathological classification, Hodgkin lymphoma (HL) and Non-Hodgkin lymphoma (NHL) compose the two main subtypes of lymphomas. 15% and 85% of all diagnoses were attributed to HL and NHL respectively (Lowry & Linch, 2013). According to the 2020 global cancer incidence statistics, NHL is estimated as the 11<sup>th</sup> most common cancer and the 11<sup>th</sup> leading cause of cancer-related deaths in the world (Ferlay et al., 2019). Although neoplasms can originate from B or T cells, 85-90% of cases are reported to be B-cell lymphomas in NHLs (Armitage et al., 2017). Depending on the growth rate, NHLs can be classified clinically as aggressive or indolent (slow-growing) in which diffuse large-B cell lymphoma (DLBCL) and follicular lymphoma (FL) exemplify the most common subtypes of these two respective forms by accounting for 40% and 25% of all NHL cases, respectively (Perry et al., 2016). Other subtypes include Burkitt's lymphoma (BL) which is an aggressive form of lymphoma, MALT lymphoma which develops slowly from marginal zone B cells found in the mucosa-associated lymphoid tissues (MALT) such as stomach, and indolent mantle cell lymphoma (MCL) (Lowry & Linch, 2013). The classification of this heterogeneous group of B cell malignancies is based on clinical findings, cell-of-origin identification by immunophenotyping and mutational landscape determination by molecular genetics.

In terms of cell of origin, DLBCL, FL and BL are described as germinal center derived mature B-cell lymphomas as they preserve some features of their natural counterparts, including somatically hypermutated immunoglobulin genes, similar bulk gene expression profiles as well

as histological phenotypes (Bahler et al., 1991) (Tamaru et al., 1995) (Küppers et al., 1997) (Alizadeh et al., 2000) (Hardianti et al., 2004) (Victoria et al., 2012).

### 1.1.3. Pathogenesis of Germinal Center Derived Mature B-Cell Lymphomas

Mature B cell lymphomas usually root from normal B cells which are primed in their potential to become lymphoma precursors by the acquisition of lymphoma predisposing alterations in their genomes. A common example of these predispositions are aberrant chromosomal translocations occurring mostly during phases of development when B cells experience DNA breaks: recombination-activating gene (RAG) endonuclease-mediated V(D)J recombination of the immunoglobulin genes for the generation of functional BCRs or AID-mediated CSR and SHM in the mature B cells (Küppers & Dalla-Favera, 2001). In BL, translocation of *MYC* and *IG* genes is observed in almost all cases. In GCB-type DLBCL *IGH-BCL2* translocation t(14; 18) is detected in 20-40%, and *MYC* translocations in 10% of patients. *IGH-BCL2* t(14; 18) translocation is also observed in FL patients at high frequencies of up to 85%. Moreover, 6-14% of FL patients are reported to contain various *BCL6* translocations (Fangazio et al., 2015). These translocations commonly result in overexpression of the proto-oncogenes mediated by immunoglobulin enhancer elements after juxtaposition. However, there are also cases where non-immunoglobulin regulators are driving the overexpression of oncogenes after the chromosomal rearrangements such as juxtaposition of *BCL6* with *CIITA*, *EIF4AII*, *IKZF1*, *TFRR*, or *PIM-1* in DLBCL patients (Yoshida et al., 1999) (Fangazio et al., 2015). Additionally, as in all other malignancies, activation of oncogenes and inactivation of tumor suppressors through somatic mutations, copy number alterations or dysregulation of epigenetic, post-transcriptional or post-translational control contribute to mature B cell's lymphomagenesis.

FL, clinically a very heterogeneous slow growing disease with an average of 10-year survival after diagnosis, remains incurable and often transforms into a more aggressive form called transformed FL (tFL). tFL usually resembles DLBCL and survival time decreases to 1-2 years (Johnson et al., 2008) (Casulo et al., 2015; Kridel et al., 2012). The *IGH-BCL2* t(14; 18) translocation which arises as a consequence of faulty repair during V(D)J recombination in early B cell development is considered as the molecular hallmark of the disease. Interestingly, this

translocation by itself is not sufficient to drive FL as it is also frequently detected in healthy individuals who are free of lymphoma (Roulland et al., 2003) (Roulland et al., 2006) (Schüler et al., 2009). Instead, ectopic overexpression of the anti-apoptotic BCL2 protein contributes to disease development by providing B cells a survival advantage even in the absence of positively selecting signals received from the microenvironment during clonal selection in the germinal centers. BCL2 overexpressing cells can escape the selecting checkpoints and enter the mutation prone germinal center reaction for several rounds without being eliminated. They may thus accumulate several additional oncogenic mutations which eventually leads to formation of cancer precursor cells and their evolution into lymphoma cells (Sungalee et al., 2014) (Carbone et al., 2019).

Microarray-based genomic profiling and sequencing studies conducted on FL samples revealed the multi-hit nature of this disease and identified many follicular lymphoma associated genetic lesions and distorted pathways which might have role in initiation, progression, relapse, or transformation (Johnson et al., 2008) (Cheung et al., 2009; Schwaenen et al., 2009) (Pasqualucci, Dominguez-Sola, et al., 2011) (Bödör et al., 2013) (Okosun et al., 2014). Especially sequencing studies performed on different temporal and spatial biopsies of patients provided valuable insights regarding the recurrent mutations and evolutionary patterns of clones. For example, recurrent, clonal, and stable mutations identified in histone-modifying genes; histone-lysine N-methyltransferase 2D (KMT2D or MLL2) and CREB binding protein (CREBBP) are considered as the early drivers of the disease and characterize tumor initiating common progenitor cells (CPC) together with the t(14; 18) translocation (Okosun et al., 2014) (Pasqualucci et al., 2014) (Okosun et al., 2016) (Araf et al., 2018). Interestingly, up to 70% of tumors possess mutations in at least in two chromatin-modifying genes and this high co-occurrence frequencies in FL indicates a cooperation between different epigenetic modulators which are yet to be described (Okosun et al., 2014) (Green et al., 2015). **Figure 1a** summarizes the development and terminal differentiation of B cells in germinal centers and highlights the stepwise evolution of germinal center derived B cell lymphomas.

#### 1.1.4. KMT2D in B cell Lymphomagenesis

Inactivating mutations of KMT2D compose the most frequently detected epigenetic change in FL, it is reported to be mutated in 75-89% of FL and 30% of DLBCL patients (Morin et al., 2011) (Green et al., 2015) (Pasqualucci, Dominguez-Sola, et al., 2011). Loss of function mutations in KMT2D skew cells into a decreased transcriptional activity profile as a result of reduced H3K4 methylation at the enhancer elements of several transcription factors and lymphoid tumor suppressors. *TNFAIP3 (A20)*, *SOCS3*, *ARID1A* and *TNFRSF14 (HVEM)* genes, which have a central role in immune signaling pathways as well as fate decision of GCB cells, exemplify some of the heavily affected tumor suppressors in this regard (Ortega-Molina et al., 2015) (Zhang et al., 2015). The role of KMT2D loss in lymphomagenesis has been investigated by two research groups using the *VavP-Bcl2* follicular lymphoma mouse model, where the induced overexpression of BCL2 in all nucleated cells of the hematopoietic system causes germinal center enlargement and development of lymphoid malignancies similar to human FL (Egle et al., 2004). In their study Ortega-Molina and colleagues showed by fetal liver cell transplantation experiments that shRNA mediated knockdown of *Kmt2d* in BCL2 overexpressing progenitor cells promoted germinal center derived lymphomagenesis, which was assessed by shortened disease onset, splenomegaly and highly abundant B220+ PNA+ follicular structures identified in histopathology. Detailed analysis of tumor cells' histone methylation profile revealed reduced methylation marks on the enhancers or promoters of tumor suppressors and several transcription factors functioning in the CD40, TLR, NF- $\kappa$ B and BCR signaling pathways (Ortega-Molina et al., 2015). On the other hand, Zhang et al. showed that KMT2D loss in B cells during the GC reaction did not affect the disease-free time of *VavP-Bcl2* animals but increased the incidence of GC derived lymphomas resembling human tumors. Also, they showed that even though inactivation of KMT2D at different B cell developmental stages (starting from pre-B cell vs during germinal center reaction, in the absence of BCL2 overexpression) induced some common transcriptional changes enhancing proliferation and survival of cells, only early B-cell stage inactivation of KMT2D resulted in elevated GCB cell numbers after the immunization. This finding indicates the critical importance of the developmental time when mutations are acquired. It has been speculated that early loss of KMT2D during B cell development might

provide more time for the establishment of the induced effects in the affected cells and thereby provide a stronger oncogenic impact during lymphomagenesis (Zhang et al., 2015).

#### **1.1.5. HVEM in B cell Lymphomagenesis**

Another gene which is concurrently mutated in FL and DLBCL patients is the immune modulator TNF receptor superfamily 14 (TNFRSF14), also called herpesvirus entry mediator (HVEM). It is reported to be inactivated by somatic mutations or lost through the recurrent chromosomal 1p36 deletions on average in half of FL patients and these aberrations are detected also in DLBCL patients especially in GCB subtype (Cheung et al., 2009) (Launay et al., 2012) (Lohr et al., 2012) (Okosun et al., 2014) (Schmitz et al., 2018). This protein is expressed on the surface of lymphoid cells and can interact with several ligands including B- and T-lymphocyte attenuator (BTLA), TNFSF14 (LIGHT), and CD160. Among these signaling axes especially HVEM-BTLA was highlighted for a potential contribution to disease development as it was reported to be disrupted in the majority of FL patients (Boice et al., 2016). Therefore, it has become a major interest for researchers to understand the normal biological functions of these modulators and their role during lymphomagenesis (Kennedy & Klein, 2019). Mintz et al. showed that activation of Tfh cells, which express high levels of BTLA on their surface, is strongly controlled and restrained by their interaction with HVEM molecules on B cells (Mintz et al., 2019). When HVEM is lost in B cells, inhibition of Tfh cells' activation is diminished through the disruption of BTLA-HVEM engagement. And in turn, Tfh cells provide stronger help in germinal center reaction by expressing more CD40 ligand (CD40L) on their surface that supports proliferation and selection of B cells in germinal centers as a result of enhanced CD40-CD40L synapses. Moreover, they also showed the additive effect of HVEM loss on BCL2 overexpressing B cells' germinal center formation capacity. In another study, contribution of HVEM silencing to germinal center lymphomagenesis was investigated by using a chimera model in which HVEM is repressed in lymphoid cells derived from the *VavP-Bcl2* fetal liver cells expressing *Hvem*-targeting shRNA (Boice et al., 2016). Animals reconstituted with silenced HVEM progenitors have a shortened disease-free period and displayed GC derived lymphomas characterized by immunopathological analysis of lymphoid tissues stained with GC markers. Molecular analysis of tumors showed an oligoclonal nature and an average of 15% increase in GCB cell frequency. Moreover, they also

identified a tumor-supportive microenvironment signature which is constituted by activated stromal cells and increased Tfh cells in HVEM deficient lymphomas.

#### **1.1.6. MYC and BCL6 in B Cell Lymphomagenesis**

Besides the founder lymphoma mutations detected as clonal events in tumors, there are several other proto-oncogenes and tumor suppressors which are targeted during disease progression and transformation. B cell lymphoma 6 protein (BCL6), an essential transcription factor expressed in GC cells, controls germinal center entry and maintenance of B cells in the central reaction. Its downregulation is required for GCB cells exit from the reaction and terminal differentiation into other subsets (Dent et al., 1997) (Ye et al., 1997). This key regulator is reported to be exposed to aberrant alterations as a result of chromosomal translocations or somatic mutations in most of the germinal center derived lymphomas. *BCL6* affecting chromosomal translocations are detected in up to 35% of DLBCL patients and in 6-14% of FL patients in which having this translocation is associated with an increased likelihood to be in the tFL group at later time points of disease (Ye et al., 1993) (Lo Coco et al., 1994) (Akasaka et al., 2003) (Kridel et al., 2015). Similarly, in 75% of DLBCL and in 45% of FL cases several somatic mutations, especially in the 5' regulatory region of the gene, are detected and some of these mutations are shown to result in deregulation of BCL6 expression, although the functional consequences of many mutations still need to be determined (Migliazza et al., 1995) (Pasqualucci et al., 2003) (Pasqualucci, 2019). This gene's contribution to lymphomagenesis was studied by Cattoretti et al. (2005) using a transgenic mouse model (I $\mu$ -BCL6) in which constitutive BCL6 expression is induced in mature B cells (Cattoretti et al., 2005). They showed that overexpression leads to increased GC formation by enhancing the germinal center reaction entry capacity of B cells and it predisposes animals at older ages to develop malignancies resembling human DLBCLs which are composed of GC-experienced mature B cell clones. Another putative proto-oncogene; c-MYC was reported to be affected specifically in transformed FL cases by translocations, copy number amplifications and point mutations (Okosun et al., 2014) (Pasqualucci et al., 2014). In normal B cells, its expression is highly controlled as it is involved in regulation of several cellular dynamics such as proliferation, cell growth, metabolism as well as fate decisions in the GC reaction. To study the role of MYC activation several mouse models were

developed. Induced expression of MYC under the control of immunoglobulin heavy locus enhancer ( $E_{\mu}$ ) or immunoglobulin K enhancer ( $E_{\kappa}$ ) resulted in clonal early B cell tumors (mature and immature) (Adams et al., 1985), whereas Ig $\lambda$ -MYC mice, which were generated by inserting BL specific mutant MYC sequence under Ig $\lambda$  control, were reported to develop clonal BL-like tumors (Kovalchuk et al., 2000). Interestingly, the latter was classified in a following research study by Pasqualucci and co-workers (2008) as a pre-GC derived lymphoma based on missing SHM signatures and BCL6 staining of tumors (Pasqualucci et al., 2008). When ectopic MYC expression is induced specifically in the germinal center B cells through a conditional system, no tumors are detected even a year after immunization of animals (Sander et al., 2012). As an example for the collaboration of BCL2 and MYC in lymphomagenesis, Oricchio et al. (2014) reported that an aggressive, tFL-like malignancy was observed in chimera animals when *c-MYC* is constitutively expressed via retroviral delivery in VavP-*Bcl2* mouse fetal liver progenitors (Oricchio et al., 2014). Compared to BCL2 alone, combined BCL2 and MYC induction was found to cause a very short disease latency accompanied by lymphoid tumors with a histological appearance of disturbed follicles although these tumors lacked the expression of a germinal center marker; peanut agglutinin (PNA). Also, in the study of Cai et al. (2020), a conditional MYC and BCL2 co-expression mouse model was generated by inserting *CAG-Stop<sup>FL</sup>-Myc-P2A-Bcl2* cassette into *Rosa26* locus of mouse (Cai et al., 2020). They described that induction of oncogenic expression starting from the pro-B cell stage or in germinal center B cells drove potent B cell lymphomagenesis assessed by enlarged lymphoid organs and increased B cell fractions (B220<sup>+</sup> and B220<sup>+</sup> FAS<sup>+</sup> B cells).

*BCL2*, *BCL6* and *MYC* potent oncogenic hits of B cell lymphomas can occur in combinations in de novo mature tumors or evolve in transformed FL cases that are attributed to the high-grade B-cell lymphoma category. They can be defined as “double-hit” or “triple-hit” lymphomas as well and usually display poor outcome with an aggressive disease course (Kapur & Levin, 2014) (Bischin et al., 2017) (Huang et al., 2018).

## 1.2. Conditionally Immortalized Hematopoietic Progenitor Cells

HSCs which have potential to give rise to all blood cell types including erythrocytes, megakaryocytes, and leukocytes, generate subsequent progenitor cell entities by becoming more restricted to certain lineages and losing their self-renewal capacity and potency (Yamamoto et al., 2018). Multipotent progenitors (MPP) compose one of the earliest progeny of HSCs and are reported to have a short-term reconstitution potential after transplantations due to their diminished self-renewal ability. During hematopoiesis, they can follow the route to differentiate into lymphoid-primed multipotent progenitor (LMPP) cells which lack erythrocyte and megakaryocyte potential but retain other blood lineage potentials including granulocytes, monocytes, and lymphocytes (Morrison & Weissman, 1994) (Yang et al., 2005) (Adolfsson et al., 2005). Further in development, with the myeloid potential exclusion from LMPP cells, common lymphoid progenitors (CLP) are formed, and they are predetermined to give rise to dendritic cells and mature lymphocytes including B, T and NK cells (Cheng et al., 2020). Execution of these complex and tightly regulated differentiation steps are dependent on signals coming from the microenvironment such as soluble stimulatory molecules released from niche cells or direct contacts with niche cells through cell adhesion and other molecules. Throughout the differentiation process, changes induced in signal transduction pathways, transcription and epigenetic profile of cells drive the development and ensure the maintenance of the committed mature cells (Barneda-Zahonero et al., 2012).

The generation of conditionally immortalized progenitor cell pools from mouse primary hematopoietic progenitors has facilitated studying molecular regulators of immune cells. Such cells can be grown for prolonged periods of time and to large numbers in culture, which permits extensive genetic manipulation and selection of cells with the desired induced genetic changes. Bone marrow cells transduced with a fusion gene construct encoding the hormone binding domain of the estrogen receptor and *Hoxb8*, can be cultured nearly limitlessly *in vitro* in the presence of estradiol and specific cytokines. *Hoxb8* expression drives a robust self-renewal program, but the cells retain the potential to differentiate into mature myeloid and lymphoid cells in the presence of appropriate differentiation signals in the absence of *Hoxb8* activity when estradiol is removed (Wang et al., 2006) (Redecke et al., 2013). *Hoxb8* cells produced with

different growth factors, or ligands including stem cell factor (SCF), granulocyte-macrophage colony-stimulating factor (GM-CSF) or Fms-like tyrosine kinase 3 ligand (Flt3-Ligand) were shown to be predisposed to certain mature lineages. For example, Hoxb8 cells generated and cultured in the presence of Flt3-Ligand, so called Hoxb8-FL, can give rise to both myeloid (macrophages, dendritic cells, granulocytes) and lymphoid (B and T) mature cell populations *in vitro* and *in vivo*. These cells were identified to represent a progenitor state close to the primary LMPP cells but with a lower T cell differentiation potential (Redecke et al., 2013) (Kucinski et al., 2020). Upon removal of estradiol and adoptive transfer into lethally irradiated mice, Hoxb8-FL cells were shown to differentiate into myeloid cells, B cells, and T cells in a time-dependent manner (Redecke et al., 2013). In these adoptive Hoxb8-FL transfer experiments, irradiated mice are co-transferred with supporting unfractionated BM cells as LMPP-resembling Hoxb8-FL cells are diminished in self-renewal capacity compared to HSCs and lack the potential to differentiate into megakaryocytes and erythroid cells.

To date, several studies have used the Hoxb8-FL model system *in vitro* and *in vivo* to answer questions involving progenitor and myeloid cell biology (Bunin et al., 2015) (Martins et al., 2016) (Grajkowska et al., 2017) (Hamey et al., 2017) (Leithner et al., 2018) (Hammerschmidt et al., 2018) (Kirkling et al., 2018) (Renkawitz et al., 2019) (Kuriakose et al., 2019) (von Gamm et al., 2019) (Schuler et al., 2019) (Piperno et al., 2020) (Kopf et al., 2020) (Govindarajah et al., 2020) (Cabal-Hierro et al., 2020) (Basilico et al., 2020) (Kucinski et al., 2020). They also highlighted the nearly interchangeable use of the Hoxb8-FL system instead of primary counterparts by showing extensive evidence for their morphological, functional, and molecular similarities. The use of the Hoxb8-FL system to explore the biology of the lymphoid lineage remains largely unexplored.

### **1.3. CRISPR/Cas9 Based Gene Editing and *PiggyBac* Transposon Mutagenesis**

#### **1.3.1. CRISPR/Cas9 Based Gene Editing**

One of the fundamental methods to study gene function relies on silencing or completely disrupting their endogenous expression in cells or organisms. For decades, several genome editing tools were established for this purpose. For example, it was first shown in *C.elegans* that

delivering double-stranded RNA can efficiently silence target genes by RNA Interference (RNAi) and generate loss-of-function phenotypes (Fire et al., 1991) (Fire et al., 1998). RNAi has been widely used to silence gene expression in mammalian cells as well (Elbashir et al., 2001). Delivering target specific double-stranded RNA molecules using short-interfering RNAs (siRNAs) or short-hairpin RNAs (shRNAs) enables to degrade messenger RNA (mRNA) of the target and prevents translation into proteins (Carthew & Sontheimer, 2009). However, incomplete shut down of mRNAs and off-target effects have remained confounding aspects of RNAi (Khan et al., 2009). Later, with the targeted use of DNA nucleases such as zinc-finger nucleases (ZFNs) and transcription activator-like effector nucleases (TALENs), complete disruption of genes and therefore their functions became possible. ZFNs and TALENs, which can be designed to target gene loci of interest, introduce double strand breaks (DSB) on the target-directed region and lead to accumulation of insertions or deletions (indels) during the repair of the break that result in frame-shift mutations bringing about loss of gene function (Urnov et al., 2010) (Joung & Sander, 2013). More recently, the discovery of the clustered regularly interspaced short palindromic repeats (CRISPR)/CRISPR-associated nuclease 9 (Cas9) system has revolutionized genome editing. As other nucleases, Cas9 also creates DSB on the target site and triggers the cells own DNA damage repair mechanisms to act on the break; error-prone non-homologous end joining (NHEJ) or the accurate homology-directed repair (HDR) pathways. Among these two general pathways, mainly NHEJ is activated, and this generally results in the disruption of the targeted gene by the induction of indels and consequent emergence of frame-shift mutations or premature mature stop codons in its reading frames (Ran et al., 2013). To be directed to the locus of interest Cas9 endonuclease requires a target-specific 20 nucleotide long guide RNA (gRNA) and the presence of a protospacer-adjacent motif (PAM) in the target DNA which is usually an NGG motif adjacent to the target-specific recognition sequence (Jinek et al., 2012). On the other hand, ZFNs and TALENs rely on target sequence-specific design of complex protein combinations in which DNA-binding proteins united with endonuclease domains for recognition and cutting of the target. Cas9s simple and flexible use over the ZFNs and TALENs has made the CRISPR/Cas9 system a broadly used powerful genome editing tool in mammalian cells (Doudna & Charpentier, 2014). Furthermore, fusing enzymatically inactive Cas9 nuclease protein (dead Cas9) with transcription repressors or activators has enabled repression (CRISPRi) or activation

(CRISPRa) of genes by CRISPR (Qi et al., 2013) (Perez-Pinera et al., 2013). CRISPR also allows introducing specific alterations into genes and integrating new sequences through genomic knock-ins mediated by the HDR pathway when an exogenous DNA repair template with homology arms designed around the targeted locus is also supplied. CRISPR-based technologies revolutionized the field of genetically modified mice as well since it became easier to generate mouse lines carrying specific mutations, reporter transgenes and conditional alleles (Yang et al., 2013). The use of different viral delivery systems such as lentiviruses, retroviruses, adeno-associated-viruses (AAV) for expression of Cas9 and gRNA has allowed to specifically target and modify a wide array of cells and organisms (Fajrial et al., 2020; Vilela et al., 2020). Recently, non-viral delivery systems including nucleofection and electroporation was introduced to efficiently deliver purified Cas9 protein, synthetically synthesized gRNAs, and repair templates for generation of CRISPR-based knockouts, large genomic rearrangements or knock-ins in many organisms and cell types including human primary cells (Liang et al., 2015) (Hendel et al., 2015) (Gundry et al., 2016) (Jacobi et al., 2017) (Lattanzi et al., 2019). The major advantage of the electroporation method is not only the circumvention of cloning and virus production steps but also the removal of unwanted side effects of viral transduction (Li et al., 2018). Moreover, a combination of delivery methods has facilitated generation of knock-ins *in vitro* and *ex-vivo*. For example, delivery of the DNA cargo with AAV and Cas9-gRNA complex with electroporation was shown to efficiently generate knock-ins in mouse and human hematopoietic stem and progenitor cells (HSPCs) (N. T. Tran et al., 2019) (Dever et al., 2016) (Bak & Porteus, 2017) (Gaj et al., 2017).

The simplicity of the gRNA design and delivery methods of CRISPR has enabled the generation of gRNA libraries for high-throughput loss-of-function screens in mammalian cells (Koike-Yusa et al., 2014) (Wang et al., 2014) (Wang et al., 2017) (Shalem et al., 2014) (Doench et al., 2016). In such screens, genome-wide or pooled targeted gRNA libraries were used to systematically identify genes responsible for certain phenotypes such as (co-)essential genes or resistance related genes in cancer cells. gRNAs might vary in their knockout efficiency depending on several factors including nucleotide composition or chromatin accessibility of the target region (Graf et al., 2019). To overcome these limitations and to have more statistical power, CRISPR libraries

usually contain several gRNAs (3-10) per target gene (Sanson et al., 2018). A typical genome-wide library for human or mouse organisms would include >100k gRNAs. Therefore, to achieve sufficient representation of each sgRNA (coverage >100x/gRNA) in the target population a high number of cells is required. This is why to date mostly immortalized cell lines were widely used for *in vitro* CRISPR screens. Recent improvements in gRNA design could reduce the requirement of number of gRNAs used per gene and therefore allow to downscale the size of targeted libraries. In spite of this progress, it is still more challenging to perform *in vivo* CRISPR screens compared *in vitro* screens due to cell number limitations, lower mutational efficiencies, immunogenicity of Cas9 protein expression, varying engraftment efficiencies in the transplant models and pre-existing intracellular heterogeneity of the targeted primary tissue in the non-transplant direct *in vivo* editing models (Chow & Chen, 2018) (Mehta & Merkel, 2020) (Noorani et al., 2020). However, *in vivo* screens as opposed to *in vitro* screens can identify relevant hits more accurately as the intact endogenous tissue microenvironment is preserved during the screen and this provides the possibility to identify context dependent phenotypes (Chow & Chen, 2018). CRISPR *in vivo* screens were applied in several studies where tumor suppressors, metastasis related genes, potential immunotherapeutic targets, immune escape, immune resistance and immune response related genes were revealed (Chen et al., 2015) (Chow et al., 2017) (Manguso et al., 2017) (Shifrut et al., 2018) (Dong et al., 2019) (Han et al., 2019) (LaFleur et al., 2019) (Bajaj et al., 2020) (Li et al., 2020).

### 1.3.2. *PiggyBac* Transposon Mutagenesis

Unbiased *in vivo* genetic screening approaches, such as retroviral and transposon-based insertional mutagenesis screens have provided a fruitful opportunity to exploit forward genetics for the identification of important regulators and their functional roles in disease. For example, given that retroviral Murine leukemia virus (MuLV) can target lymphoid tissue *in vivo* with high efficiency, Webster et al. (2018) developed a retroviral-mutagenesis screen in BCL2 overexpressing mouse models: VavP-*Bcl2* where the *Bcl2* oncogene is expressed in all blood cells and Emu-*Bcl2*-22 where the *Bcl2* oncogene is expressed in only B cells. They observed an increased incidence in B cell lymphomas when additional somatic mutations were induced in the presence of BCL2 overexpression. Moreover, by sequencing of the viral integration sites in

tumors they could identify novel modulators of NHL and describe clonal and subclonal events during disease development (Webster et al., 2018). Even though screens performed in mice using retroviral insertional mutagenesis yielded several key modulators, the lack of viral tropism for several tissues has prevented its wide-spread use (van Lohuizen et al., 1991) (Kool et al., 2010) (Kool & Berns, 2009). Alternatively, transposon-based *in vivo* screens enabled studying the effect of induced somatic mutations in all tissues. Transposons, which are natural genetic units with the ability to move through the genome, are normally found silenced in higher organisms. However, with the engineering of *Sleeping Beauty (SB)* and *PiggyBac (PB)* transposon systems, insertional mutagenesis could be achieved in mammalian cells as well as in mice (Ivics et al., 1997) (Horie et al., 2001) (Ding et al., 2005) (Collier et al., 2005) (Rad et al., 2010). Engineered transposon systems include two main components: a transposase enzyme and a transposon DNA fragment. Transposase activation leads to initiation of transposon hopping in the genome via molecular cut and paste mechanisms. Depending on the transposon integration direction and location relative to a nearby gene, either activation or inactivation of gene expression can follow.

In the *PiggyBac (PB)* mouse system, a constitutive or conditional PB transposase is knocked-in to the *R26* locus in one transgenic line. Complementing *ATP* (activating transposon) transgenic mouse strains carry in their genomes multicopy transposon DNA arrays, which include a promoter/enhancer element, splice donor, splice acceptors (SAs) and a bidirectional SV40 polyadenylation signal serving for activation or inactivation of the genes after mobilization (Friedrich et al., 2017). Interbreeding of a constitutively expressed *PB* mouse line with different *ATP* strains was shown to drive malignancies with different outcomes. For example, MSCV promoter bearing *ATP2* lines mostly generated hematopoietic cancers with a rare B cell lymphoma incidence, whereas CAG promoter containing *ATP1* lines mostly generated solid cancers and PGK promoter driven *ATP3* lines generated both blood and solid cancers (Rad et al., 2010) (Weber et al., 2019). This screening platform was employed for the successful discovery of several novel cancer regulators and pathways and for the cataloguing of evolutionary relationships in disease events in subsequent publications (Noorani et al., 2020) (Rad et al., 2015) (Wartewig et al., 2017) (Chapeau et al., 2017). In a recent study, Weber et al. (2019) identified

recessive tumor suppressors of B-cell lymphomas with *in vivo* mutagenesis screens by combining the *PB* line with *ITP* transposon lines, where the transposon DNA cassette is designed as to generate only inactivating mutations through promoter interference in a loss of heterozygosity triggering genetic background (Weber et al., 2019).

#### 1.4. Aim of the Study

The malignant transformation of GC-derived B cells constitutes the most commonly observed neoplasm among all human lymphomas. Genetically, epigenetically, and phenotypically heterogeneous GC derived lymphomas remain a major cause of morbidity and mortality despite the development of novel therapies. Over the past decades, several high-throughput sequencing studies revealed the enormously complex genetic landscape of these lymphomas. Now, in order to identify the pathogenic role of the recurrent mutations, to understand the dynamic clonal evolution, and to determine novel regulators of lymphomagenesis, functional studies are required. The generation and analysis of genetically engineered mouse models and lymphoma cell lines led to the discovery of the disease-causing mechanisms of critical genetic aberrations. Although these model systems were instrumental for conducting functional studies, they are not without shortcomings, such as missing the genetic complexity seen in human lymphomas in *in vivo* models or lacking the contributions of lymphoma microenvironments in *in vitro* cell culture setups. Furthermore, the autochthonous mouse models are low throughput, and the introduction of genetic alterations is a slow and laborious process. To overcome some of the limitations of the current model systems, I aimed to establish a novel adoptive cell transfer-based mouse model to investigate critical regulators of the biology and pathology of GCB cells and GC derived lymphomas. To achieve this aim, I set out to address the following two major objectives (**Figure 1b-c**):

1) To generate and test conditionally immortalized hematopoietic progenitor cells from VavP-*Bcl2* transgenic mice and diverse compound genetically engineered derivatives in order to allow conditional gene targeting via the Cre-LoxP system and gene editing through CRISPR/Cas9

approaches *in vivo*. To establish genome editing protocols in these Hoxb8-FL cells in order to introduce defined lymphoma-associated genetic alterations.

2) To establish and characterize a VavP-*Bcl2* Hoxb8-FL cell based adoptive-transfer model to dissect the molecular processes regulating the differentiation, transformation, and clonal evolution of GCB cells.

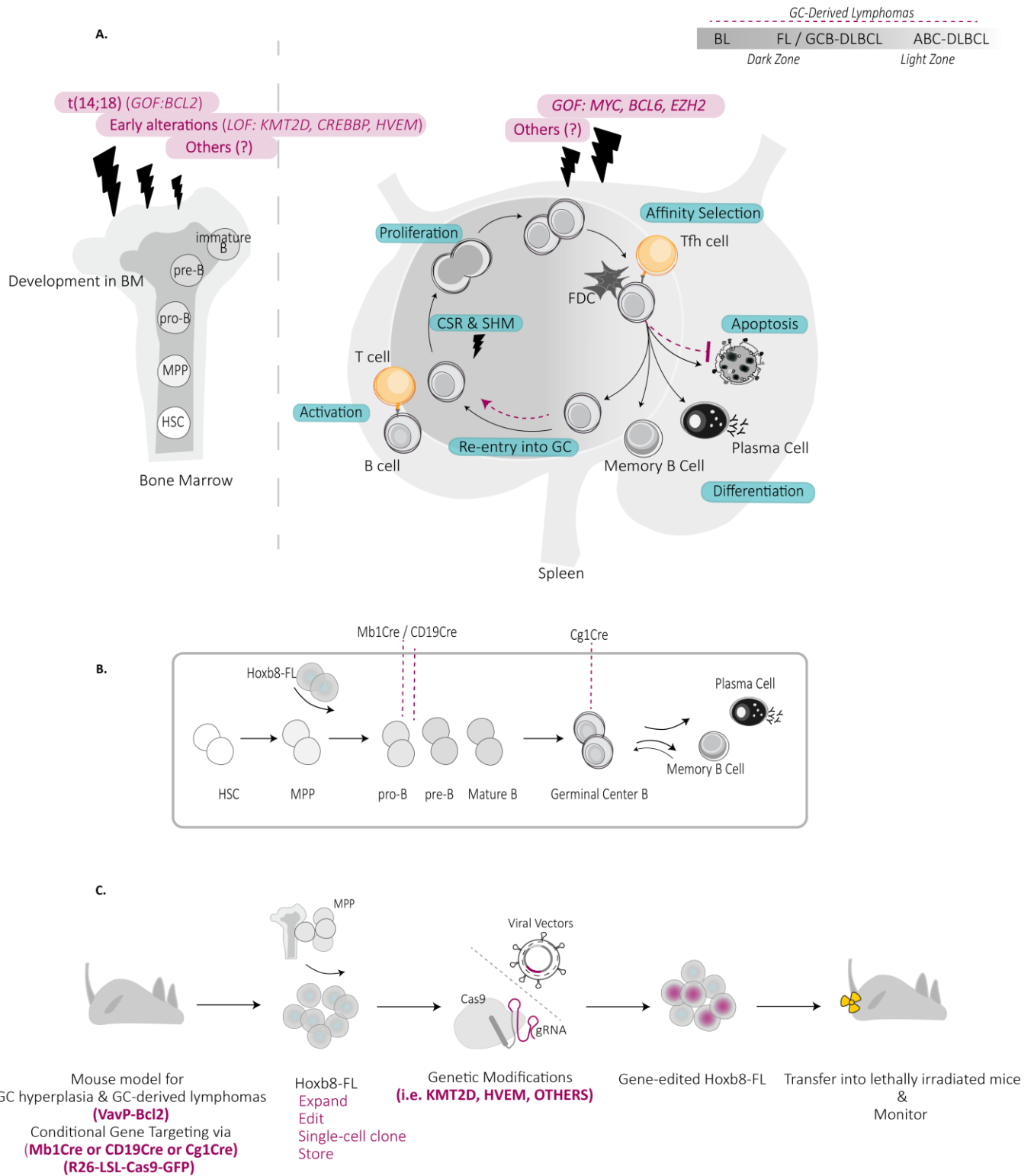


**Figure 1: Scheme of terminal B cell differentiation, evolutionary steps of lymphomagenesis, and proposed VavP-Bcl2 Hoxb8-FL adoptive transfer model to investigate regulators of GCB cells and GC derived B-cell lymphomas**

**Figure 1: Scheme of terminal B cell differentiation, evolutionary steps of lymphomagenesis, and proposed VavP-Bcl2 Hoxb8-FL adoptive transfer model to investigate regulators of GCB cells and GC derived B-cell lymphomas**

**A)** In the bone marrow, progenitor B cells developing from hematopoietic stem cells undergo the V(D)J recombination process to assemble immunoglobulin heavy chain gene segments in order to generate functional BCRs. In rare cases, as a result of errors during recombination, developing B cells acquire chromosomal translocations that lead to constitutive expression of proto-oncogenes. In FL, the t(14;18) translocation places expression of the BCL2 protein under the control of immunoglobulin heavy chain regulatory regions, which leads to overexpression of the anti-apoptotic protein, starting by the early stages of B cell differentiation. Besides the ectopic expression of BCL2, other alterations including mutations in epigenetic modifiers (KMT2D, CREBBP) and immune modulators (HVEM) occur at the early developmental stages of B cells and these cells could be considered as lymphoma founder clones. In secondary lymphoid organs, antigen-activated naïve B cells enter the germinal center reaction where they undergo CSR and SHM to generate high-affinity immunoglobulins with effector functions. During affinity maturation, GCB cells acquiring sufficient help from Tfh cells are selected to differentiate into memory B cells or antibody-secreting plasma cells (for graphical simplicity, plasma cells are shown to leave the germinal center in the light zone, although recent evidence points to a dark zone exit (Meyer-Hermann et al., 2012)). On the other hand, low-affinity GCB-cells are eliminated by apoptosis from the reaction, as they lack the survival signals provided by Tfh cells and FDCs. Forced expression of BCL2 in t(14;18)-carrying cells prevents or reduces removal of unfit clones from the system leading to vastly increased numbers of cells undergoing iterative rounds of cyclic re-entry and thereby accumulation of further genetic lesions and propagation of clonal evolution towards FL development. Similarly to FL, BL and DLBCL also manifest features of GC lymphomas including the increased genomic instability, enhanced proliferation, clonal expansion, and accumulated mutations affecting oncogenes and tumor suppressors. (GOF: Gain of function, LOF: Loss of function, GC: Germinal Center, FDC: Follicular dendritic cell, Tfh: T follicular helper cell, HSC: Hematopoietic stem cell, MPP: Multipotent progenitors, FL: Follicular lymphoma, BL: Burkitt lymphoma, ABC-DLBCL: Activated B Cell-like diffuse large B cell lymphoma, GCB-DLBCL: Germinal center B cell-like diffuse large B cell lymphoma, CSR: Class switch recombination, SHM: Somatic hypermutation) **B)** Cre-drivers employed to introduce lymphoma-associated alterations at distinct stages of B cell development. Mb1cre and CD19cre for expression of Cre in early B cells, while Cγ1cre mediates Cre expression in GCB cells. **C)** Bone marrow from diverse compound genetically engineered derivatives of VavP-Bcl2 Hoxb8-FL mice is used for the generation of different Hoxb8-FL cell pools. VavP-Bcl2 Hoxb8-FL cells can be genetically manipulated and subcloned in the presence of estradiol and FLT3L. Upon adoptive transfer into irradiated recipients, they differentiate in a developmental wave into myeloid and lymphoid cells, including functional GCB and plasma cells. Compound genetic mouse strains including Cre-drivers or CRISPR gene-editing components allow for *in vivo* conditional mutagenesis to monitor clonal evolution in response to induced pathogenic alterations.

## 2. MATERIALS AND METHODS

### 2.1. Materials

#### 2.1.1. Equipment

| Product           | Description       | Distributor      |
|-------------------|-------------------|------------------|
| CytoFLEX LX       | Flow Cytometer    | Beckman Coulter  |
| CytoFLEX S        | Flow Cytometer    | Beckman Coulter  |
| FACS Aria IIITM   | Cell Sorter       | Becton Dickinson |
| FACS FusionTM     | Cell Sorter       | Becton Dickinson |
| Nanodrop One/OneC | Spectrophotometer | Thermo Fisher    |
| Neon              | Electroporator    | Thermo Fisher    |
| Gulmay RS 225A    | X-ray irradiator  | Gulmay Medical   |

#### 2.1.2. Consumables

| Product                                | Cat. No     | Distributor     |
|--|-------------|-----------------|
| Gibco-ACK lysis buffer                 | A1049201    | Thermo Fisher   |
| Neon 10 ul kit                         | MPK1096     | Thermo Fisher   |
| Anti-APC MicroBeads                    | 130-090-855 | Miltenyi Biotec |
| eBioscience™ Foxp3 Staining Buffer Set | 00-5523-00  | eBioscience™    |
| QIAquick PCR Purification Kit          | 28104       | Qiagen          |
| Nuclease-Free Water                    | AM9937      | Ambion          |
| QIAquick Gel Extraction Kit            | 28704       | Qiagen          |
| QIAamp DNA Mini Kit                    | 51304       | Qiagen          |
| NucleoSpin Plasmid miniprep            | 740499.50   | Macherey-nagel  |
| DNA LoBind Tubes (1.5 ml)              | 30108051    | Eppendorf       |
| Protein LoBind Tubes (1.5 ml)          | 30108116    | Eppendorf       |
| Roti®-Histofix 4 %                     | P087.4      | Carl-Roth       |
| RNAse AWAY                             | 10328-011   | Thermo Fisher   |
| RnAlater                               | R0901       | Sigma-Aldrich   |
| Fast Alkaline Phosphatase (FastAP)     | EF0654      | Thermo Fisher   |
| FastDigest Esp3I (Bsmbl)               | FD0454      | Thermo Fisher   |
| FastDigest Bpil (BbsI)                 | FD1014      | Thermo Fisher   |
| AarI                                   | ER1581      | Thermo Fisher   |
| XhoI                                   | R0146S      | NEB             |

|   |            |               |
|---|------------|---------------|
| T4 DNA Ligase Reaction Buffer           | B0202S     | NEB           |
| T4 Polynucleotide Kinase (PNK)          | M0201S     | NEB           |
| Quick Ligation™ Kit                     | M2200S     | NEB           |
| Gibson Assembly® Master Mix             | E2611L     | NEB           |
| LR Clonase II Enzyme Mix                | 11791020   | Thermo Fisher |
| Q5® Hot Start High-Fidelity MM          | M0494S     | Thermo Fisher |
| Phusion High-Fidelity DNA Polymerase    | F-530L     | NEB           |
| GoTaq hotstart green mastermix          | m512b      | Promega       |
| Heparin treated Microvette              | 16443      | Sarstedt      |
| Lipofectamine 2000                      | 11668019   | Thermo Fisher |
| Lipofectamine                           | 18324020   | Thermo Fisher |
| Polybrene                               | TR-1003-G  | Sigma-Aldrich |
| 0.8 um Syringe Filter Cellulose Acetate | 16592      | Sartorius     |
| 1-kb Plus DNA ladder                    | 10787026   | Thermo Fisher |
| CleanCap® Cre mRNA- (5moU)              | L-7211     | TriLink       |
| CleanCap® GFP mRNA- (5moU)              | L-7201     | TriLink       |
| Opti-MEM, reduced serum medium          | 31985062   | Thermo Fisher |
| UltraComp eBeads™ Compensation Beads    | 01-2222-42 | Thermo Fisher |
| Ampicillin                              | A5354      | Sigma-Aldrich |
| QuickExtract DNA extraction             | QE09050    | Epicentre     |
| DMSO                                    | A994.1     | Carl Roth     |

### 2.1.3. Antibodies

| Name   | Coupling | Clone    |
|--|----------|----------|
| LIVE/DEAD™ Fixable Near-IR Dead Cell Stain Kit | NA       | NA       |
| Zombie UV™ Fixable Viability Kit               | NA       | NA       |
| 7-AAD  | NA       | NA       |
| Anti-CD16/CD32                                 | NA       | NA       |
| Anti-CD3ε                                      | PE/Cy7   | 145-2C11 |
| Anti-CD8a                                      | FITC     | 53-6.7   |
| Anti-IgG1                                      | APC      | X56      |
| Anti-CD95                                      | PE       | Jo2      |
| Anti-CD95                                      | BV650    | Jo2      |
| Anti-CD38                                      | PE/Cy7   | 90       |
| Anti-CD138                                     | PE       | 281-2    |
| Anti-CD138                                     | APC      | 281-2    |
| Anti-B220                                      | FITC     | RA3-6B2  |

|                   |             |              |
|-------------------|-------------|--------------|
| Anti-B220         | eF450       | RA3-6B2      |
| Anti-B220         | PE/Cy7      | RA3-6B2      |
| Anti-B220         | PerCP-Cy5.5 | RA3-6B2      |
| Anti-B220         | BV650       | RA3-6B2      |
| Anti-NK1.1        | BV650       | PK136        |
| Anti-Streptavidin | PerCP-Cy5.5 | NA           |
| Anti-Streptavidin | BV650       | NA           |
| Anti-TCR $\beta$  | eFluor450   | H57-597      |
| Anti-TCR $\beta$  | FITC        | H57-597      |
| Anti-TCR $\beta$  | PerCP/Cy5.5 | H57-597      |
| Anti-hBCL2        | PE          | 10C4         |
| Anti-hBCL2        | FITC        | 10C4         |
| Anti-CD19         | eFluor450   | eBio1D3      |
| Anti-CD19         | PE/Cy7      | eBio1D3      |
| Anti-CD19         | PerCP/Cy5.5 | eBio1D3      |
| Anti-IgM          | PE/Cy7      | II/41        |
| Anti-IgD          | FITC        | 11-26c/11-26 |
| Anti-IgD          | eF450       | 11-26c/11-26 |
| Anti-IgD          | APC         | 11-26c/11-26 |
| Anti-Bcl6         | PE/Cy7      | K112-91      |
| Anti-CD23         | FITC        | B3B4         |
| Anti-CD23         | PE          | B3B4         |
| Anti-CD21         | FITC        | 7G6          |
| Anti-AA4.1        | APC         | AA4.1        |
| Anti-Taci         | APC         | ebio8F10-3   |
| Anti-CD44         | PE/Cy7      | IM7          |
| Anti-CD44         | APC         | IM7          |
| Anti-CD44         | PerCP/Cy5.5 | IM7          |
| Anti-CD44         | eF450       | IM7          |
| Anti-CD44         | PE          | IM7          |
| Anti-CD45.1       | PerCP/Cy5.5 | A20          |
| Anti-CD45.1       | PE/Cy7      | A20          |
| Anti-CD45.2       | eFluor450   | 104          |
| Anti-CD45.2       | APC         | 104          |
| Anti-CD45.2       | PE/Cy7      | 104          |
| Anti-CD1d         | PE          | 1B1          |
| Anti-CD1d         | PerCP/Cy5.5 | 1B1          |
| Anti-CD8a         | eFluor450   | 53-6.7       |
| Anti-CD11b        | eFluor450   | M1/70        |
| Anti-CD11b        | APC         | M1/70        |

|             |           |       |
|-------------|-----------|-------|
| Anti-Thy1.1 | APC       | HIS51 |
| Anti-Thy1.1 | eFluor450 | HIS51 |
| Anti-GL7    | eFluor450 | GL7   |

#### 2.1.4. Plasmids

| Backbone                                       | ID             | Gift from     |
|--|----------------|---------------|
| MSCV_hU6_ccdB_gRNA_PGK_Puro_T2A_Thy1.1         | -              | Martin Turner |
| MSCV_hU6_ccdB_gRNA_hU6_gRNA_PGK_Puro_T2A_eBFP2 | pSB2           | -             |
| MSCV_hU6_ccdB_PGK_Puro_T2A_eBFP2               | Addgene- 86457 | Ralf Kuehn    |
| pKLV2_hU6_ccdB_PGK_Puro_T2A_BFP                | Addgene-67974  | Kosuke Yusa   |
| MSCV_IRES_eGFP                                 | Addgene-27490  | Warren Pear   |
| MSCV_3HA_ERHBDG400VHOXB8                       | -              | Hans Häcker   |

#### 2.1.5. Oligos

| sgRNA oligo sequences used in viral targeting experiments |           |                       |
|---|-----------|-----------------------|
| Target  | Name      | Sequence              |
| KMT2D   | sgKMT2D_A | CGTGGTCAGCAGGCGTATGG  |
| KMT2D   | sgKMT2D_B | TCCGAACCTCCATCGGCCCG  |
| KMT2D   | sgKMT2D_C | AGCCCGTAAGACTGATCGAC  |
| KMT2D   | sgKMT2D_D | TGGGTACCACAACCTCGACCT |
| KMT2D   | sgKMT2D_E | AAATGGCTGTTGATCCCATG  |
| KMT2D   | sgKMT2D_F | G TTCACCATTAATACCCCA  |
| KMT2D   | sgKMT2D_G | ATTGACGCCACGTTGACCGG  |
| HVEM  | sgHVEM_A  | CAGGATGGGGGTCGGCACCC  |
| HVEM  | sgHVEM_B  | TGGAACCTCTCCAGGATGG   |
| CD44  | sgCD44    | GTGCCAGGCTCAACTGCAAG  |
| GFP   | sgGFP     | GGCCACAAGTTCAGCGTGTC  |
| LACZ  | sgLACZ    | TGCGAATACGCCACGCGAT   |

| ssODN sequences  |                |   |                     |
|------------------|----------------|---|---------------------|
| Conversion       | Name           | Sequence  | Reference           |
| GFP to BFP       | BFP ssODN_1    | ACCCTGAAGTTCATCTGCACCACCGCAAGCTGCC<br>GTGCCCTGGCCACCCTCGTGACCACCCTGAGCCAC<br>GGGGTGCAGTGCTTCAGCCGCTACCCCGACCACAT<br>GAAGCAGCACGACTTCTCAAGTCCGCCATGCC  | Glaser et al., 2016 |
| GFP to BFP       | BFP ssODN_2    | GGCATGGCGGACTTGAAGAAGTCGTGCTGCTTCAT<br>GTGGTCGGGGTAGCGGCTGAAGCACTGCACCCCGT<br>GGCTCAGGGTGGTCACGAGGGTGGCCAGGGCAC<br>GGGCAGCTTGCCGGTGGTGCAGATGAACTTCAGGG<br>T   | Glaser et al., 2016 |
| CD45.2 to CD45.1 | CD45.1 ssODN_1 | TTTCTGATAATAGAACTTCTCTGCCAGCATCGTACC<br>TGGCTCACAGTGGAGTACATATGAAATATTGCACT<br>GTTGCATTTTCTGAAATCAAGGTTTTCTGTTTTCCAT<br>TCAAGACAGATTGAAGTGTTAGCCTTTTCTTTGGT<br>GTGCAGTCATGTAGCGAAAACCTGTCAGTCCCTGTG<br>GAGGAAACGGAGAGGTGC |                     |
| CD45.2 to CD45.1 | CD45.1 ssODN_2 | TTTCTGATAATAGAACTTCTCTGCCAGCATCGTACC<br>TGGCTCACAGTGGAGTACATATGAAATATTGCACT<br>GTTGCATTTTCTGAAATCAAGGTTTTCTGTTTTCCAT<br>TCAAGACAGATTGAAGTGTTAGCCTTTTCTTTGGT<br>GTGCAGTC   |                     |

| Primer-pairs used in TIDE assay |           |                        |                        |
|---------------------------------|-----------|------------------------|------------------------|
| Target                          | sgRNA     | Primer-1 (5'--> 3')    | Primer-2 (5'--> 3')    |
| KMT2D                           | sgKMT2D_A | GCGTTGTGCTCTCTGTAAC    | TGCACAGGGAAAGTGGTAAAG  |
| KMT2D                           | sgKMT2D_B | GGTGACTCCTACCTGTCTCTT  | GCAGTCCTCACCTGGTAAATC  |
| KMT2D                           | sgKMT2D_C | GAGGCAGTTTGATAGGGAGAC  | GGCTTGGGTAAGGAGGATAAG  |
| KMT2D                           | sgKMT2D_D | CTGCTGGCTGTCTACCTC     | GACATCAGGTGCCTTTAACTCC |
| KMT2D                           | sgKMT2D_E | CCTAGCCCACTCCACT       | TTGTAGCTCCTGGGTCTTCT   |
| KMT2D                           | sgKMT2D_F | CACTGACCCTGAGCTTGATAC  | GCCCACTGGGTAAGGTTAG    |
| HVEM                            | sgHVEM_A  | CTGAGGCTCTGTTTGGACTTTA | CACTCTGTGAGGGTGCTTATC  |
| HVEM                            | sgHVEM_B  | CTGAGGCTCTGTTTGGACTTTA | CACTCTGTGAGGGTGCTTATC  |

| Primer-pairs used for identification the induced genomic deletions of dual sgRNA targeting (via virus) |                         |                       |                       |     |
|--|-------------------------|-----------------------|-----------------------|-----|
| Target   | sgRNA pair              | Primer-1 (5'--> 3')   | Primer-2 (5'--> 3')   |     |
| KMT2D  | sgKMT2D_G and sgKMT2D_F | GGGTCAGGGCTCTCCTCTTA  | CACTGACCCTGAGCTTGATAC | PP1 |
| KMT2D  | sgKMT2D_A and sgKMT2D_C | GCGTTGTGCTCTCTGTAAC   | GGCTTGGGTAAGGAGGATAAG | PP2 |
| KMT2D  | sgKMT2D_C and sgKMT2D_F | GAGGCAGTTTGATAGGGAGAC | GCCCACTGGGTAAGGTTAG   | PP3 |

| Primer-pairs used for identification the induced genomic deletions of dual sgRNA targeting (via RNP) |                             |                       |                       |     |
|--|-----------------------------|-----------------------|-----------------------|-----|
| Target   | sgRNA pair                  | Primer-1 (5'--> 3')   | Primer-2 (5'--> 3')   |     |
| KMT2D  | KMT2D RNP_A and KMT2D RNP_G | GCGTTGTGCTCTCTGTAAC   | GGGTCAGGGCTCTCCTCTTA  | PP5 |
| KMT2D  | KMT2D RNP_C and KMT2D RNP_G | GAGGCAGTTTGATAGGGAGAC | GGGTCAGGGCTCTCCTCTTA  | PP6 |
| KMT2D  | KMT2D RNP_A and KMT2D RNP_C | GCGTTGTGCTCTCTGTAAC   | GGCTTGGGTAAGGAGGATAAG | PP2 |

| Primer-pairs used for identification of T2A-BFP tag in ACTB locus |                                |                               |
|---|--------------------------------|-------------------------------|
| Target  | Primer-1 (5'--> 3')            | Primer-2 (5'--> 3')           |
| ACTB  | TCTCAGATCTATCCATACAGTTTCACCTGC | CAACCAACTGCTGTGCCTTCACCGTTCCA |

## 2.2. Methods

### 2.2.1. Genetically Modified Mouse Strains

All mouse lines used in this study were previously published and they are used on the C57BL/6 background. Mice were housed in the Centre for Preclinical Research of the MRI (Zentrum für Präklinisches Forschung, ZPF), Munich, and Charles River Calco, Italy. They were bred and kept in specific pathogen-free (SPF) conditions or specific and opportunistic pathogen-free (SOPF) conditions under the guidelines of the Region of Upper Bavaria (Regierung von Oberbayern) and the European Union.

#### VavP-Bcl2

The VavP-Bcl2 transgenic mouse line was generated by introducing to the genome the transgenic vector allowing the expression of the human Bcl2 cDNA under the control of the Vav promoter (Ogilvy et al., 1999). In these transgenic animals, all nucleated hematopoietic cells

express human *BCL2* constitutively. *VavP-Bcl2* transgenic animals develop germinal center hyperplasia starting from 18 weeks of age. They are highly susceptible to acquire autoimmune-type glomerulonephritis (~25%, by 40 weeks of age) and at older ages to develop B cell lymphomas resembling the human follicular lymphoma (30-50%, >10 months) (Egle et al., 2004).

### **Mb1cre**

Mb1cre mice were generated by targeting the exon2 and exon3 of the *CD79a (Mb1)* gene with a mammalian codon-optimized Cre-recombinase. In these mice, the expression of Cre starts at the pro-B cell stage and continues throughout B-cell development. Moreover, mice carrying homozygous Mb1Cre knock-in alleles lack mature B cells due to the block in B cell development as a result of the full knockout of the Ig- $\alpha$  subunit of the B cell antigen receptor (Hobeika et al., 2006).

### **CD19cre**

CD19cre mice express the Cre-recombinase under the control of CD19 promoter elements. It was constructed by inserting the Cre-coding sequence into the first coding exon of the *CD19* and activates Cre expression in B cells starting from early B-cell developmental stages (pro and pre-B cells) onwards (Rickert et al., 1997).

### **Cy1cre**

Cy1cre mice were developed by inserting an IRES-Cre cassette into the 3' untranslated region (UTR) of the immunoglobulin heavy constant gamma 1 locus (*Ighg1*). Cre-mediated recombination appears in germinal center B cells and is detected in class-switched memory B, and plasma cells and therefore can be used to investigate gene functions in GC reaction (Casola et al., 2006).

### **R26-Cas9-eGFP and R26-LSL-Cas9-eGFP**

R26-Cas9 and R26-LSL-Cas9 mice enable the expression of Cas9 (CRISPR associated protein 9) for gene editing by CRISPR-based applications. Cas9, one of the major components of the CRISPR system was inserted either with (R26-LSL-Cas9-eGFP) or without (R26-Cas9-eGFP) a *loxP*-flanked

stop cassette (LSL) into the *Rosa26* locus in combination with a 5' CAG promoter and with a 3' eGFP tag following a ribosomal skip cleavage peptide sequence (P2A). While R26-Cas9 mice provide ubiquitous whole-body Cas9 expression, R26-LSL-Cas9 mice allow tissue specific Cas9 expression in cells which experienced Cre recombinase-mediated stop cassette deletion (Platt et al., 2014).

### **R26-LSL-PB**

Transposition-based insertional mutagenesis systems in mice are engineered in a way that transposon and transposase elements are found in different animals. For a conditional *piggyBac* transposition system, an insect version of the *piggyBac* transposase (iPBase), rendered conditional through a 5' loxP-flanked stop cassette (LSL), was knocked-in to the *Rosa26* locus (Rad et al., 2015).

### **ATP2-H32**

The ATP2-H32 transgenic mouse line has 25 copies of the bi-functional “activating/inactivating” transposon ATP2 on chromosome 2. The ATP2 construct contains the murine stem cell virus long terminal repeat (MSCV) promoter placed between PB and SB inverted terminal repeats (ITRs) along with splice acceptors (SA) and bidirectional polyadenylation signals (pA). It was reported that mostly hematopoietic malignancies arose from the combination of ATP2 and R26-PB in mice (Rad et al., 2010).

### **Compound genetic mouse strains and derived Hoxb8-FL cells for the investigation of GC derived lymphomas**

In order to establish an Hoxb8-FL-based adoptive transplantation model to study the dynamics of GC B cells and lymphoma development, *VavP-Bcl2* mice were bred to different Cre-expressing lines (*Mb1cre*, *CD19cre*, *Cy1cre*) and finally crossed to R26-LSL-Cas9-eGFP mice (*VavP-Bcl2 Mb1-Cre<sup>i/wt</sup> R26-LSL-Cas9-eGFP<sup>i/wt</sup>*, *VavP-Bcl2 CD19-Cre<sup>i/wt</sup> R26-LSL-Cas9-eGFP<sup>i/wt</sup>*, *VavP-Bcl2 Cy1-Cre<sup>i/wt</sup> R26-LSL-Cas9-eGFP<sup>i/wt</sup>*). Moreover, Hoxb8-FL cells were generated from *VavP-Bcl2 CD19-Cre<sup>i/wt</sup> R26-LSL-PB<sup>i/wt</sup> ATP2-H32* mice with the aim of conducting further forward genetic screens in adoptive transplantation models. By the age of 6-10 weeks, bone marrow cells of the indicated

mice were isolated and used to generate Hoxb8-FL lines. In the transplantation models, as supporting bone marrow (BM) cells, 6–10-week-old *Mb1-Cre<sup>i/i</sup>* B cell-deficient animals were used to generate a mature B cell-deficient hematopoietic environment for the Hoxb8FL-derived cells in the recipient mice.

To identify lymphoma contributing genes through *in vivo* conditional screens, *VavP-Bcl2* mice were bred to different Cre lines (*Mb1cre*, *CD19cre*, *Cy1cre*). Then to introduce insertional mutagenesis they were bred to R26-LSL-PB and ATP2-H32 lines. Generated experimental animals (*VavP-Bcl2 Mb1-Cre<sup>i/wt</sup> R26-LSL-PB<sup>i/wt</sup> ATP2-H32*, *VavP-Bcl2 CD19-Cre<sup>i/wt</sup> R26-LSL-PB<sup>i/wt</sup> ATP2-H32*, *VavP-Bcl2 Cy1-Cre<sup>i/wt</sup> R26-LSL-PB<sup>i/wt</sup> ATP2-H32*) were aged and monitored closely to assess the disease development and progression according to the license for animal experiments (TVA 55.2-1-54-2532-234-2015) granted by the Regierung of Upper Bavaria.

During the aging period, animals were continuously monitored and tracked for signs of sickness including autoimmunity (i.e., weight loss, paleness, anemia) and cancer development (i.e., splenomegaly, enlargement in the lymph nodes).

### **2.2.2. Adoptive Transfer of Hoxb8-FL Cells into Recipient Mice**

For the Hoxb8-FL adoptive transfer experiments, early passage frozen Hoxb8-FL cells were thawed and expanded. On the day of injection, 10-15 million Hoxb8-FL cells were centrifuged and washed with PBS. In parallel, as supportive cells, either freshly isolated or thawed frozen *Mb1-Cre<sup>i/i</sup>* unfractionated bone marrow cells were added (0.4 - 0.8 million per injection). After mixing the cell number-adjusted supportive bone marrow and Hoxb8-FL cells, they were resuspended in 200 ul PBS and transferred by intravenous injection to C57BL/6N animals, which had been lethally irradiated with 8.5 Gray (Gy) using an in-house Gulmay irradiation machine. In the following two weeks, mice were monitored every day for irradiation-related symptoms and 24% Borgal® antibiotic was added to the drinking water by 1:1000 dilution. To check the reconstitution after transplantation, mice were bled, and the collected peripheral blood samples were further processed for FACS analysis following red blood cell lysis with ACK buffer.

### **2.2.3. Organ Collection and Processing**

After euthanasia blood was collected from the heart by syringe into a heparin treated Microvette®. The serum was frozen at -20°C after separation from the cell pellets by centrifugation (500g, 20 min, 4°C). If the cell pellet was to be further analyzed, red blood cell lysis with ACK was performed for 15 min on ice. Following two washes with PBS, samples were further processed according to the FACS protocol. Inguinal, brachial, axillary, and superficial cervical lymph nodes were collected and pooled when needed. Spleen, mesenteric lymph nodes, liver, kidneys, thymus, tibia, and femur were harvested. Tumors were treated in the same way as other organs. In case of multiple tumors, they were treated as individual entities and processed separately. Organs were kept on ice throughout the processing. Lymph nodes, spleen, thymus, and tumor(s) were processed to single cell suspensions using 70 µm cell strainers, washed with PBS, and pelleted by centrifugation. Bone marrow cells were flushed from femur and tibia with PBS using a syringe and transferred to falcon tubes for pelleting. Spleen, bone marrow, and tumor single suspension cells were incubated with ACK lysis buffer on ice for 5-10 min to lyse red blood cells. Single-cell suspensions were diluted with Trypan Blue to count the viable cells using the Neubauer counting chamber.

### **2.2.4. DNA and RNA Preservation in RNAlater**

For DNA and RNA preservation, tissues were trimmed to small pieces (~2-3 mm<sup>3</sup>) and dipped into 1-2 ml RNAlater solution. They were left overnight room temperature or 4°C for better penetration of the solution into tissues and then transferred to -20°C for longer storage.

### **2.2.5. Flow Cytometry**

Up to 3 million cells were stained in 96 well V-bottom plates for flow cytometric analyses. In all the steps of the FACS preparations up to fixation, Hoxb8-FL cells were kept and incubated at room temperature (RT) as they are cold-sensitive, whereas mouse single cell suspensions were kept on ice. Initially, to prevent nonspecific Fc receptor binding of antibodies, cells were incubated with anti-mouse CD16/CD32 antibody along with a fixable live/dead dye in PBS for 20 min. After washing with PBS, cells were stained for 30 min with different antibody mixes

prepared in FACS buffer to identify the immune populations based on the expression profile of extracellular marker proteins. When a biotinylated antibody was included in the staining mix, after the washing a second incubation with fluorescence-tagged streptavidin (SA) was performed in FACS buffer. For intracellular protein staining, cells were fixed at room temperature for 30 min either with a final 2% Roti®-Histofix solution diluted in PBS or with BD Cytofix/Cytoperm™ solution. After fixation and washing, cells were permeabilized with absolute methanol for 5 min at -20°C, followed by 1h room temperature FACS buffer blocking and 1h intracellular antibody staining. As an alternative permeabilization method to methanol, in which tandem dyes signals were lost, cells were permeabilized and stained overnight at 4°C in the permeabilization buffer of the eBioscience™ Foxp3/Transcription Factor Staining Buffer Set. After intracellular and extracellular staining cells were washed and resuspended in FACS buffer for acquisition. Then samples were acquired with CytoFLEX S or CytoFLEX LX flow cytometers. FACS-sorting was performed with BD FACS Aria™ III or BD FACS Aria™ Fusion machines. For compensation, single color stainings were performed using splenocytes or UltraComp eBeads™ Compensation Beads. Flow cytometric data analysis was conducted using the software FlowJo version 9. Default starting gating strategies included first doublet exclusions (FSC-H vs. FSC-A, SSC-H vs. SSC-A), then gating on living cells (SSC-A vs. live/dead) and lymphocytes (SSC-A - FSC-H).

#### **2.2.6. Cell Culture**

All cell types (HEK293T, Hoxb8-FL, primary mouse cells) were incubated in a humidified incubator at 37 °C with 5% CO<sub>2</sub> and passaged regularly every 2-3 days. All cell lines and primary cells were frozen and thawed by the following protocol: to freeze, cells were pelleted and dissolved in 10% DMSO containing FBS, directly transferred into cryotubes and transferred with a pre-cooled freezing box to -80°C. For longer preservations, they were stored in liquid nitrogen. To thaw, cells were transferred from -80°C or liquid nitrogen to a 37°C water bath, incubated for 1-2 min in the water bath, dissolved in 9ml of medium, centrifuged and dissolved in the respective growth medium for further culturing.

### 2.2.7. HEK293T Transfection and Virus Production

For retrovirus production one day before transfection, HEK293T cells were trypsinized using 0.05% trypsin. They were seeded in D-10 medium (D-10: DMEM with GlutaMAX with 10% FBS and 1% PenStrep) at a density of 0.45 million cells in 2ml per well in a 6-well plate. Next day, first the plasmid cocktail was prepared by mixing 1 ug of cargo plasmid (pMSCV) with 1 ug of packaging plasmid (pCL-Eco) and dissolved in Opti-MEM™. In parallel, 4 ul of Lipofectamine™ 2000 was added to the Opti-MEM™ in another tube. After 5 min incubation, plasmid cocktail with Opti-MEM™ was mixed with Lipofectamine™ 2000 dissolved in Opti-MEM™. This mixture was kept at room temperature for 30 min, then added dropwise onto HEK293T cells. After 6 hours incubation, medium was changed with Hoxb8-FL medium for virus production in the following 48 hours. Virus containing medium was collected and passed through a 0.8 um Minisart® Syringe Filter. 0.35 - 1 million cells were spin-infected (800g, 30°C, 90 min) with the virus preparations in the presence of a final concentration of 5 ul/ml polybrene.

For lentivirus production, 2 million HEK293T cells were seeded in a 25 cm<sup>2</sup> cell culture flask one day before the transfection. The next day, as in the retrovirus production protocol, first the plasmid cocktail was prepared by mixing 3.1 ug of lentiviral cargo plasmid with 2.6 ug of packaging plasmid (psPAX2) and 1.7 ug of envelope plasmid (pMD2.G) by dissolving in Opti-MEM™. In parallel, 16 ul of Lipofectamine™ 2000 was diluted in Opti-MEM™. After 5 min incubation, the components were mixed and incubated at room temperature for 30 min, finally added dropwise onto HEK293T cells. After 6h, the medium was replaced with Hoxb8-FL medium. At the end of 48 hour, produced viral particles were harvested and cells were infected as described above in the retroviral protocol.

AAV-DJ vector carrying the donor template for beta-actin (*Actb*) loci, Actb (AAV-DJ-Actb), was a kind gift of Van Trung Chu (Max-Delbruck-Center for Molecular Medicine, Berlin).

For longer storage, viral preparations were snap frozen in liquid nitrogen and kept at -80°C. They were thawed by incubating at 37°C for 2-10 min (for aliquots in 15ml tubes thawing occurred in

a cell culture incubator, smaller volume aliquots in cryopreservation vials were thawed in a water bath).

### **2.2.8. Hoxb8-FL Generation**

From 6-10 weeks old animals, femur and tibia were harvested. Bone marrow cells were isolated by flushing the bones with medium (RPMI 1640 GlutaMAX™ with 10% heat inactivated FBS and 1% PenStrep). Cells were pelleted and seeded on 6-well plates by dissolving in stem cell medium which contained recombinant mouse IL-3 (5 ng/ml), IL-6 (20 ng/ml) and 1% cell culture supernatant from SCF-producing B16 melanoma cells in RPMI 1640 GlutaMAX™. After 48 hours of culture, cells were centrifuged and dissolved in the progenitor outgrowth medium (POM: RPMI 1640 GlutaMAX™ with additives of 10% non-heat inactivated FBS, 0.1% 2-Mercaptoethanol, 1% PenStrep, 1  $\mu$ M  $\beta$ -estradiol and supernatant from an Flt3L-producing B16 melanoma cell line which equals to a final concentration of 35 ng/ml). Afterwards, cells were spin-infected (800g, 30°C, 90 min) with the MSCV–ERHBD–Hoxb8 retrovirus and cultured with POM until Hoxb8-FL cells grew out. From the first batches several vials were frozen for later uses.

### **2.2.9. Generation of Single Cell-Derived Clones**

In order to generate monoclonal cell clones from Hoxb8-FL cell preparations, a low-density seeding method in 96-well plate was applied. Cells were brought to a dilution where theoretically 0.5 cells/well in 100ul of medium were seeded to U-bottom 96-well plates. The next day, plates were screened for wells containing only one cell. These wells were marked and grown by changing the medium every 2-3 days. After they reached approximately thousand cells, they were transferred into bigger plates.

### **2.2.10. Magnetic Activated Cell Sorting (MACS)**

Single-cell suspensions of retrovirally transduced Hoxb8-FL cells were first blocked by anti-CD16/CD32 monoclonal antibody at RT for 15 min, then washed and labelled with either anti-THY1.1-APC and/or anti-hCD2-APC antibodies for 20 min. Samples were washed, resuspended in PBS (80  $\mu$ l/10 million), and labeled with anti-APC MicroBeads (20  $\mu$ l/10 million) for 15 min at

RT. After the incubation and final washing, cells were resuspended in PBS and loaded on pre-equilibrated MACS columns (LS or MS depending on the cell number). Cell enrichment purity was assessed by Flow Cytometry.

### 2.2.11. Molecular Cloning

For CRISPR targeting, sgRNAs were designed by using the sgRNA design tool of the Broad Institute (GPP portal), MA, USA. Targets were restricted to 20 nucleotides and NGG was set always as PAM sequence. Among the software-ranked sgRNA designs, the ones which had the lowest off-target score with a high potential efficacy were chosen to proceed with. As control, *LacZ*-targeted sgRNA (sgLacZ) was used. sgRNA oligos were phosphorylated and annealed in the presence of 10x T4 Ligation Buffer (NEB) and T4 PNK (NEB) in the thermocycler by incubation for 30 min at 37 °C followed by a temperature ramp from 95°C to 25 °C at 5°C/min. Retroviral or lentiviral CRISPR sgRNA vector backbones were digested by FastDigest Esp3I (BsmBI) or FastDigest BpiI (BbsI) or AarI and dephosphorylated by using Fast Alkaline Phosphatase at 37°C for 30 min. Then, the reactions were run on 1.5% agarose gels to separate the stuffer from the digested vector and the cut backbone was purified by using QIAquick Gel Extraction Kit (Qiagen). The concentration of digested backbone was determined using NanoDrop™ One/OneC (Thermo Scientific). Ligation of the cut backbone and sgRNA oligos was performed at room temperature for 10 min in 2x Quick Ligation Buffer (NEB) and Quick Ligase (NEB). Reactions were transformed into chemically competent Stb13 bacteria by heat shock (45 sec at 42 °C) and then bacteria were chilled on ice for 5 min, followed by incubation in LB medium at 37 °C for 40 min. Bacteria were grown overnight at 37 °C on ampicillin agar plates. Following single colony selection and LB medium growth in the presence of 100 µg/ml ampicillin, plasmids were purified using NucleoSpin Plasmid miniprep kit (Macherey-Nagel) and concentrations were measured with nanodrop. In the case of multiplexed sgRNA clonings, a two-step cloning procedure was applied.

For cloning of the multiplexing sgRNA plasmid, pMSCV\_hU6\_ccdB\_PGK\_Puromycin\_eBFP backbone was cut with XhoI (NEB) restriction enzyme and a gBlock (IDT), which is a double-stranded DNA fragment containing the second hU6 and gRNA scaffold unit with AarI restriction sites, was inserted by Gibson Assembly®. DB3.1 bacteria were transformed with the cloning

reaction and plated on ampicillin plates. 4-5 clones were selected and sequenced for successful integration.

In order to clone human *MYC* and flag-tagged mouse *Bcl6* genes into conditional expression retroviral vectors, Gateway LR reactions were performed by targeting the entry plasmid clones of *hMYC* and flag-tagged *mBcl6* into the destination vectors MSCV-LSL-ccdB-IRES-THY1.1-F2A-PURO-WPRE and MSCV-LSL-ccdB-IRES-hCD2 respectively.

#### 2.2.12. Gene Editing Assessment at DNA Level

In order to assess the gene-editing spectrum and frequencies, genomic DNA was recovered from CRISPR edited and control cells using QuickExtract (Epicentre) and QIAamp DNA Mini (Qiagen) Kits. Targeted genomic loci were PCR amplified with high fidelity polymerases (Phusion, Q5<sup>®</sup> Hot Start Thermo Scientific) and two primers covering a ~400-600 bp region around the Cas9 cut site. After the PCR clean-up (QIAquick PCR Purification Kit, Qiagen) of amplicons, they were sequenced by Sanger sequencing. Sequencing results of targeted and control samples were uploaded and analyzed by the TIDE software tool (Tracking of Indels by DEcomposition) which provides a sequence trace decomposition algorithm for detection of editing events (Brinkman et al., 2014). Alternatively, a similar commercial web tool termed ICE v2 (Inference of CRISPR Edits), which had been developed using the algorithm of TIDE but with a few additional features including knockout/in efficiency score prediction, was also used in the analysis (Hsiao et al., 2018).

In the gene-editing experiments where multiple sgRNAs were used to generate genomic deletions in a locus, two sets of primers were designed to determine the presence of the genomic knockout. One primer set ("out primers") was designed outside of the sgRNA target sites. A second primer set ("in primers") was designed in between the two sgRNA target sites. In the absence of deletions, the "in primers" amplified the wild type sequence and resulted in a single amplicon, whereas the "out primers" cannot amplify the DNA because they had been designed too far apart to produce an amplicon within the given PCR conditions. In the presence of genomic deletions, the "out primers" can amplify an amplicon with the same PCR conditions

as they were brought closer together due to the CRISPR-mediated deletion. By using this method, single cell-derived clones were also screened for homozygous and heterozygous deletions. As there was no need for high fidelity amplification for the initial screening of deletions, Gotaq Hotstart 2X master mix was used for PCR reactions.

### **2.2.13. Gene Editing by Electroporation**

#### **RNP complex formation, electroporation, and AAV-mediated HR**

In the presence of 2-part guide RNA (Alt-R CRISPR-Cas9 crRNA and Alt-R CRISPR-Cas9, IDT), a RNA duplex was formed by mixing equimolar concentrations of crRNA and tracrRNA for a final 44  $\mu$ M duplex concentration. For duplex formation, the mixed RNAs were cooled down to room temperature after heating for 5 min at 95 °C. When a pre-made complete sgRNA (Alt-R CRISPR-Cas9 sgRNA, IDT) was used, the duplex formation step was skipped. For RNP complex formation 44  $\mu$ M of either duplex RNA or sgRNA was incubated with 36  $\mu$ M of Cas9 enzyme (Alt-R® S.p. Cas9 Nuclease V3 or purified recombinant Cas9-NLS from the MPIB Max Planck Core Facility) at room temperature for 30 min. In case the HDR template or Alt-R Cas9 Electroporation Enhancer (IDT) were used, they were added to the complex only in the very final step, just before the electroporation. When optimization experiments were performed the same protocol was followed but the amounts individual reagents were varied .

To electroporate Hoxb8-FL cells the Neon® transfection kit and device (Invitrogen) was used. For the 10  $\mu$ l reaction format, 0.35 million cells were pelleted and washed with PBS. Cells were dissolved in Neon resuspension buffer R or T, and mixed with sgRNA duplex, RNP complex, HDR template and Alt-R Cas9 Electroporation Enhancer (IDT) either in combinations or alone depending on the testing condition. 10  $\mu$ l of the suspension was electroporated with the Neon electroporation device. Electroporated cells were transferred into a 24-well plate and 2 ml of medium added.

For AAV-mediated HR, initially Hoxb8-FL cells were electroporated with RNP complex and incubated in their medium for 30 min at 37 °C incubator. After 30 min, cells were spin-infected (800g, 30°C, 60 min) with the donor template-carrying AAV-DJ virus preparations at varying

multiplicities of infection (MOI). 48 hours after infection, the cells were analyzed by FACS for expression of the inserted transgene.

#### **2.2.14. His-TAT-NLS-Cre Transduction**

For TAT-Cre treatment, cells were centrifuged and washed with PBS. Per reaction  $5 \times 10^6$  cells were dissolved in Optimem containing recombinant His-TAT-NLS-Cre protein. Cells were seeded on non-treated cell culture plates and incubated for 1 hour in a tissue culture incubator with Cre containing medium at varying concentrations. After Cre-treatment, the medium was removed, cells were thoroughly washed with PBS and resuspended in fresh medium for further culturing.

#### **2.2.15. Statistical Analysis and Software**

Total cell numbers and other calculations were performed using Excel (Microsoft). Flow cytometry plots were generated using FlowJo version 9 (Tree Star Inc.). Bar charts and heatmaps were generated with GraphPad Prism version 7 (GraphPad Software). Adobe Illustrator (Adobe Systems) was used for figure preparations. Statistical analyses were calculated using the functions of GraphPad Prism. D'Angostino and Pearson normality tests were used to test the normal distribution of samples. For normally distributed populations T-test or One-way ANOVA (Holm-Sidak's multiple comparisons test) were applied for statistical analyses. For samples with no normal distribution of the data the Kurskal-Wallis nonparametric test (Dunn's multiple comparison test) was used. sgRNA sequences for CRISPR/Cas9 based genome editing were determined with Broad Institute Genetic Perturbation Platform sgRNA designer tool (<https://portals.broadinstitute.org/gpp/public/analysis-tools/sgrna-design>). TIDE (Tracking of Indels by DEcomposition, (Brinkman et al., 2014) ) and ICE (Inference of CRISPR Edits) softwares were used to track the sequence decompositions in gene edited samples.

### 3. RESULTS

#### 3.1. Generation of Hoxb8-FL Lines and Establishment of Gene Editing Protocols in Hoxb8-FL Cells

##### 3.1.1. Generation of Hoxb8-FL Lines

With the aim of investigating the important regulators of germinal center reaction and germinal center derived B cell lymphomas *in vivo*, I wanted to establish a versatile genetic model system that permits high throughput genome manipulation of B lineage cells at different developmental stages *in vivo* to understand the effects of the induced alterations. As the *VavP-Bcl2* transgenic mouse line is characterized by germinal center hyperplasia and an increased incidence to develop follicular lymphoma (Egle et al., 2004), I generated conditionally immortalized hematopoietic progenitor Hoxb8-FL cell pools (Redecke et al., 2013) from the bone marrow of *VavP-Bcl2* transgenic mice (**Supplementary Table 1**). *VavP-Bcl2*tg Hoxb8-FL cells provide a pool of BCL2-overexpressing progenitor cells that can be expanded *in vitro* owing to their unlimited proliferation potential. My aim was to evaluate whether these cells could be efficiently genetically modified and adoptively transferred into mice, where they should differentiate into mature hematopoietic cells, especially into germinal center B cells and plasma cells (**Figure 1c**). This would allow to investigate how the nature of the prevalent alterations influences clonal growth, clonal evolution, and transformation of B cells.

Importantly, I wanted to develop a fine-tuned system where I can control the integration of genetic modifications in B cells during B-cell developmental stages. With the aim of this, I crossed *VavP-Bcl2* animals with different B cell-specific Cre lines (*Mb1cre*, *CD19cre*, *Cy1cre*) (**Supplementary Table 1**). While *Mb1cre* and *CD19cre* allow conditional gene targeting starting from the early B cell developmental stages, *Cy1cre* would facilitate targeting in GCB cells for genetic manipulation (**Figure 1b**).

For CRISPR-mediated gene editing applications, ubiquitous Cas9 expression levels would be a desirable advantage for efficient gene editing. Therefore, I also generated Hoxb8-FL lines from *R26-Cas9* and *R26-LSL-Cas9* strains (Platt et al., 2014) (**Supplementary Table 1**). For example, B cell-specific Cre strains crossed with *VavP-Bcl2* mice were bred to *R26-LSL-Cas9* mice and used

to produce BCL2-overexpressing Hoxb8-FL cell lines which can serve for the conditional CRISPR activation in B cells (**Figure 1C**).

Similarly, to deploy conditional *PiggyBac* transposon mutagenesis using the Hoxb8-FL system, VavP-*Bcl2*-CD19*cre* animals were crossed to *R26-LSL-PB* and *ATP2-H32* transgenic mice (Rad et al., 2010) and Hoxb8-FL cells were generated from their bone marrow cells (**Supplementary Table 1**). These Hoxb8-FL cells could be directly used for B cell-specific insertional mutagenesis screens *in vivo*, but alternatively also by *in vitro* activation of Cre, transposon hopping in the genome can be already induced in the progenitor cells and further proceeded after *in vivo* transfer leading to further transposon hopping, selection and evolution of clones.

### 3.1.2. Establishment of Gene Editing Protocols in Hoxb8-FL Cells

#### 3.1.2.1. Genetic Modification of Hoxb8-FL Cells by Viral Systems

As I wanted to use Hoxb8-FL cells for loss and gain of function studies first I focused on the optimization of genetic manipulation applications in Hoxb8-FL cells. Initially, I tested the infectability of Hoxb8-FL cells by using retroviral and lentiviral eGFP fluorescent reporter expression vectors. Retroviral or lentiviral transduction of VavP-*Bcl2* Hoxb8-FL cells resulted in up to 95% and 70% GFP-expressing cells, respectively (**Figure 2a**). Similarly, transduction of cells with retro- or lentiviral sgRNA expression vectors carrying the BFP reporter resulted in high infection efficiencies reaching up to 70% and 50% respectively (**Figure 2a**). Given the high viral infection efficiencies I next tested the applicability of CRISPR/Cas9 based gene editing by transducing ubiquitously Cas9-expressing Cas9-GFP Hoxb8-FL cells with sgRNA-expressing vectors. Initially, I targeted CD44, a surface protein whose levels can be quantified by flow cytometry and the fluorescent protein GFP. After non-targeting control LACZ, CD44 and GFP targeting sgRNAs were cloned into individual retroviral sgRNA expression vectors, cells were transduced. FACS analysis of BFP<sup>+</sup> infected cells showed that cells transduced with the target sgRNAs showed high knockout efficiencies reaching up to 93% for both CD44 and GFP proteins (**Figure 2b**). Furthermore, I also tested multiplexing sgRNAs in Hoxb8-FL cells since it would provide the advantage to target multiple locations in the genome either to target different genes

at the same time or to generate regional deletions. To do so, CD44 and GFP targeting sgRNAs were cloned into a retroviral multiplexing vector; pSB2 where respective sgRNA expression is driven by individual sgRNA expression cassettes that are regulated by two independent human-U6 (hU6) promoters. In pSB2, CD44 and GFP targeting sgRNAs were brought into gRNA scaffold positions in two different combinations: hU6<sup>1</sup>-sgCD44-hU6<sup>2</sup>-sgGFP-eBFP and hU6<sup>1</sup>-sgGFP-hU6<sup>2</sup>-sgCD44-eBFP. Afterwards, Cas9-GFP Hoxb8-FL cells were transduced with these two vectors and analyzed by FACS for CD44 and GFP expression (**Figure 2b**). Depending on the gRNA scaffold position of the sgRNAs, knockout efficiencies were slightly altered. For example, when the GFP targeting sgRNA was inserted after the 5'-proximal U6 promoter (hU6<sup>1</sup>), it performed less efficiently than when it was inserted after the 3'-proximal U6 promoter (hU6<sup>2</sup>), 65% knockout vs 91% knockout, respectively. Likewise, CD44 targeting sgRNA resulted with ~77% knockout efficiency when inserted after hU6<sup>1</sup> while ~89% knockout efficiency was observed when it was inserted after the hU6<sup>2</sup>. Importantly, with both positional combinations, I obtained in more than half of the infected cells a double knockout phenotype demonstrating efficient multiplexing.

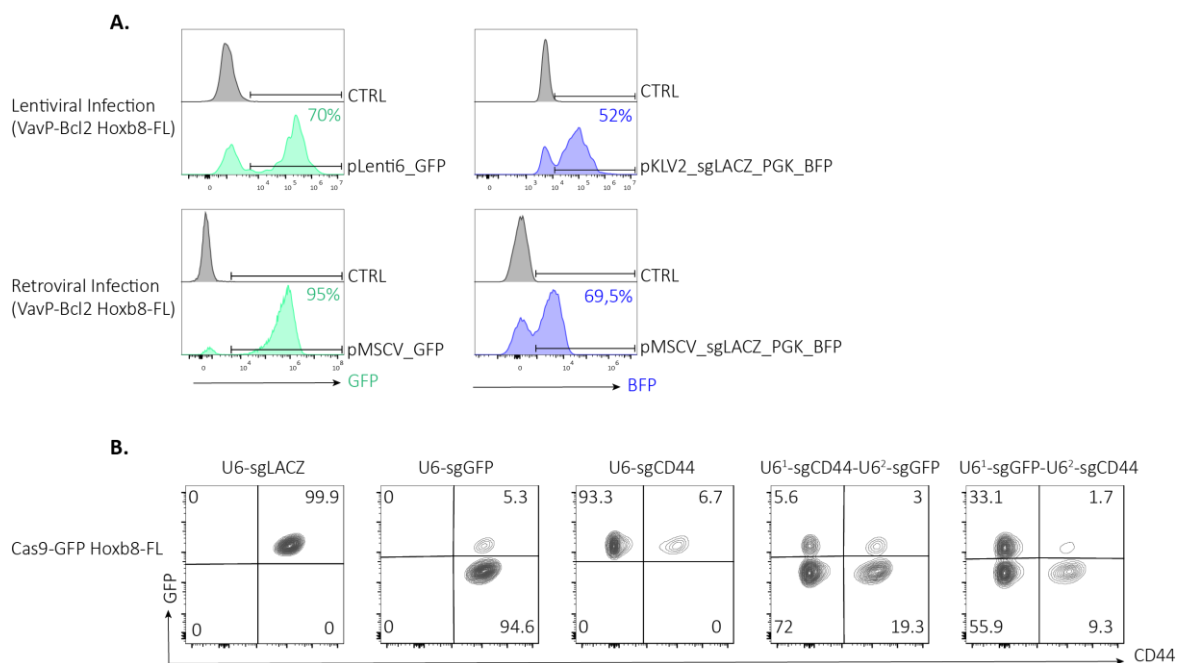


**Figure 2: Genetic modification of Hoxb8-FL cells through viral transduction: A)** Representative FACS plots of VavP-Bcl2 Hoxb8-FL cells transduced with lentiviral (pLenti6\_GFP and pKLV2\_sgLACZ\_PGK\_BFP) or retroviral (pMSCV\_GFP and pMSCV\_sgLACZ\_PGK\_BFP) vectors. Cells were fixed and analyzed by flow cytometry 5 days after the infection. Numbers indicate the percentages of the gated populations. GFP (Green Fluorescent Protein), BFP (Blue Fluorescent Protein). Data are representative of 2 (lentiviral) - 7 (retroviral) experiments. **B)** Representative FACS plots of GFP and CD44 expression in Cas9-GFP Hoxb8-FL cells transduced with single or dual sgRNA expressing retroviral vectors. Cas9-GFP Hoxb8-FL cells were transduced with the indicated vectors carrying the following sgRNAs; non-targeting sgLACZ, CD44 targeting sgCD44 and GFP targeting sgGFP. Cells were FACS analyzed 15 days later, graphs represent the GFP and CD44 expression in infected GFP<sup>+</sup> living cells. Numbers in quadrants indicate percentages. U6<sup>1</sup>: sgRNA at position-1; U6<sup>2</sup>: sgRNA at position-2. Data are representative of 2 experiments.

### 3.1.2.2. Genetic Modification of Hoxb8-FL Cells by Electroporation

To increase the gene-editing application tools that can be used for Hoxb8-FL cells, I wanted to establish an electroporation-based gene-editing protocol using the Neon<sup>®</sup> transfection device.

Initially, I optimized electroporation conditions by targeting CD44 in Cas9-GFP Hoxb8-FL cells. Control (LACZ) or CD44-targeting crRNAs (CD44\_A and CD44\_B) were complexed with tracrRNA and electroporated into Cas9-GFP Hoxb8-FL cells using three different programs (P1, P2, P3) that were adapted from the established Neon<sup>®</sup> electroporation programs of murine and human hematopoietic progenitor cells (Gundry et al., 2016). In my optimization tests I also included two different resuspension buffers of the Neon<sup>®</sup> system (R and T buffers) to determine the conditions which can provide an efficient gene targeting with high viability. Cells electroporated with the R buffer showed a significant decrease in viability compared to non-electroporated cells especially when used in combination with P2 and P3 programs (**Figure 3a**). On the other hand, resuspension of cells with the T buffer showed less toxicity and cells remained highly viable after electroporation. Even with the use of program P3, the harshest program among others for R buffer samples, 75% viability was achieved in T buffer resuspended cells. When the CD44 targeting efficiencies were compared between these different combinations, T buffer-resuspended cells always showed higher knockout efficiencies compared to R buffer-resuspended cells (**Figure 3b**). Among the tested programs, the P1 electroporation program underperformed in knockout efficiencies when an inferior sgRNA was used to target CD44 (CD44\_B). On the other hand, P2 and P3 programs performed highly similarly in the depletion of CD44 for both sgRNA designs. As program P2 resulted with slightly more viable cells than P3 I decided to electroporate T buffer resuspended cells with program P2 in my future experiments. With this combination, CD44 could be depleted in 76% of CD44\_A duplex electroporated and 60% CD44\_B electroporated Cas9-GFP Hoxb8-FL cells. By using this condition, electroporation of GFP-targeting crRNA:tracrRNA gRNA complex yielded 85% depletion in GFP positive cells (**Supplementary Figure 1a-b**). Increasing the gRNA concentration 5-fold higher brought the knockout efficiency up to 94% without causing toxicity on the viability of cells.

As next, to induce CRISPR-based gene editing in Hoxb8-FL cells lacking Cas9 expression, I optimized the delivery of Cas9/gRNA complexes (RNPs) by electroporation. After assembling CD44-targeting RNP (CD44\_A) by incubating crRNA:tracrRNA gRNA complex with Cas9 protein at different molar ratios, I electroporated these complexes using the program P2 into the VavP-Bcl2 Hoxb8-FL cells that were resuspended in T buffer. Previously it was shown that using random, non-homologous single-stranded oligo sequences along with RNPs during the electroporation can increase the indel efficiencies possibly by simulating the error-prone repair pathway in cells and by enhancing the uptake of RNPs into the cells (Jacobi et al., 2017) (Richardson et al., 2016) (Shapiro et al., 2020). Therefore, additionally I also tested the potential contribution of non-homologous single-stranded oligo sequences to the knockout efficiency by using the commercially available reagent Alt-R™ Cas9 Electroporation Enhancer-IDT (EE). My results showed that RNP precomplexed at a 1:0.8 gRNA: Cas9 molar ratio provided the highest knockout levels (in the absence and presence of EE; 71% and 78%, respectively) and an increase in the Cas9 molarity didn't further improve the efficiencies (**Figure 3c**). Therefore, I determined the optimal condition as 1:0.8 gRNA: Cas9 molar ratio together with EE. Addition of Alt-R™ Electroporation Enhancer slightly improved the knockout levels in all tested molarity ratios, however the most dramatic improvement was observed when it was used in combination with the 1:0.4 gRNA: Cas9 molar ratio by bringing up the total knockout levels from 55% to 71%. Therefore, addition of EE could be helpful especially to improve gene editing when lower molar ratios have to be used. Similarly, I showed that targeting CD44 in VavP-Bcl2 Hoxb8-FL cells with another CD44 targeting RNP complex (CD44\_B) at 1:0.8 molarity ratio could generate more than 80% knockout cells (**Supplementary Figure 1c**). Furthermore, efficient ablation of CD44 by RNP electroporation could also be achieved in WT Hoxb8-FL cells (**Figure 3d**). In these cells, I also tested the effect of using different amounts of Cas9 protein on depletion efficiency while keeping the 1:0.8 gRNA: Cas9 molar ratio constant (**Figure 3d**). Depletion of CD44 was dependent on RNP dose used and in the absence of EE it reached the plateau at 1.5 uM Cas9. When EE was used together with RNPs, 0.75 uM Cas9 was also sufficient to generate the same ablation levels observed in higher Cas9 amounts. Overall, I could determine the optimal electroporation conditions for gene targeting in Hoxb8-FL cells and I demonstrated that efficient gene ablations could be achieved with the use of optimal gRNA to Cas9 ratios.

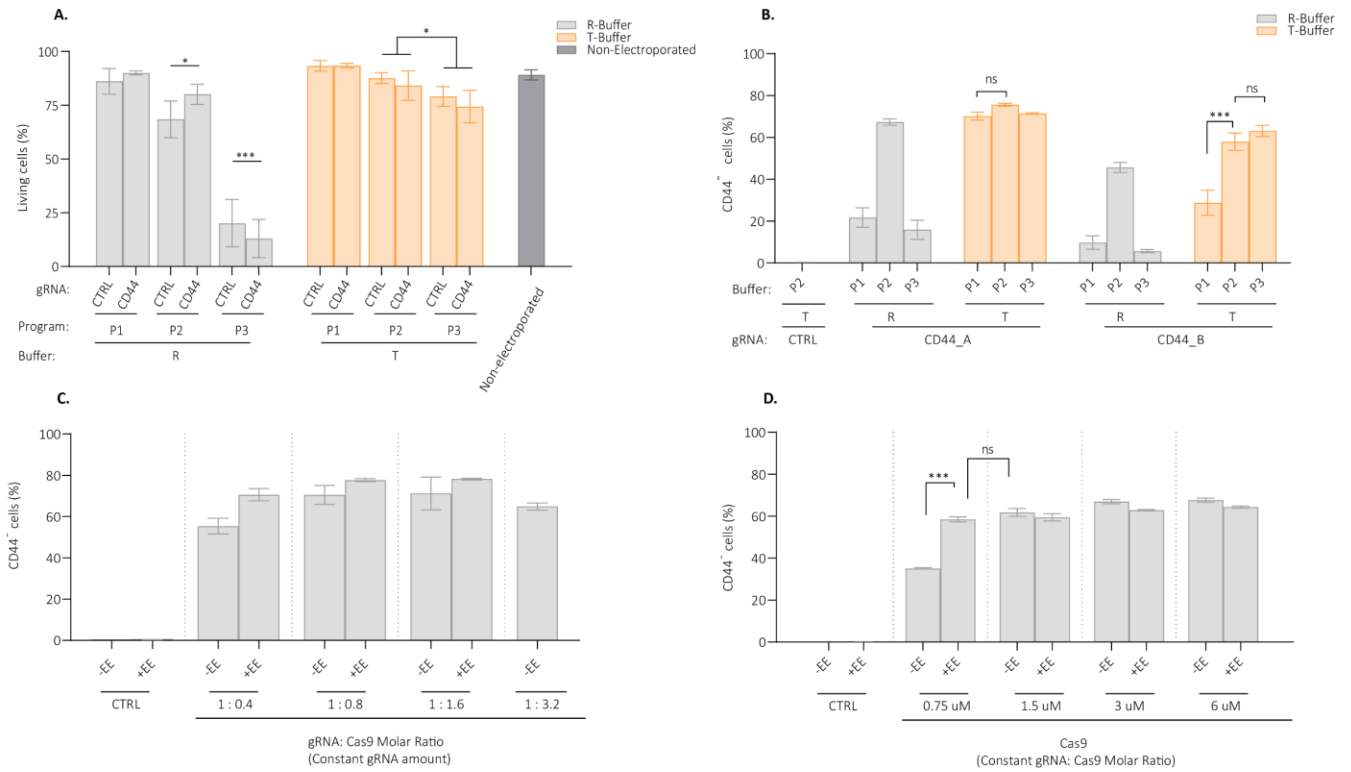


**Figure 3: Optimization of Hoxb8-FL electroporation conditions**

**A)** Flow cytometry–based viability (PF840) assessment in Cas9-GFP Hoxb8-FL cells; 48 hours after electroporation with control (LACZ) or CD44-targeting (CD44\_A, CD44\_B) crRNA:tracrRNA gRNA complexes (n=4, mean±SD). Dunnett’s multiple comparisons test comparing the control and CD44-targeted sample pairs of different conditions to non-electroporated cultured cells, and two-tailed Student’s t-test comparing P2 and P3 conditions of T buffer (\*P < 0.05, \*\*\*P < 0.001). **B)** Flow cytometry–based assessment of CD44 gene editing in Cas9-GFP Hoxb8-FL cells; 48 hours after electroporation with control (LACZ) or CD44-targeting (CD44\_A, CD44\_B) crRNA:tracrRNA gRNA complexes (n=2, mean±SD). Sidak’s multiple comparisons test comparing all conditions to each other (ns P > 0.05, \*\*\*P ≤ 0.001). **C)** Flow cytometry–based assessment of CD44 gene editing in VavP-Bcl2 Hoxb8-FL cells 4 days after electroporation with RNPs. Control (LACZ) or CD44-targeting (CD44\_A) RNPs were precomplexed at different gRNA:Cas9 molar ratios by keeping the gRNA amount used constant. Complexes electroporated into the cells in the presence or absence of the electroporation enhancer (EE) (n=2-5, mean±SD). Sidak’s multiple comparisons test comparing all conditions to each other (\*\*\*P ≤ 0.001). **D)** Flow cytometry–based assessment of CD44 gene editing in WT Hoxb8-FL cells 4 days after electroporation. Control (LACZ) or CD44-targeting (CD44\_A) RNPs were precomplexed in all reactions at 1:0.8 gRNA:Cas9 molar ratio. With increasing Cas9 amount, gRNA was also increased to keep the 1:0.8 ratio constant and RNPs were electroporated into the cells in the presence or absence of the electroporation enhancer (EE) (n=2, mean±SD). Sidak’s multiple comparisons test comparing all conditions to each other (ns P > 0.05, \*\*\*P ≤ 0.001).

Given the demand to target different loci at the same time in individual cells, I next tested the applicability of multiplexing by electroporating cells with two different RNPs. With this aim, I targeted CD44 and CD45 surface proteins in WT and VavP-Bcl2 Hoxb8-FL cells. RNPs targeting CD44 (CD44\_A) and CD45 (CD45) were complexed individually and electroporated either alone or together into cells using my optimized protocol and cells were analyzed by flow cytometry 2 days later. Singularly transfected cells efficiently generated CD44 or CD45 knockout Hoxb8-FL cells (VavP-Bcl2; 73% and 71% respectively) (WT; 69% and 84% respectively) (**Figure 4a-b**). In co-transfected cells, in addition to the detected single-knockout CD44 or CD45 populations, a

double knockout population was also identified in both cell lines (VavP-Bcl2; 40% and WT; 46%). Moreover, when two RNPs were provided together, the total editing ratios were not heavily affected and therefore it enabled to ablate multiple genes simultaneously with a high efficiency. Multiplexing can also serve to generate a pool of cells with three possible editing outcomes. I also tested the addition of EE in CD44 and CD45 multiplexing of VavP-Bcl2 Hoxb8-FL cells. Presence of EE improved the knockout efficiencies of single RNPs and this was also reflected in the co-transfection. Use of EE elevated the double knockout population from 40% to 52% and the total editing from 70% to 82% (**Supplementary Figure 1d**).

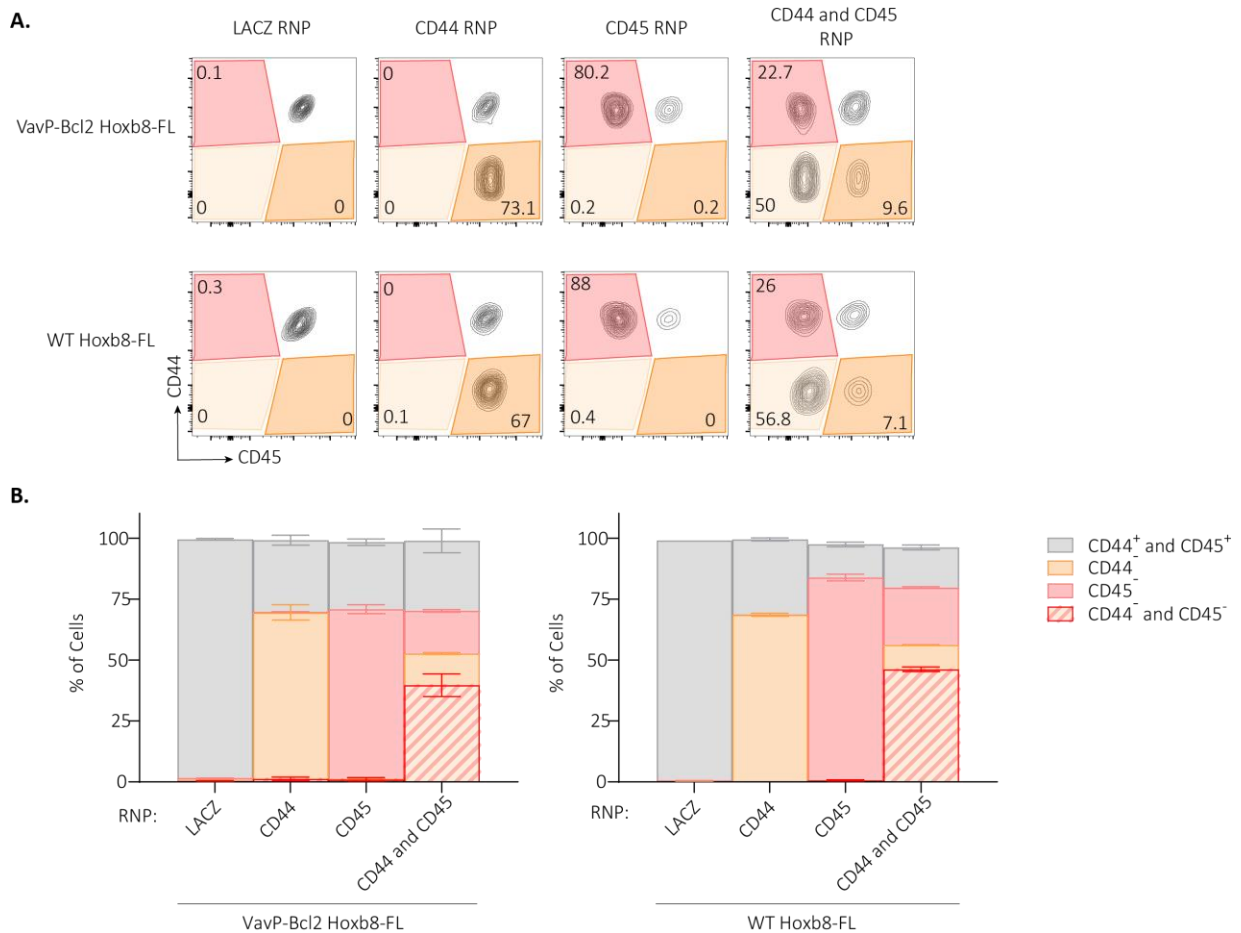


**Figure 4: Multiplexed gene knockout in Hoxb8-FL cells via RNP electroportation**

**A)** Representative FACS plots of CD44 and CD45 expression in VavP-Bcl2 Hoxb8-FL and WT Hoxb8-FL cells 2 days after electroportation with RNPs. Numbers indicate the percentages of the gated populations. Data are representative of 2 experiments. **B)** Flow cytometry-based assessment of CD44 and CD45 depletion in VavP-Bcl2 Hoxb8-FL and WT Hoxb8-FL cells 2 days after electroportation with RNPs. Control (LACZ), CD44-targeting (CD44\_A) or CD45-targeting (CD45) RNPs were precomplexed individually and electroportated into cells singularly or in combination (n=2, mean±SD).

In some experimental setups, uncoupling of sgRNA and Cas9 can provide flexibility as an alternative approach in gene targeting methods. For example, it was shown that human primary cells that are transduced with pooled sgRNA-expressing lentiviral libraries can be electroporated with non-targeting RNP complexes to enable efficient, genome-scale, functional CRISPR screens (even in the absence of genetically encoded Cas9-expression) by eliminating the need for the viral transduction of large Cas9 vectors (Ting et al., 2018). Electroporation of Cas9 as RNP (i.e., Cas9 precomplexed with a non-targeting sgRNA) into stably sgRNA-expressing cells was shown to significantly improve the editing efficiencies over Cas9 electroporation alone as it increased the overall Cas9 uptakes into cells in which eventually a guide-exchange (Guide Swap mechanism) took place before the final targeting. In this line, I tested whether Hob8FL cells which are transduced with retroviral sgRNA expression vectors would result in gene ablation upon Cas9 electroporation. After retroviral transduction of VavP-Bcl2 Hoxb8-FL cells with a CD44-targeting sgRNA expression plasmid carrying the THY1.1 reporter indicating infected cells, I electroporated cells either with Cas9 alone or with RNPs which were generated by complexing Cas9 together with different gRNAs (GFP, LACZ, CD44\_B). Electroporating the cells with Cas9 alone led to an average of 10% knockout in the infected (THY1.1<sup>+</sup>) cells. On the other hand, electroporating cells with non-targeting RNPs resulted in improved knockout efficiencies reaching over 40% in both gRNAs (**Figure 5a**). As non-homologous DNA sequences also enhance the uptake of Cas9 into cells, I reasoned that electroporating Cas9 together with the Alt-R™ Electroporation Enhancer into the sgRNA expressing cells might generate a similar effect on the editing levels as non-targeting RNP does. Indeed, cells that received Cas9 with electroporation enhancer resulted in 46% CD44 knockout levels which was highly comparable to non-targeting RNPs' editing levels. Interestingly, combination of non-targeting RNPs with the electroporation enhancer did not markedly further enhance the knockout frequencies. Overall, I showed that in constitutively sgRNA expressing Hoxb8-FL cells, gene ablation can be achieved by electroporating Cas9 protein and targeting levels can be increased by combining Cas9 with non-targeting gRNAs or EE.

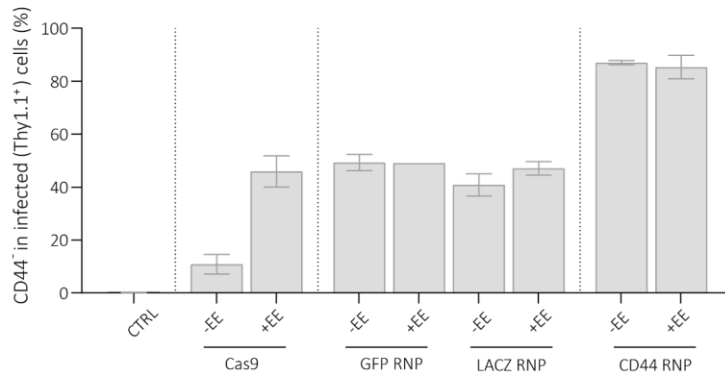


**Figure 5: Gene disruption in constitutively sgRNA-expressing Hoxb8-FL cells via Cas9 RNP-delivery**

Flow cytometry-based assessment of CD44 depletion in THY1.1<sup>+</sup> cells. VavP-Bcl2 Hoxb8-FL cells were retrovirally transduced with CD44-targeting sgRNA vector and electroporated with Cas9 or RNP in the presence or absence of electroporation enhancer. RNPs were generated by complexing Cas9 either with non-targeting gRNAs (GFP, LACZ) or with CD44-targeting gRNA (CD44\_B). Control cells are mock electroporated in the absence of Cas9/RNP. 7 days after electroporation, cells were analyzed by FACS, retrovirally infected gRNA-expressing cells were identified by expression of virus-encoded THY1.1. (GFP RNP+EE n=1, rest n =2-3, mean±SD)

### 3.1.2.3. Targeted Gene Knock-in in Hoxb8-FL Cells

My established CRISPR/Cas9 based knockout strategies in Hoxb8-FL cells can be very useful to conduct loss of function studies. However, I considered improving my gene-editing protocol further to introduce specific and precise alterations in the genomes of Hoxb8-FLs which could enable me to investigate the roles of particular mutations, to tag endogenous genes or to modify their genome with other inserted sequences. To do so, I employed Cas9-mediated homology-directed repair (HDR) induction; I electroporated cells with CRISPR components (i.e., gRNA/Cas9) for the generation of double-strand breaks in the targeted region and provided the repair templates via two different strategies.

A) In the first strategy, to make amino acid substitutions in targeted genes I used synthetically produced single-stranded donor oligonucleotides (ssODN) as repair templates and electroporated them together with the CRISPR components into cells. To enable rapid assessment of HDR-mediated point mutation induction in my system, initially I introduced a point mutation that is identifiable through flow cytometry: The conversion of the CD45.2 surface protein into the naturally occurring CD45.1 allelic variant by changing a single amino acid at position 302 (K<sup>302</sup> → E<sup>302</sup>) (Mercier et al., 2016). I electroporated Cas9-GFP Hoxb8-FL cells with a gRNA targeting CD45.2 (CD45.2) along with ssODN repair templates (CD45.1 ssODN\_1 or CD45.1 ssODN\_2) carrying the sequence for CD45.1 substitution. Then, I assessed the CD45.1

substitution by FACS analysis (**Figure 6a-b**). All samples which received a donor template had CD45.1<sup>+</sup> cells indicating for the successful HDR. With the use of 80 pmol ssODN-1 or ssODN-2 I detected in 9% and in 3% of the cells CD45.1 expression, respectively. Moreover, a further increase in the used donor template amount (to 160 pmol) did not improve the HDR levels. As next step, I tested the applicability of this approach in VavP-Bcl2 Hoxb8-FL cells which lack endogenous Cas9 expression. Previously, Glaser et al., established a GFP to BFP conversion assay to assess gene editing events in different cell lines (Glaser et al., 2016). I implemented this assay in VavP-Bcl2 Hoxb8-FL cells. First, I transduced cells with a retroviral GFP expression vector (pMIGR) and then electroporated them with the GFP-targeting RNP (GFP) along with ssODNs (BFP ssODN\_1 and BFP ssODN\_2) designed to convert GFP into BFP with a single amino acid substitution. Cells transfected with RNP and 80 pmol ssODN\_1 or ssODN\_2 resulted in ~13% and ~6% BFP<sup>+</sup> cells respectively; among those ~1% and ~0.5% had GFP signal in addition to the BFP, which most likely reflects partial gene conversion in cells carrying more than one retroviral integrations expressing GFP (**Figure 6c-d**). Similar to the CD45.2 to CD45.1 conversion, with the use of 160 pmol donor template I did not detect a further improvement in the HDR mediated knock-in efficiencies. Remarkably, I could FACS purify and culture BFP converted (i.e., BFP<sup>+</sup>-only or BFP<sup>+</sup> GFP<sup>+</sup> double-positive) VavP-Bcl2 Hoxb8-FL cells stably (**Figure 6c**).

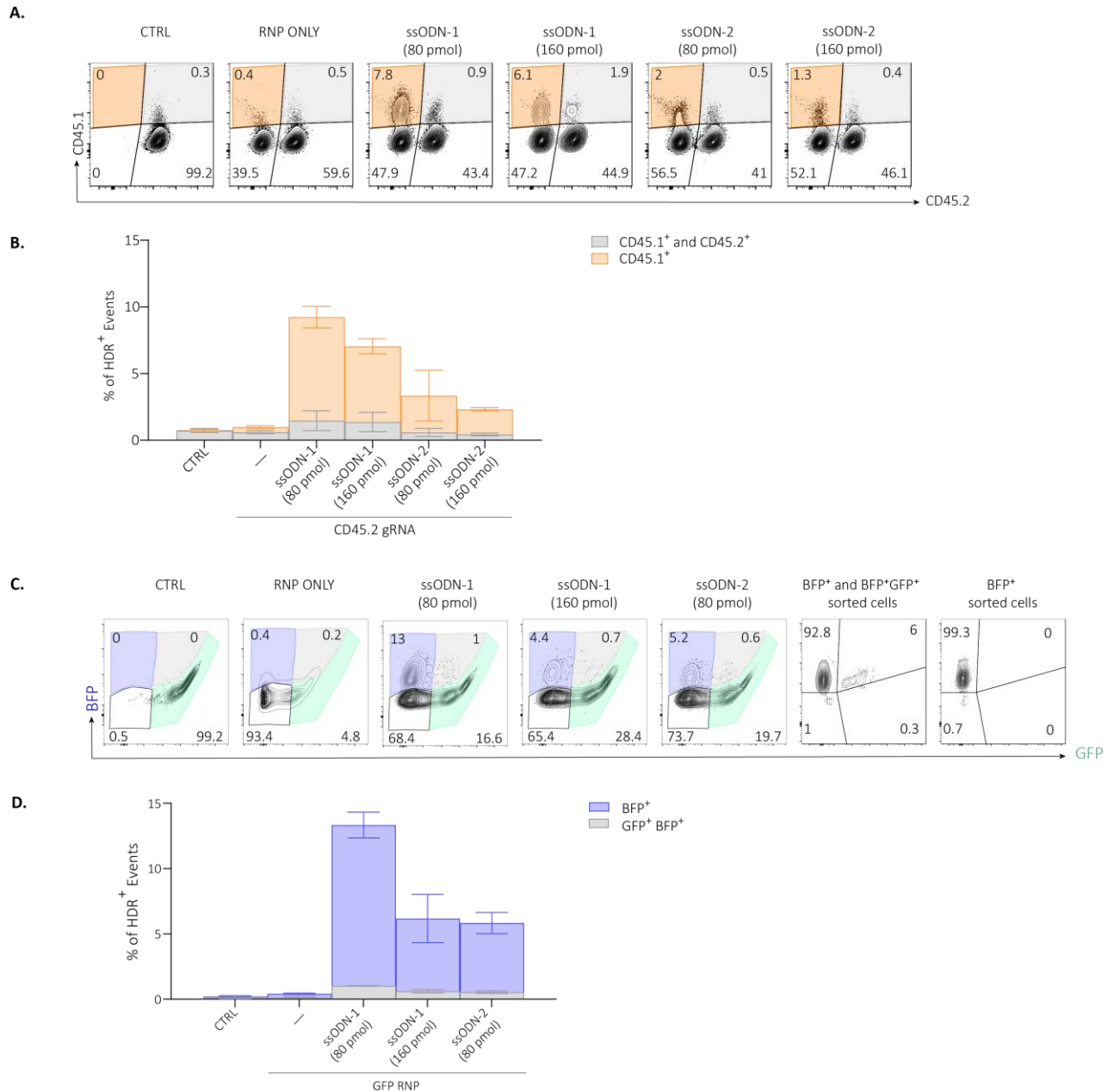


**Figure 6: Targeted introduction of CRISPR/Cas9-mediated point mutations in Hoxb8-FL cells**

**A)** Representative FACS plots of Cas9-GFP Hoxb8-FL cells electroporated with control (LACZ) or CD45.2-targeting (CD45.2) gRNA along with CD45.1 ssODN donor templates (CD45.1 ssODN<sub>1</sub> and CD45.1 ssODN<sub>2</sub>) for conversion of CD45.2 allelic variant into CD45.1 variant by a single amino acid substitution. 80 pmol and 160 pmol ssODN templates were tested for both templates. Cells were analyzed 5 days after the electroporation. Numbers indicate the percentages of the gated populations. Data are representative of 3 experiments. **B)** Flow cytometry-based assessment of CD45.2 to CD45.1 conversion in Cas9-GFP Hoxb8-FL cells 5 days after the electroporation with control (LACZ) or CD45.2-targeting (CD45.2) gRNA along with CD45.1 ssODN donor templates (CD45.1 ssODN<sub>1</sub> and CD45.1 ssODN<sub>2</sub>). 80 pmol and 160 pmol of ssODN were tested for both templates. (n=2-3, mean±SD). **C)** Representative FACS plots of VavP-Bcl2 Hoxb8-FL cells which were transduced with GFP-expressing retroviral plasmid pMIGR and electroporated with control (LACZ) or GFP targeting (GFP) RNP along with BFP ssODN-donor templates (BFP ssODN<sub>1</sub> and BFP ssODN<sub>2</sub>) for conversion of GFP into BFP by a single amino acid substitution. Cells were transduced with pMIGR and GFP<sup>+</sup> cells were sorted. 5 days after the electroporation cells were analyzed by FACS. 13 days after electroporation, BFP<sup>+</sup> or BFP<sup>+</sup>GFP<sup>+</sup> double positive VavP-Bcl2 Hoxb8-FL cells were FACS-sorted. Numbers indicate the percentages of the gated populations. Data are representative of 2 experiments. **D)** Flow cytometry-based assessment of the GFP to BFP conversion in GFP<sup>+</sup> VavP-Bcl2 Hoxb8-FL cells 5 days after the electroporation with control (LACZ) or GFP-targeting (GFP) RNP along with BFP ssODN donor templates (BFP ssODN<sub>1</sub> and BFP ssODN<sub>2</sub>). 80 pmol and 160 pmol of ssODN were tested for BFP ssODN<sub>1</sub> template, while only 80 pmol of ssODN was tested for BFP ssODN<sub>2</sub> template. (n = 2, mean±SD).

B) Having established a system for the induction of small substitutions in the genome of Hoxb8-FL cells by the use of ssODN templates, I developed a second strategy for bringing larger repair templates that can introduce longer DNA sequences into these cells. In my second approach for bringing the repair template into the RNP electroporated cells, I benefited from the single-stranded genome of the adeno-associated viruses (AAV) whose cargo size (~4.7 kb) can allow integration of longer DNA sequences into the targeted genes during homologous recombination. Previously Tran and colleagues showed that recombinant adeno-associated virus (rAAV)-DJ donor templates can efficiently generate gene knock-ins in mouse HSPCs when used in combination with RNPs (Ngoc Tung Tran et al., 2019). They showed that ~20% of mouse HSPCs' *Actb* locus could be modified through the integration of T2A-BFP fluorescence tag via electroporation of an ACTB targeting RNP along with the infection of the recombinant AAV-DJ repair template including the BFP-tag sequence (rAAV-DJ-Actb). When I utilized this setup in VavP-Bcl2 Hoxb8-FL cells to target the last exon of mouse *Actb*, I could successfully bring the T2A-BFP tag into the 3'UTR of the gene by infecting cells with the rAAV-DJ-Actb virus after ACTB RNP electroporation (**Figure 7a-b**). With the use of the template at a multiplicity of infection (MOI) of  $10^7$  virus genome copies (GCs) per cell, ~17% of cells were identified as BFP<sup>+</sup> 2 days after the treatment. Use of a MOI of  $4 \times 10^7$  virus GC/cell did not further improve the HDR mediated knock-in in the cells. Successful insertion of the T2A-BFP (~0.8 kb) tag in the *Actb* locus was also verified via PCR on the genomic DNA; in the presence of the targeting RNP and the viral repair template a shift from the WT amplicon (1.8 kb) to the higher size (2.1 kb) was identified indicating the successful targeted insertion (**Figure 7c**). Overall, with these experiments I showed that targeted precise alterations can be efficiently achieved in Hoxb8-FL cells using different alternative methods.

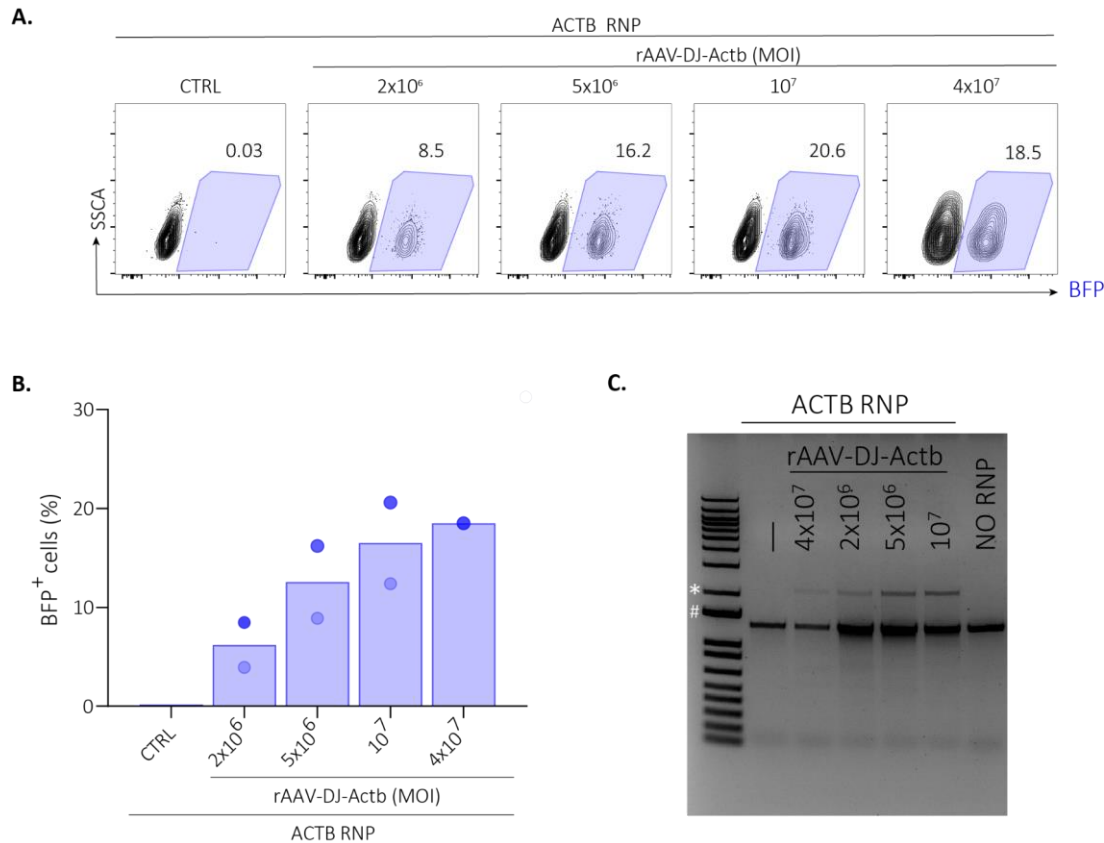


**Figure 7: CRISPR/Cas9 and AAV-mediated targeted gene knock-in in VavP-Bcl2 Hoxb8-FL cells**

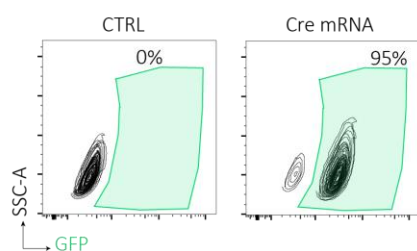
**A)** Representative FACS plots of VavP-Bcl2 Hoxb8-FL cells electroporated with Actb-targeting (ACTB) RNP and infected with rAAV-DJ-Actb donor for the insertion of a ~0.8 kb T2A-BFP tag into the *Actb* locus. Following the electroporation of (ACTB) RNP into cells, cells were infected with rAAV-DJ-Actb donor at the MOI of  $2 \times 10^6$ ,  $5 \times 10^6$ ,  $10^7$ ,  $4 \times 10^7$  GC/cell and 2 days later BFP<sup>+</sup> cells were identified by FACS. Numbers indicate the percentages of the gated populations. Data are representative of 2 experiments (for MOI  $4 \times 10^7$  n=1, rest n=2). **B)** Flow cytometry-based assessment of T2A-BFP insertion in *Actb* locus of VavP-Bcl2 Hoxb8-FL cells. Darker blue circles represent the samples depicted in Figure 7a. (For MOI  $4 \times 10^7$  n=1, rest n=2). **C)** Agarose gel electrophoresis of PCR amplicons covering the *Actb* targeted region in cells. Wild-type (WT) and/or NHEJ amplicons are expected to be at 1.3 kb size and HDR mediated insertion amplicon is at 2.1 kb size. # corresponds to 1.5 kb and \* corresponds to 2 kb band in the DNA ladder.

### 3.1.2.4. *In vitro* Cre/loxP-Mediated Recombination in Hoxb8-FL Cells

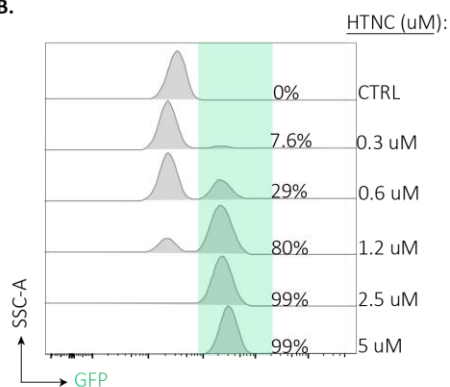
Cre/loxP-mediated conditional gene targeting allows investigating the roles of induced alterations in certain cell types, at defined developmental stages. To benefit of this control in my experiments, I generated several Hoxb8-FL lines carrying the elements of the Cre/loxP system. For example, to activate Cas9 expression in BCL2-overexpressing GCB cells I generated the VavP-Bcl2 Cy1cre LSL-Cas9-GFP Hoxb8-FL line. However, besides having the advantage to induce alterations *in vivo* at particular developmental stages using these cell lines, I considered having the option to bring alterations *in vitro* already in the progenitor state as this could enable alternative approaches to answer questions related to the timing of induced alterations. With

this aim, for the *in vitro* recombination activation in my cell lines, I tested electroporation of cells with an mRNA encoding Cre recombinase protein (Cre-mRNA) or transduction of cells with the histidine-tagged Cre recombinant protein containing a nuclear localization signal in addition to the basic TAT peptide integral to Cre (His-TAT-NLS-Cre, HTNC) (Van den Plas et al., 2003) (Peitz et al., 2002). Electroporation of VavP-Bcl2 LSL-Cas9-GFP cells with 0.5 ug Cre-mRNA resulted in 95% of GFP<sup>+</sup> cells, indicating an efficient Cre-mediated loxP recombination and stop cassette deletion (**Figure 8a**). Similarly, HTNC transduction of these cells led to an average of 99% loxP-site excision with a dose of 2.5 uM (**Figure 8b-c**). Therefore, by both Cre mRNA electroporation and Cre protein transduction, I could efficiently recombine loxP-flanked gene segments in Hoxb8FL cells.

**A.**



**B.**



**C.**

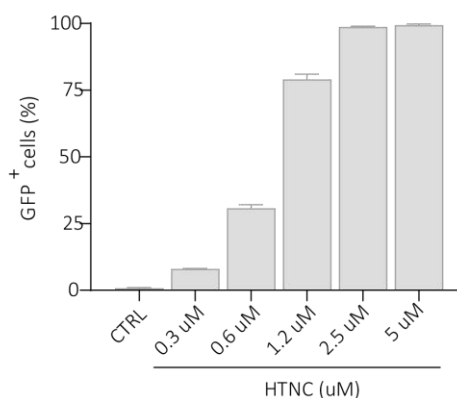


**Figure 8: *In vitro* Cre-mediated excision of the loxP-flanked stop cassette in VavP-Bcl2 LSL-Cas9-GFP Hoxb8-FL cells**

**A)** Representative FACS plots of VavP-Bcl2 LSL-Cas9-GFP Hoxb8-FL cells that were mock or Cre-mRNA electroporated. 2 days after the electroporation, cells were analyzed by FACS for GFP expression resulted by the Cre-mediated stop cassette deletion. Data are representative of 3 experiments. Numbers indicate the percentages of the gated populations. **B)** Representative FACS plot of VavP-Bcl2 LSL-Cas9-GFP Hoxb8-FL cells that were mock or HTNC transduced. 2 days after the transduction of cells with varying HTNC molarities, cells were analyzed by FACS for GFP expression resulted by the Cre-mediated stop cassette deletion. Data are representative of 2 experiments. **C)** Flow cytometry-based assessment of GFP expression resulted by Cre-mediated stop cassette deletion after transduction of VavP-Bcl2 LSL-Cas9-GFP Hoxb8-FL cells with HTNC at varying molarities. (n=2, mean ±SD).

## 3.2. Targeting GC Derived Lymphoma-Associated Tumor Suppressor Genes in Hoxb8-FL Cells

### 3.2.1. Targeting Histone-lysine N-methyltransferase 2D (KMT2D)

The Histone-lysine N-methyltransferase 2D (*KMT2D*), one of the highly mutated FL driver genes identified by whole-genome sequencing of human FL and tFL samples (Okosun et al., 2014), was shown to contribute to lymphoma development when inactivated with shRNAs in BCL2-overexpressing fetal liver HSPCs-reconstituted mice (Ortega-Molina et al., 2015). Since the inactivation of KMT2D is reported to be a recurrent event (in ~80% of FL cases), in my effort to generate transplantable FL progenitor clones, I wanted to target KMT2D with CRISPR in VavP-Bcl2 Hoxb8-FL cells. With this purpose, initially I designed several sgRNAs targeting the open reading frame of the gene spreading between early and late exons (**Figure 9a**). Then to identify high-performing sgRNAs I determined the indel efficiencies of sgRNAs by TIDE in ubiquitously Cas9-expressing sgRNA vector transduced cells (**Figure 9b**). Because of its large genomic size (39.5 kb, 55 exons, 19.8 kb CDS), I utilized a multiplexing approach to inactivate the gene by inducing locus deletions. sgRNAs targeting the early, mid, and late exons of *Kmt2d* were combined in pairs to make deletions ranging from ~3 kb to ~31 kb. These deletions were identified by a PCR-based strategy in which two different primer pairs for each combination were used to amplify the genomic DNA of cells (**Figure 9a**). In this strategy, one primer pair (out-PCR) was designed external to the deletion region, therefore allowing to amplify DNA resulting from the deletion and the other primer pair (in-PCR) was designed internal to the deleted region, to detect DNA that is intact or carries indels separately induced by the two sgRNAs. Following the cloning of sgRNAs in pairs into the pSB2 multiplexing retroviral vector, Cas9-GFP Hoxb8-FL cells were transduced and selected with puromycin (**Figure 9c**). Genotyping PCR analysis of their genomic DNA revealed that all KMT2D-targeting sgRNA combinations resulted in the expected deletion-amplicons, whereas control sgRNA transduced cells were free of these deletion-amplicons (**Figure 9d**). Similarly, I used my established RNP-multiplexing approach to engineer *Kmt2d* deletions into the VavP-Bcl2 Hoxb8-FL cells lacking endogenous Cas9 expression. After electroporation of cells with the KMT2D-targeting RNP pairs, genotyping PCRs were performed to identify deletions (**Figure 10a**). In all tested RNP combinations, including targeted deletions

reaching up to 31 kb in size, I detected deletion-amplicons showing efficient RNP multiplexing in Hoxb8-FL cells (**Figure 10b**). Furthermore, I also generated single-cell derived clones from these electroporated cells and identified mono-allelic or biallelic deletions by my PCR-based screening strategy (**Figure 10c**). Among the screened clones of the 12 kb deletion, 10% had bi-allelic and 25% carried mono-allelic deletions (**Figure 10d**). Subsequent sanger-sequencing of the deletion amplicons of bi-allelic single-cell clones which were generated from 12 kb or 31 kb targeting provided me with sequences of the deletion events (**Supplementary Figure 2a-c**).

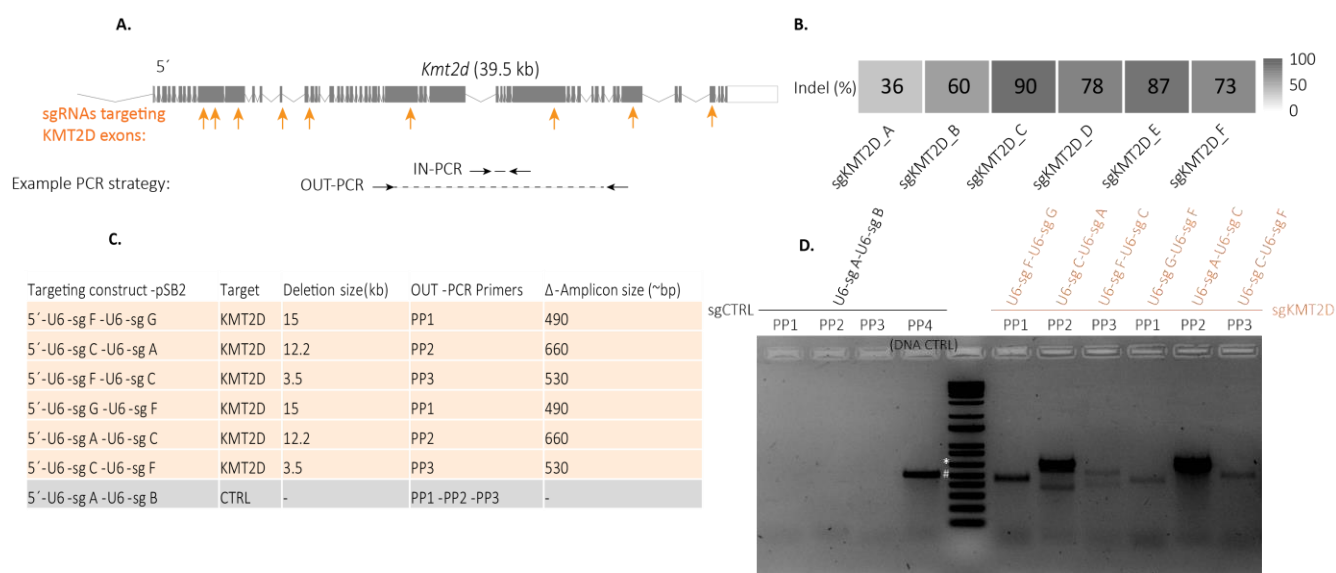


**Figure 9: Targeting KMT2D in Hoxb8-FL cells by CRISPR/Cas9**

**A)** Schematic diagram of the mouse *Kmt2d* genomic locus (Ensembl) and PCR-based identification strategy of induced deletions by CRISPR/Cas9-multiplexing. sgRNAs were designed over the coding sequence and used in pairs to generate locus deletions. To identify targeted deletions in the region, a PCR-based approach was applied. Amplicon resulting from genomic deletions were detected using two primers designed outside of the two sgRNAs (out-PCR), while intact loci or loci harboring only individual indels were detected using primers designed between the two sgRNAs (in-PCR). **B)** Editing efficiencies of some sgRNAs targeting the coding regions of *Kmt2d*. Cas9-expressing cells were transduced with retroviral vectors expressing KMT2D-targeting sgRNAs (sgKMT2D\_A to sgKMT2D\_F), then selected with puromycin, and 20 days after the transduction editing levels were assessed by the TIDE assay. Insertion and deletion (indel %) efficiencies of sgRNAs are represented as means. Indel data are derived from 3-8 TIDE experiments. **C)** Multiplexing set-up to generate genomic deletions in the *Kmt2d* locus of Cas9-GFP Hoxb8-FL cells. Control sgRNAs (Here sgCTRL\_A and sgCTRL\_B depicts sgLACZ and sgGFP) or KMT2D-targeting sgRNAs (sgKMT2D\_A, sgKMT2D\_C, sgKMT2D\_F, sgKMT2D\_G) were cloned as pairs into the retroviral multiplexing plasmid pSB2 in two different positions for each combination. Based on the sgRNA combination used, the sizes of the expected genomic deletions were calculated. Using the indicated out-PCR primers the sizes of amplicons resulting from deletions ( $\Delta$ ) were determined. **D)** Representative gel image of the out-PCRs identifying the multiplexed *Kmt2d* deletions in bulk Cas9-GFP-Hoxb8 FL cells. Cells were transduced with the pSB2 retroviral vectors carrying the indicated sgRNA combinations and then selected with puromycin followed by genotyping-PCRs 15 days after transduction. PP1, PP2, PP3 primer pairs were used for out-PCRs and the PP4 primer pair was used as DNA control for the control sample. # corresponds to the 500 bp-band and \* corresponds to the 650 bp-band in the ladder. Data are representative of 3 experiments.

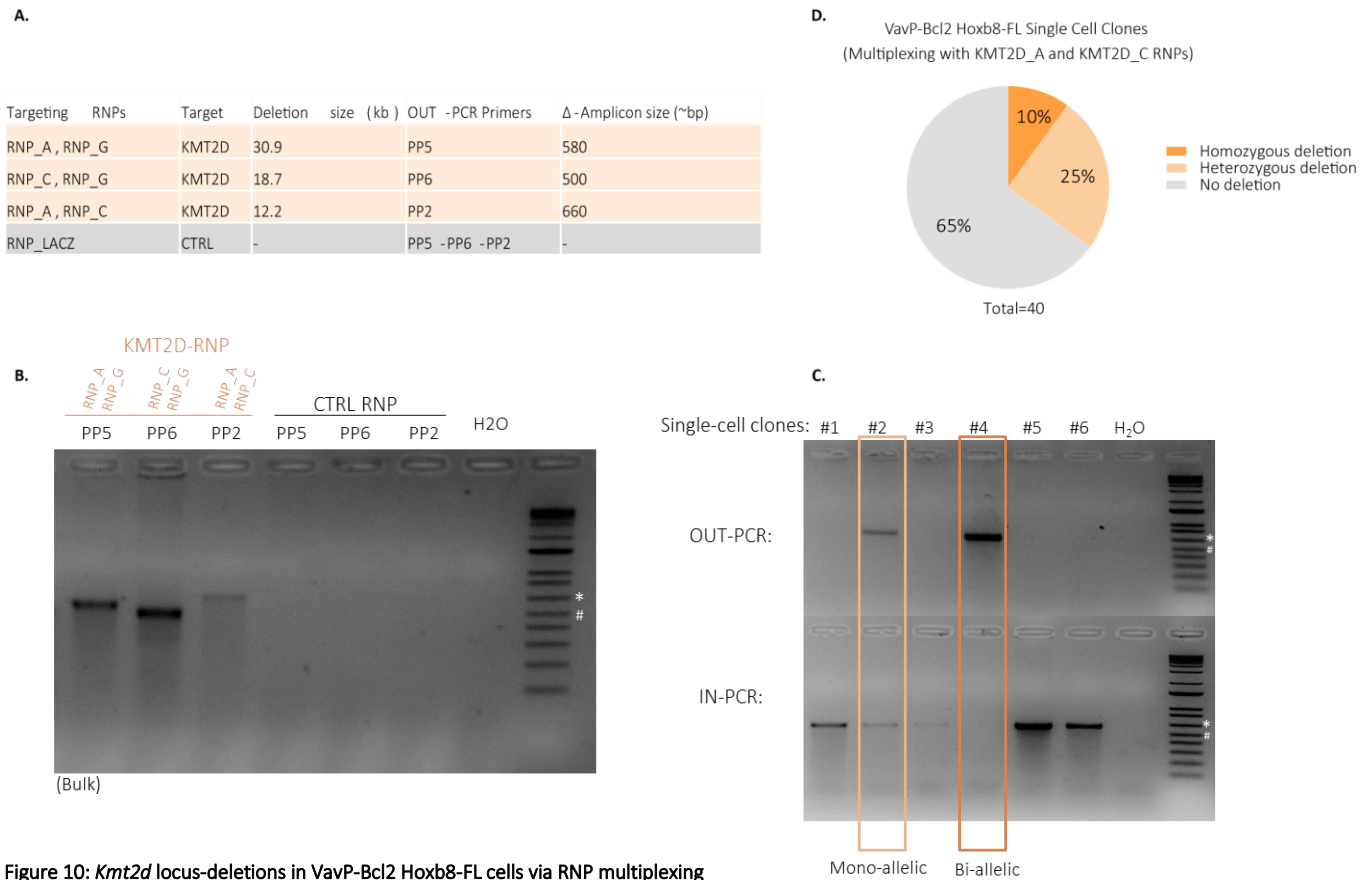


**Figure 10: *Kmt2d* locus-deletions in VavP-Bcl2 Hoxb8-FL cells via RNP multiplexing**

**A)** Multiplexing set-up to generate deletions in the *Kmt2d* locus of VavP-Bcl2 Hoxb8-FL cells by RNP electroporation. For targeted deletions ranging from ~12 kb to ~31 kb indicated RNP pairs (Control (LACZ) or KMT2D-targeting (KMT2D\_A, KMT2D\_C, KMT2D\_G) RNPs) were used. Using the corresponding out-PCR primers, the sizes of amplicons resulting from deletions ( $\Delta$ ) were determined. **B)** Representative gel image of out-PCRs identifying the RNP targeted *Kmt2d* deletions in bulk VavP-Bcl2 Hoxb8-FL cells. Cells were electroporated with indicated RNP combinations, and genotyping PCRs were performed four days later. PP5, PP6, PP2 primer pairs were used for out-PCRs. # corresponds to the 500 bp-band and \* corresponds to the 650 bp-band in the ladder. Data are representative of 2 experiments. **C)** Representative gel images of in- and out-PCRs identifying the *Kmt2d* deletions in VavP-Bcl2 Hoxb8-FL single-cell clones that were isolated from the bulk cells electroporated with KMT2D\_A and KMT2D\_C RNPs (12 kb deletion). After combined electroporation of two RNPs, cells were serially diluted in 96-well plate. Single-cell derived clone's deletion status (mono-allelic, bi-allelic, none) were determined with in- and out-PCRs. For out-PCR, primer pair PP2; for in-PCR, primer pair PP7 were used. **D)** Pie chart summarizing the frequency of monoallelic and bi-allelic deletion events in the *Kmt2d* locus of screened single-cell VavP-Bcl2 Hoxb8-FL clones multiplexed with KMT2D\_A and KMT2D\_C RNPs.

### 3.2.2. Targeting Herpes Virus Entry Mediator (HVEM)

Another gene highly mutated in follicular lymphoma is Herpes Virus Entry Mediator (HVEM), also known as *TNFRSF14*. HVEM is an immune receptor whose inactivation was shown to accelerate experimental lymphoma progression in mice. HVEM-deficient murine lymphoproliferations display microenvironment reprogramming very similar to that observed in FL patients carrying HVEM mutations (Boice et al., 2016). I aimed to inactivate this gene in my Hoxb8-FL system to assess its role in disease development. To this end, I designed sgRNAs against *HVEM* (sgHVEM\_A, sgHVEM\_B) and cloned them into retroviral sgRNA expression vectors co-expressing the THY1.1

reporter. Then, VavP-Bcl2 LSL-Cas9-GFP cells which were electroporated with Cre-mRNA to induce ubiquitous Cas9 expression, were transduced with these vectors. FACS analysis of THY1.1<sup>+</sup> GFP<sup>+</sup> VavP-Bcl2 Hoxb8-FL cells showed that both sgRNAs resulted in the loss of HVEM in ~66 % of cells, indicating the successful CRISPR targeting of the gene (**Figure 11**).

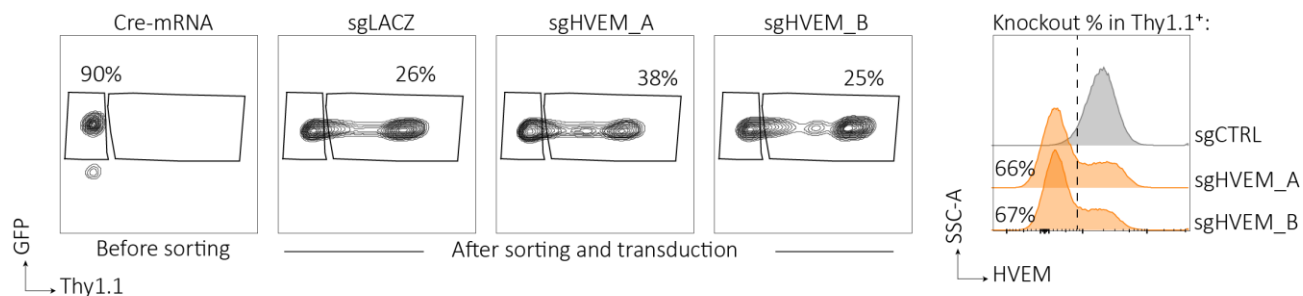


**Figure 11: Targeting HVEM in VavP-Bcl2 Cas9-GFP Hoxb8-FL cells by CRISPR/Cas9**

Representative FACS plots of VavP-Bcl2 Cas9-GFP Hoxb8-FL cells transduced with control (sgLACZ) or HVEM-targeting (sgHVEM\_A and sgHVEM\_B) retroviral sgRNA-expression vectors. VavP-Bcl2 LSL-Cas9-GFP Hoxb8-FL cells were electroporated with Cre-mRNA and GFP<sup>+</sup> cells were purified by FACS. Sorted VavP-Bcl2 Cas9-GFP Hoxb8-FL cells were transduced with sgRNA-expressing retroviral vectors carrying the THY1.1 reporter. 15 days later cells were analyzed by FACS. HVEM expression in THY1.1<sup>+</sup> cells is depicted in the histograms on the right. Data are representative of 2 experiments. Numbers indicate the percentages of the gated populations.

### 3.2.2. Combining KMT2D and HVEM Targeting with Insertional Mutagenesis for Hoxb8-FL Based Genetic Screens

I reasoned that early driver mutations of FL including KMT2D and HVEM can be combined in my progenitor cell lines to investigate the nature of serially acquired subsequent mutations and their associations with the founder mutations during the progression of the disease. With this aim, I targeted KMT2D and HVEM in my VavP-Bcl2 CD19cre LSL-PB ATP Hoxb8-FL lines, which entails the possibility to introduce unbiased genetic perturbations in B cells in addition to the *in vitro*-induced inactivating founder mutations in KMT2D and HVEM. In this regard, I co-electroporated VavP-Bcl2 CD19cre LSL-PB ATP Hoxb8-FL cells with KMT2D and HVEM targeting RNP complexes (**Figure 12a**). To check indel efficiencies I amplified targeted regions by PCR and analyzed them by TIDE after sanger sequencing (**Figure 12b**). Targeting KMT2D with the KMT2D\_A RNP resulted in a ~77% indel ratio. However, half of the described indels were 3 bp insertion events (**Figure 12b**), which might not lead to the loss of protein as the addition of a

single amino acid may not suffice to inactivate KMT2D. KMT2D\_C RNP electroporation resulted in ~51% indel ratio and an indel spectrum comprising several alterations that could result in knockout of the protein. The co-electroporated HVEM\_A RNP resulted in about 20% and 13% indel ratios in both combinations. The quantification of HVEM surface levels on these cells by FACS loss of surface HVEM in 19% and 17% of the cells, respectively (**Figure 12c**). Transplantation of these bulk engineered Hoxb8FL cells into recipient animals will allow me to experimentally address clonal evolution in lymphoma cells by enabling clones with different mutational signatures to compete *in vivo* and to be selected for carrying synergistically advantageous combinations with an outgrowth potential during lymphomagenesis.

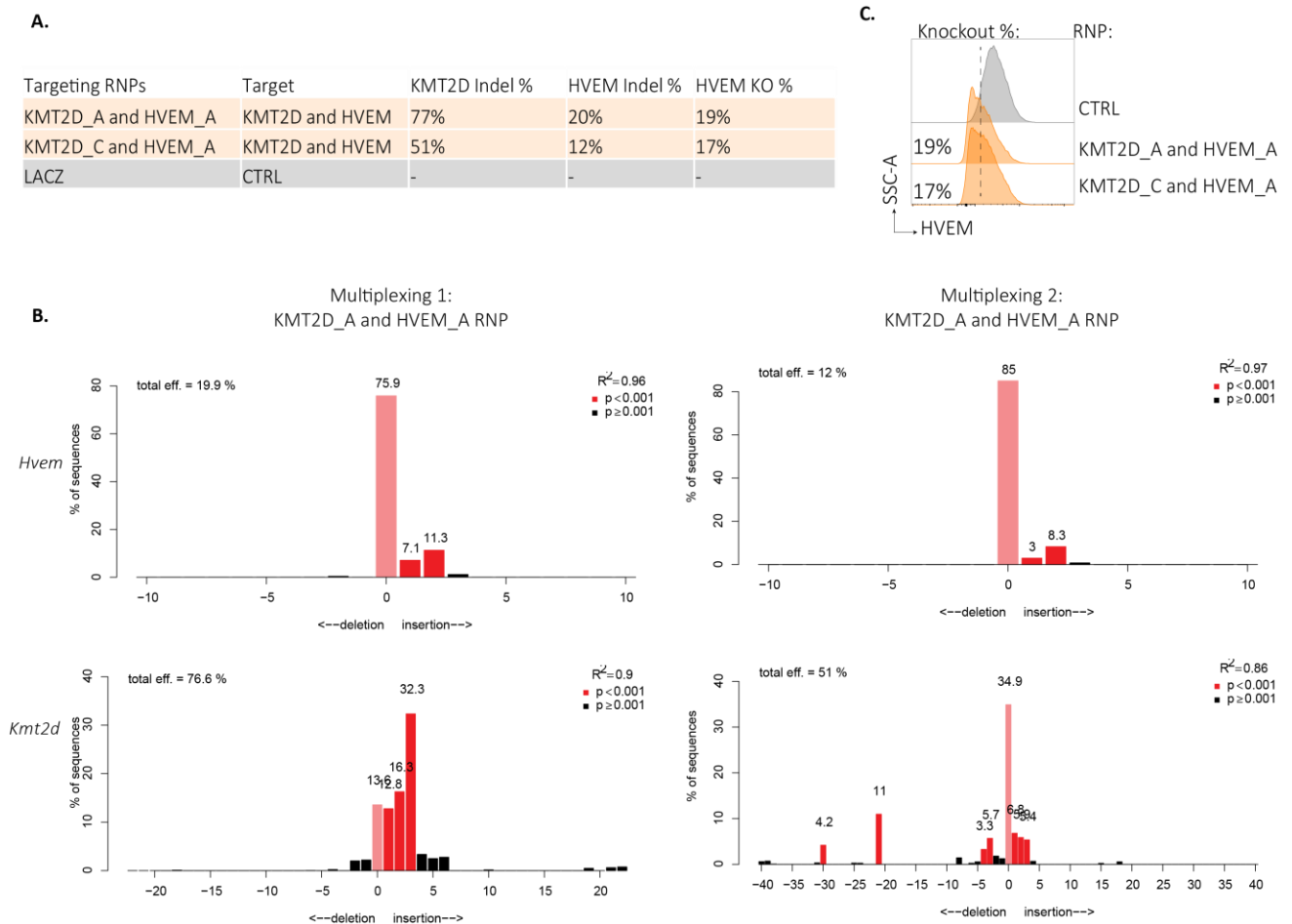


**Figure 12: Targeting KMT2D and HVEM in VavP-Bcl2 CD19cre LSL-PB ATP Hoxb8-FL cells via RNPs**

**A)** Multiplexing set-up to target KMT2D and HVEM in VavP-Bcl2 CD19cre LSL-PB ATP Hoxb8-FL cells via RNPs. Cells electroporated with control (LACZ) or KMT2D (KMT2D\_A, KMT2D\_C) and HVEM (HVEM\_A) RNPs were analyzed by TIDE to determine indel ratios. For the assessment of HVEM knockout levels, cells were also analyzed by FACS. **B)** TIDE results showing the indel spectrum and frequencies in corresponding locus regions of targets. **C)** FACS plots of HVEM expression in control and multiplexed RNP-treated cells 4 days after the electroporation.

### 3.3. *In vivo* Use of VavP-Bcl2 Hoxb8-FL Cells for the Investigation of Regulators of GCB cells and GC derived lymphomas

#### 3.3.1. Establishment of VavP-Bcl2 Hoxb8-FL Adoptive Transfer System to Study Regulators of GCB cells

My ultimate goal was to develop mature, germinal center derived B-cell lymphoma models allowing the investigation of novel immune-cell regulators *in vivo* using functional genomics. With this aim, I first generated several Hoxb8-FL progenitor cell lines from the VavP-Bcl2 transgenic mouse strain since VavP-Bcl2 mice display germinal center hyperplasia and can develop follicular lymphoma. For *in vivo* reconstitution experiments, I modified the Hoxb8-FL adoptive transfer protocol (Redecke et al., 2013) by transplanting VavP-Bcl2 Hoxb8-FL progenitor cells into lethally irradiated mice in the presence of unfractionated B-cell deficient bone marrow cells. I reasoned that using B-cell deficient bone marrow supportive cells could improve the engraftment and maybe also the long-term sustainability of Hoxb8-FL-derived B cells in recipient mice by eliminating the competition of B cells that are continuously produced from the bone marrow hematopoietic stem cells (**Figure 13a**). To determine mature hematopoietic cells that had differentiated from the injected VavP-Bcl2 Hoxb8-FL cells, I analyzed peripheral blood of the transplanted mice by FACS using a human-BCL2 (hBCL2) specific antibody. 10 days after the transfer, VavP-Bcl2 Hoxb8-FL derived hBCL2<sup>+</sup> myeloid and B cells were detected in the blood, composing 37±13% and 51±13% of all lymphocytes respectively (**Figure 13b-c**). Importantly, all detected B cells displayed hBCL2 expression indicating the efficient clearance of endogenous B cells from the recipient mice by lethal irradiation and the tight B-cell deficiency of the co-injected supportive bone marrow cells. In addition to B220, peripheral hBCL2<sup>+</sup> B cells also expressed CD19 and IgM demonstrating the successful completion of B cell maturation steps (**Figure 13d**). By day 20, VavP-Bcl2 Hoxb8-FL derived myeloid cells were highly decreased in the blood (4±4%), on the other hand, hBCL2<sup>+</sup> B cells were still detected at high ratios (53±14%). Peripheral blood T cells expressing human Bcl2 were observed only in later analysis time points. Of note, among the four independent VavP-Bcl2 Hoxb8-FL lines transplanted, Line-2 reconstituted animals had up to 9% hBCL2<sup>+</sup> T cells in the blood by d70,

whereas Line-1 only had a maximum of 1.5%, indicating possible line-specific lineage-potential differences. A similar difference was observed in Line-3's B-cell reconstitution capacity, which resulted in significantly reduced B cell proportions after the transplantation compared to other tested lines (**Figure 13c, Supplementary Figure 3a**).

Since follicular lymphoma is an indolent disease, the maintenance of Hoxb8-FL-derived B cells in transplanted animals for extended periods of time would be highly desirable. I therefore tracked persistence of B cells in the blood of aged transplanted mice and found that hBCL2<sup>+</sup> B cells were still detectable 7 months after the transfer with similar percentages to the initial time points of the reconstitution (**Figure 13e**).

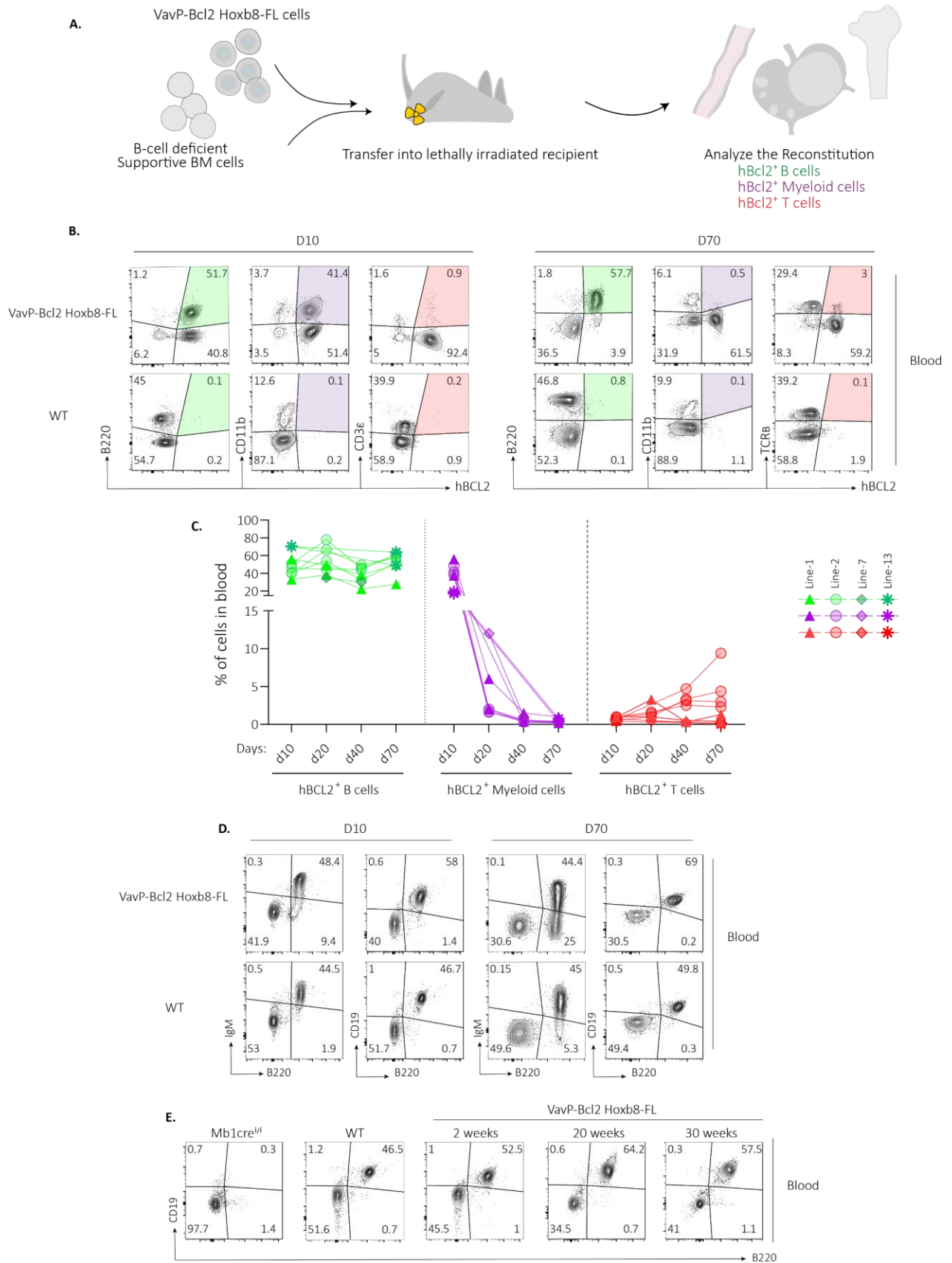


Figure 13: Adoptive transfer of VavP-Bcl2 Hoxb8-FL cells into irradiated recipient mice

**Figure 13: Adoptive transfer of VavP-Bcl2 Hoxb8-FL cells into irradiated recipient mice**

**A)** Experimental scheme of adoptive transfer of VavP-Bcl2 Hoxb8-FL cells together with unfractionated B-cell deficient bone marrow cells into lethally irradiated mice. **B)** Representative FACS plots of human BCL2 (hBCL2) expression in peripheral blood of lethally irradiated mice transplanted with VavP-Bcl2 Hoxb8-FL cells (10 and 70 days after transplantation). Samples are pregated on CD45.2<sup>+</sup> cells. Numbers in quadrants indicate percentages. Plots are representative of the data obtained from nine mice transferred with one of the four independent VavP-Bcl2 Hoxb8-FL cell lines (Line-1, Line-2, Line-7, Line-13). Line-2 day 10 and day 70 are depicted. Data are representative of 3 experiments. **C)** Percentage of hBCL2<sup>+</sup> B (B220<sup>+</sup>), myeloid (CD11b<sup>+</sup>) and T (CD3ε<sup>+</sup>/TCRβ<sup>+</sup>) cells over time in the peripheral blood of lethally irradiated mice transplanted with VavP-Bcl2 Hoxb8-FL cells. Samples are pregated on CD45.2<sup>+</sup> cells. (n=9, four independent VavP-Bcl2 Hoxb8-FL cell lines were transplanted: Line-1, Line-2, Line-7, Line-13). Data are representative of 3 experiments. **D)** Representative FACS plots of CD19, B220 and IgM expression on CD45.2<sup>+</sup> cells in the peripheral blood of lethally irradiated mice transplanted with VavP-Bcl2 Hoxb8-FL cells (10 and 70 days after the transplantation). Numbers in quadrants indicate percentages. Plots are representative of the data obtained from mice transplanted with one of the two independent VavP-Bcl2 Hoxb8-FL cell lines (Line-1 and Line-2). Line-2 day 10 and day 70 are depicted. Data are representative of 3 experiments (n=13). **E)** Representative FACS plots of CD19 and B220 expression over the time in the peripheral blood of lethally irradiated mouse transplanted with VavP-Bcl2 Hoxb8-FL cells. Numbers in quadrants indicate percentages. Plots are representative of the data obtained from mice transferred with one of the five independent VavP-Bcl2 Hoxb8-FL cell line (Line-1, Line-2, Line-3, Line-6, Line-7) (n=8-19). Data are representative of 2-4 experiments.

As next step I analyzed B cell dynamics in the immunological organs of VavP-Bcl2 Hoxb8-FL transplanted mice together with VavP-Bcl2 transgenic and WT animals. In transplanted animals, B220<sup>+</sup> CD19<sup>+</sup> B cells could be identified in all secondary lymphoid organs including spleen, lymph nodes, mesenteric lymph nodes, and hBCL2 staining confirmed that they all originated from VavP-Bcl2 Hoxb8-FL cells (**Figure 14a, Supplementary Figure 5**). hBCL2<sup>+</sup> B cells composed approximately 36±13% of all splenocytes, which was highly similar to the B cell frequencies in the spleens of WT 43±10% and VavP-Bcl2 49±14% transgenic animals (**Supplementary Figure 4a**). Although the total number of B cells (B220<sup>+</sup> CD19<sup>+</sup>) in the spleen of the WT mice and VavP-Bcl2 Hoxb8-FL transplanted mice were similar, they were 10-fold less compared to VavP-Bcl2 transgenic animals (**Supplementary Figure 4a**). Importantly, it is critical that all mature B-cell subsets are generated in VavP-Bcl2tg Hoxb8-FL reconstituted mice in order to study mature B-cell biology and genetics of mature B-cell lymphomas. Therefore, I next checked mature B-cell compartments including MZB, FOB, and GCB cells. I confirmed the presence of MZB and FOB cells by CD23 and CD21/35 staining patterns on B220<sup>+</sup> AA4.1<sup>-</sup> mature B cells in transplanted mice (**Figure 14b**). There was a tendency toward reduced MZB and FOB percentages in the spleens of VavP-Bcl2 transgenic and VavP-Bcl2 Hoxb8-FL transplanted mice. However, the sample size should be increased for testing the significance of these observations (**Supplementary Figure 4b**). Importantly, analysis of B cells in secondary lymphoid organs for germinal center markers revealed that germinal center hyperplasia, the hallmark of the VavP-Bcl2 transgenic line, could be recapitulated using the VavP-Bcl2 Hoxb8-FL transplantation model (**Figure 15a, Supplementary Figure 6a**). Similar to the GCB cells in VavP-Bcl2 transgenic mice, VavP-Bcl2 Hoxb8-FL derived GCB

cells expressed high levels of CD95, GL7, and had diminished IgD expression indicating the active CSR in germinal centers. Starting as early as 1 month after the transplant, the percentage of GCB cells, defined as CD95<sup>high</sup> CD38<sup>low</sup> or CD95<sup>high</sup> GL7<sup>high</sup>, increased dramatically in the spleen, lymph nodes and mesenteric lymph nodes of the transplanted animals when compared to WT mice (**Figure 15b, Supplementary Figure 4c**). Furthermore, in transplanted animals, upregulation of the key germinal center transcriptional modulator BCL6 in GCBs compared to naive B cells was confirmed (**Figure 15c**). Interestingly, in the bone marrow of the transplanted and the transgenic mice, I observed elevated percentages of CD95<sup>high</sup>CD38<sup>low</sup> B cells which might be pointing to the presence of circulating activated B cells in BCL2 overexpressing animals (**Figure 15b, Supplementary Figure 6a**). Besides robust spontaneous differentiation of GCB cells, I detected higher plasma cell ratios in VavP-Bcl2 transgenic, and VavP-Bcl2 Hoxb8-FL transplanted mice compared to WT counterparts (**Figure 15d, Supplementary Figure 6b**). Due to the induced germinal center formation via BCL2 overexpression, B220<sup>low</sup> CD138<sup>+</sup> TACI<sup>+</sup> plasma cells' ratios were significantly elevated in these animals even in the absence of immunization (**Figure 15e, Supplementary Figure 4d**). Overall, my VavP-Bcl2 Hoxb8-FL transplantation system resulted in enlarged germinal centers and provided a useful experimental platform to study dynamics of mature B cells including GCB and PC differentiation axes *in vivo* in a similar fashion to VavP-Bcl2 transgenic animals.

Besides the strong B cell reconstitution in secondary lymphoid tissues of VavP-Bcl2 Hoxb8-FL transplanted animal, I also observed hBCL2<sup>+</sup> T cells by 3 months after the transfer (**Figure 14a, Supplementary Figure 5**). However, similar to my data in peripheral blood, tissue analysis showed that T cell reconstitution capacity was highly dependent on the VavP-Bcl2 Hoxb8-FL line used. In contrast to Line-1's reduced T cell reconstitution, the spleens of animals reconstituted with Line-2 Hoxb8-FL cells had hBCL2<sup>+</sup> T cells accounting for 20% of all T cells in the spleens (**Supplementary Figure 3c**).

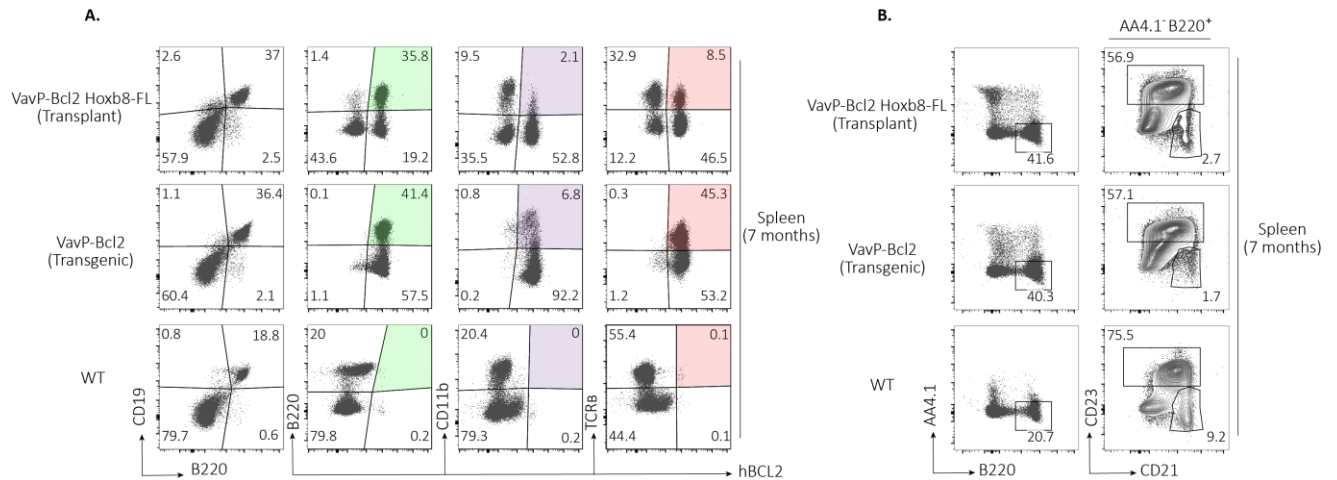


**Figure 14: Adoptive transfer of VavP-Bcl2 Hoxb8-FL cells and ensuing B-cell differentiation *in vivo***

**A)** Representative FACS plots of hBCL2 expression in splenocytes from lethally irradiated mice transplanted (TP) with VavP-Bcl2 Hoxb8-FL cells (7 months after the transplantation). Samples are pregated on CD45.2<sup>+</sup> cells. Numbers in quadrants indicate percentages. Plots are representative of data obtained from four mice transferred with one of the two independent VavP-Bcl2 Hoxb8-FL cell line. Tissue from untreated control mice (WT) and from transgenic (TG) VavP-Bcl2 mice were used for comparison. B cells (B220<sup>+</sup> CD19<sup>+</sup>), myeloid cells (CD11b<sup>+</sup>) and T cells (TCRβ<sup>+</sup>). Data are representative of 3 experiments (Analysis up to 10 months). **B)** Representative FACS plots of marginal zone B (MZB, B220<sup>+</sup> AA4.1<sup>-</sup> CD23<sup>-</sup> CD21<sup>high</sup>) and follicular B (FOB, B220<sup>+</sup> AA4.1<sup>-</sup> CD23<sup>+</sup> CD21<sup>low</sup>) cells in spleen, 7 months after the transplantation (TP) of VavP-Bcl2 Hoxb8-FL cells. Samples are pregated on CD45.2<sup>+</sup> cells. Two independent VavP-Bcl2 Hoxb8-FL cell lines were tested. Numbers in quadrants indicate percentages. Data are representative of 3 experiments (Analysis up to 7 months).

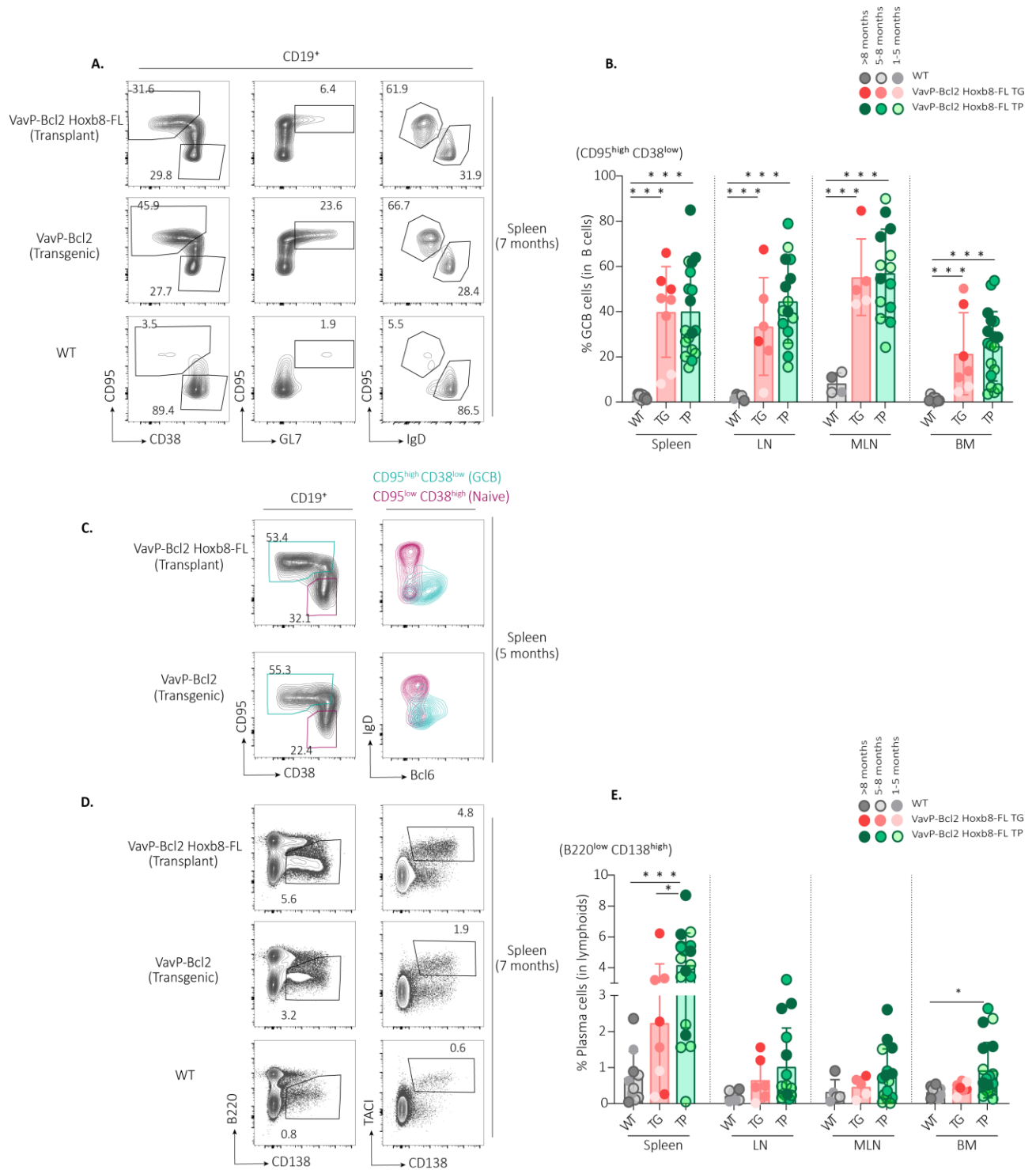


**Figure 15: Adoptive transfer of VavP-Bcl2 Hoxb8-FL cells and ensuing GCB-cell and PC differentiation *in vivo***

**A)** Representative FACS plots of splenic germinal center B (GCB, CD19<sup>+</sup> CD95<sup>high</sup> CD38<sup>low</sup> / CD95<sup>+</sup> GL7<sup>+</sup> / CD95<sup>+</sup> IgD<sup>-</sup>) and naive-B (CD19<sup>+</sup> CD95<sup>-</sup> CD38<sup>+</sup> / CD95<sup>-</sup> IgD<sup>+</sup>) cells, 7 months after the transplantation (TP) of VavP-Bcl2 Hoxb8-FL cells. Four independent VavP-Bcl2 Hoxb8-FL cell lines were tested. Numbers in quadrants indicate percentages. Data are representative of 6 experiments (Analysis up to 10 months). **B)** Percentage of germinal center B cells (GCB, CD19<sup>+</sup> CD95<sup>high</sup> CD38<sup>low</sup>) in spleen, lymph nodes (LN), mesenteric lymph nodes (MLN) and bone marrow (BM) of mice transplanted with VavP-Bcl2 Hoxb8-FL cells (TP), untreated control WT and VavP-Bcl2 Hoxb8-FL transgenic (TG) mice. Four independent VavP-Bcl2 Hoxb8-FL cell lines were tested.

**Figure 15 (continued):** were tested. (n=2-7 for each time-interval, mean±SD) Sidak's multiple comparisons test comparing all conditions to each other (\*P < 0.05, \*P < 0.01, \*\*\*P ≤ 0.001). Data are representative of 6 experiments. **C)** Representative FACS plots of IgD and BCL6 expression in germinal center B cells (GCB, CD19<sup>+</sup> CD95<sup>high</sup> CD38<sup>low</sup>) and naïve-B (CD19<sup>+</sup> CD95<sup>+</sup> CD38<sup>+</sup>) cells in the spleens of mice transplanted with VavP-Bcl2 Hoxb8-FL cells and VavP-Bcl2 transgenic mice. The analysis was conducted 5 months after transplantation, n=2. Numbers in quadrants indicate percentages. **D)** Representative FACS plots of plasma cells (PC, B220<sup>low</sup> CD138<sup>high</sup>) in spleen, 7 months after the transplantation (TP) of VavP-Bcl2 Hoxb8-FL cells. Samples are pregated on CD45.2<sup>+</sup> cells. Four independent VavP-Bcl2 Hoxb8-FL cell line were tested. Numbers in quadrants indicate percentages. Data are representative of 6 experiments (Analysis up to 10 months). **E)** Percentage of plasma cells (PC, B220<sup>low</sup> CD138<sup>high</sup>) in spleen, lymph nodes (LN), mesenteric lymph nodes (MLN) and bone marrow (BM) of VavP-Bcl2 Hoxb8-FL transplanted (TP), untreated control WT and VavP-Bcl2 Hoxb8-FL transgenic (TG) mice. Four independent VavP-Bcl2 Hoxb8-FL cell line were tested. (n=2-7 for each time-interval, mean±SD) Sidak's multiple comparisons test comparing all conditions to each other (\*P < 0.05, \*P < 0.01, \*\*\*P ≤ 0.001). Data are representative of 6 experiments.

### 3.3.2. Adoptive Transfer of Retrovirally Transduced VavP-Bcl2 Hoxb8-FL Cells

Since I wanted to introduce genetic perturbations into VavP-Bcl2 Hoxb8-FL lines in order to be able to conduct *in vivo* functional studies, as the next step I determined whether viral manipulation of cells would have an effect on Hoxb8-FL cells engraftment and subsequent *in vivo* maturation process and whether the system can be implemented in future to assess the clonal evolution of cells carrying different genetic perturbations. To do so, VavP-Bcl2 Hoxb8-FL cells were transduced with a retroviral vector expressing control sgRNA and the THY1.1 marker (**Figure 16a**). Infected cells were enriched by MACS and then spiked in at different ratios (45%, 23%, 7.5%, and 1.5% THY1.1<sup>+</sup>) into uninfected Hoxb8-FL cells. Different THY1.1<sup>+</sup> percentage containing cell populations were transferred into lethally irradiated mice together with unfractionated B cell-deficient BM cells. 3 months later mice were analyzed and THY1.1 expression was assessed in VavP-Bcl2 Hoxb8-FL derived B cells. Notably, initial *in vitro* spike-in ratios were detected at highly similar ratios in lymphoid organs of all reconstituted animals (**Figure 16b-c**). Moreover, comparison of THY1.1 expression in GCB and naïve-B cells, revealed that THY1.1<sup>+</sup> cells were represented in both compartments at similar ratios indicating for a neutral effect of the manipulation (**Figure 16d**). Overall, highly preserved representation of the proportions of infected THY1.1<sup>+</sup> B cells compared to the adoptively transferred Hoxb8-FL cells highlighted the potential use of the system later in investigation of clonal relationships in functional studies.

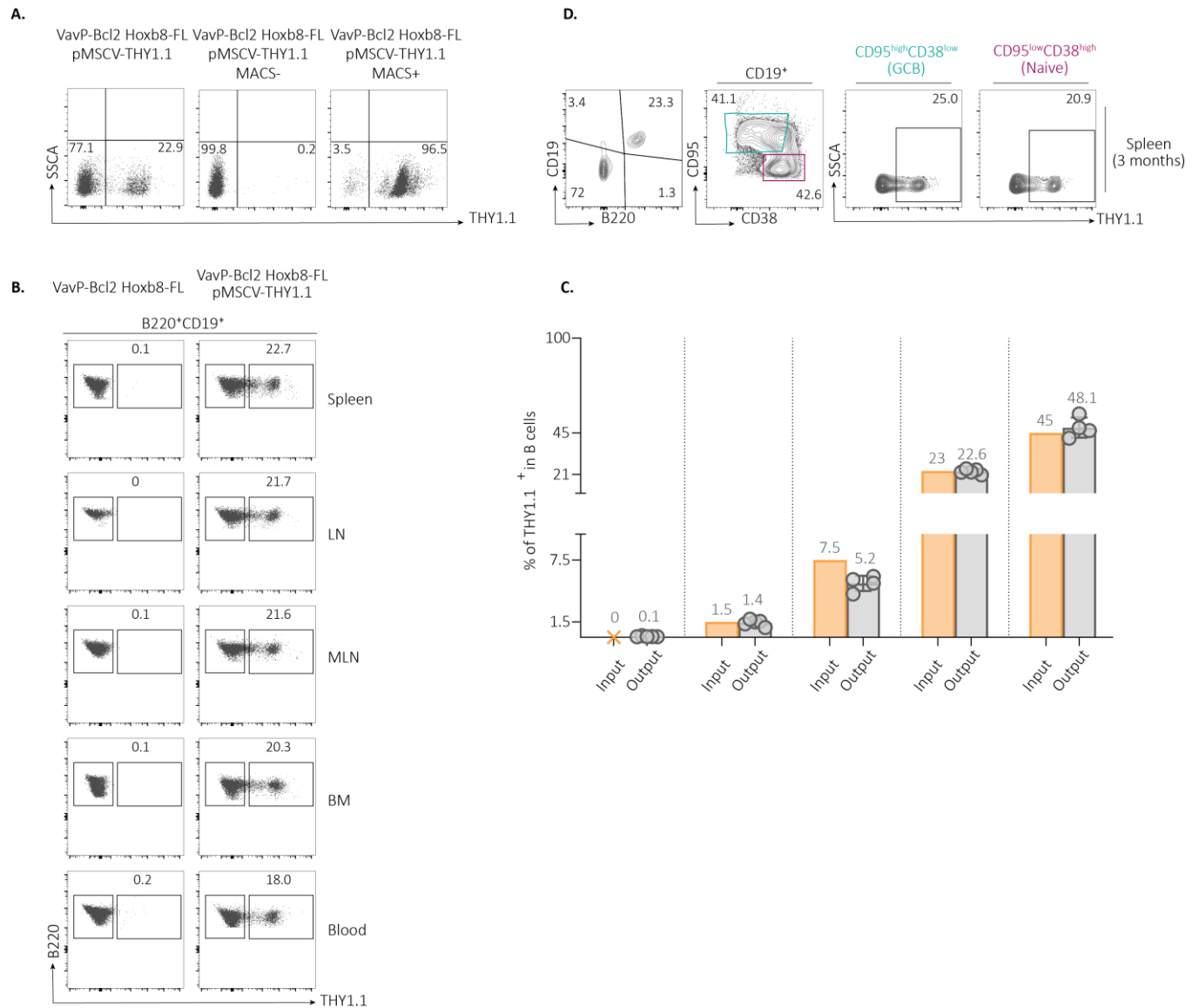


**Figure 16: Adoptive transfer of retrovirally transduced VavP-Bcl2 Hoxb8-FL cells**

**A)** FACS plots of THY1.1 expression in VavP-Bcl2 Hoxb8-FL cells that were transduced with THY1.1-expressing retroviral vectors. Plots of cells before and after MACS enrichment. Numbers in quadrants indicate percentages. **B)** Representative FACS plots identifying THY1.1 expressing B (CD19<sup>+</sup> B220<sup>+</sup>) cells in spleen, lymph nodes (LN), mesenteric lymph nodes (MLN), bone marrow (BM) and blood of mice transplanted with VavP-Bcl2 Hoxb8-FL cells containing 23% THY1.1<sup>+</sup> retrovirally transduced cells. Numbers in quadrants indicate percentages 3 months after the transplantation. **C)** Flow cytometry-based assessment of THY1.1 expression on B (CD19<sup>+</sup> B220<sup>+</sup>) cells of reconstituted mice. VavP-Bcl2 Hoxb8-FL cells were spiked in with MACS enriched THY1.1<sup>+</sup> VavP-Bcl2 Hoxb8-FL cells at varying ratios (percentage of "input") and transplanted into lethally irradiated mice. 3 months later, THY1.1<sup>+</sup> cells' percentages in B cells of lymphoid tissues analyzed (percentage of "output"). **D)** Representative FACS plots of THY1.1 expression on germinal center B cells (GCB, CD19<sup>+</sup> CD95<sup>high</sup> CD38<sup>low</sup>) and naive-B (CD19<sup>+</sup> CD95<sup>low</sup> CD38<sup>high</sup>) cells in the spleens of mice transplanted with VavP-Bcl2 Hoxb8-FL cells containing 23% THY1.1<sup>+</sup> retrovirally transduced cells. Numbers in quadrants indicate percentages 3 months after the transplantation.

### 3.3.3. *In vivo* Conditional Gene Targeting in VavP-Bcl2 Hoxb8-FL Derived GCB cells

To induce genetic alterations in specific B cell subsets or at particular developmental stages I generated several different Hoxb8-FL lines harboring different Cre knock-ins as well as conditional Cas9 knock-ins. For instance, VavP-Bcl2 C $\gamma$ 1cre LSL-Cas9-GFP Hoxb8-FL lines were generated to induce Cas9 activation in GCB cells. To test Cre-mediated recombination in my adoptive transplant system, I transferred these cells as described before and analyzed lymphoid tissues for GFP expression. While naive B cells were barely detected within the GFP<sup>+</sup> cells, GCB cells were highly enriched for GFP<sup>+</sup> expression, indicative of germinal center specific recombination events (**Figure 17a**). In the absence of immunization, on average 30% of GCB cells expressed GFP as a result of the deletion of the stop cassette in the R26 locus in all secondary lymphoid organs (**Figure 17b**). Similarly, this ratio was also reflected in PCs, indicating their differentiation from recombined GCB cells (**Figure 17a-b**). Overall, this experiment showed that *in vivo* conditional gene targeting can be achieved with the Hoxb8-FL adoptive transfer system. Importantly, it also showed that my VavP-Bcl2 C $\gamma$ 1cre Hoxb8-FL cells can be used to study gene function in GCB and plasma cells in the absence of immunization.

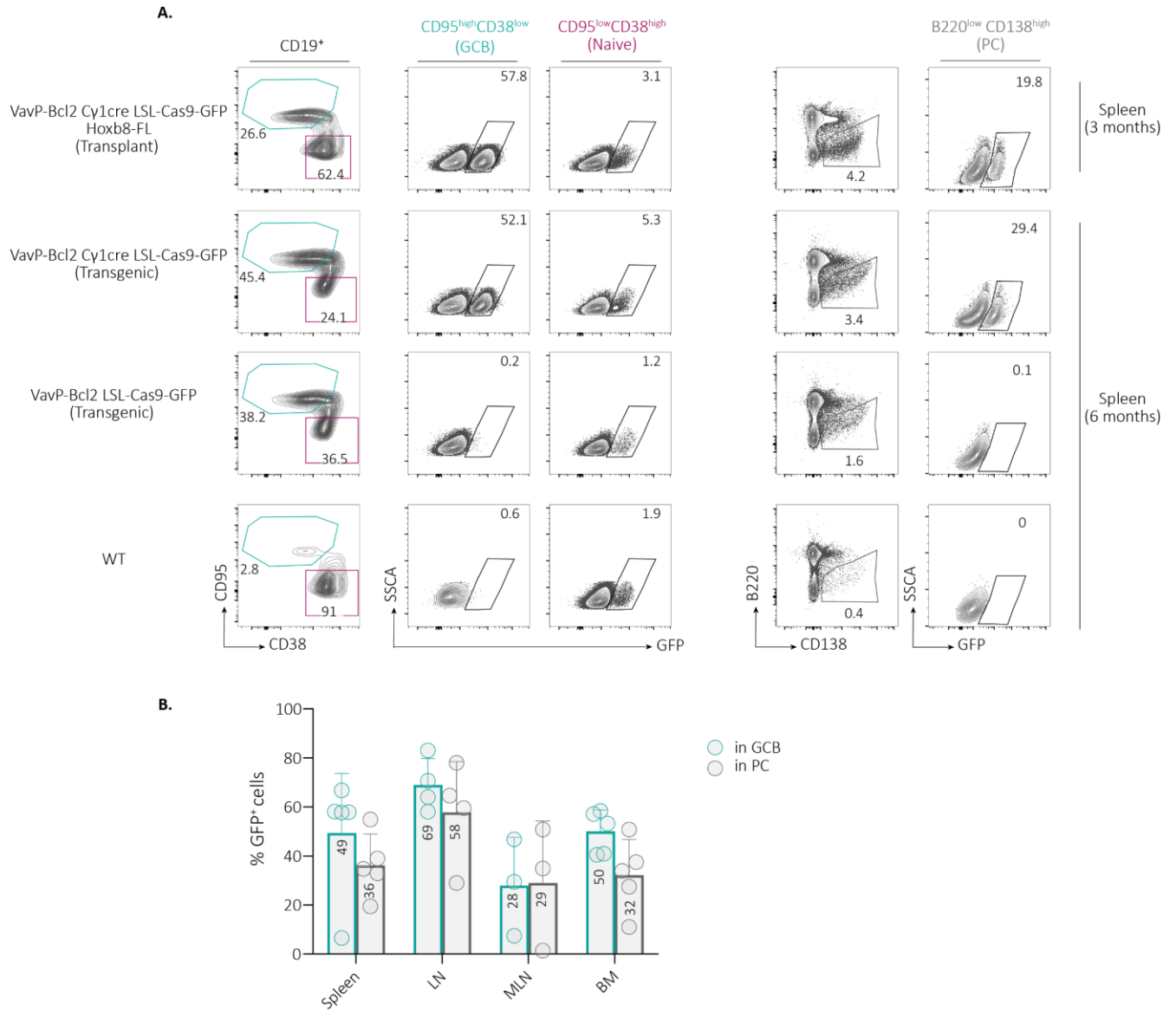


**Figure 17: *In vivo* conditional gene targeting in VavP-Bcl2 Hoxb8-FL derived GCB cells**

**A)** Representative FACS plots of GFP expression in germinal center B cells (GCB, CD19<sup>+</sup>CD95<sup>high</sup>CD38<sup>low</sup>), naive-B (CD19<sup>+</sup>CD95<sup>low</sup>CD38<sup>high</sup>) cells and plasma cells (PC, B220<sup>low</sup>CD138<sup>high</sup>) in the spleens of mice transplanted with VavP-Bcl2 Cy1cre LSL-Cas9-GFP Hoxb8-FL cells. Tissues from VavP-Bcl2 Cy1cre LSL-Cas9-GFP, VavP-Bcl2 LSL-Cas9-GFP transgenic mice and untreated WT control mice were used for comparison. Numbers in quadrants indicate percentages. **B)** Flow cytometry-based assessment of GFP expression in germinal center B cells (GCB, CD19<sup>+</sup>CD95<sup>high</sup>CD38<sup>low</sup>) and plasma (PC, B220<sup>low</sup>CD138<sup>high</sup>) cells of mice transplanted with VavP-Bcl2 Cy1cre LSL-Cas9-GFP Hoxb8-FL cells. Two independent VavP-Bcl2 Cy1cre LSL-Cas9-GFP Hoxb8-FL lines were used for reconstitution experiments and 10 months after the transfer spleen, lymph nodes (LN), mesenteric lymph nodes (MLN) and bone marrow (BM) of mice were analyzed (n=2-3 for each line, mean±SD).

### 3.3.4. Generation of Lymphoma Mouse Models via VavP-Bcl2 Hoxb8-FL Adoptive Transfer System

After showing that the VavP-Bcl2 Hoxb8-FL adoptive transfer system enables the genetic interrogation of mature B-cell biology *in vivo*, I wanted to employ *in vitro* manipulation followed

by transfer into recipient mice in order to generate mature B-cell lymphoma mouse models and investigate genetic interactors of BCL2 in lymphoma development.

Initially, to model double and/or triple-hit high-grade B-cell lymphomas which arise from combinatorial oncogenic activation of *c-MYC*, *BCL2*, and/or *BCL6*, I transduced VavP-Bcl2 Cy1cre LSL-Cas9-GFP Hoxb8-FL cells with retroviral vectors conditionally overexpressing human *c-MYC* or mouse *Bcl6*. Cy1cre should limit oncogene expression to GCB cells and the conditional Cas9-GFP knock-in serves as reporter for Cre-mediated recombination in this case. I employed the following conditional expression constructs; pMSCV-LSL-hMYC-IRES-PURO-F2A-THY1.1 and pMSCV-LSL-mBcl6-IRES-thCD2; THY1.1 and truncated human CD2 (thCD2) serve for the identification of infected cells carrying the integrated retroviral provirus. In these vectors, Cre-mediated recombination of loxP sites, leads to the excision of a translational stop cassette (UAG stop codon), which is found upstream of *MYC* or *Bcl6*. This allows the ectopic expression of these proteins in infected cells expressing Cre and in their progeny (Turner et al., 2010). After transducing cells with these two retroviruses together, I identified single (THY1.1<sup>+</sup> or thCD2<sup>+</sup>) or double (THY1.1<sup>+</sup> and thCD2<sup>+</sup>) infected cell populations by FACS (**Supplementary Figure 7**). As next step, these transduced bulk cell populations were transplanted into lethally irradiated mice in the presence of B-cell deficient bone marrow cells, and mice were aged while being monitored for disease development. Notably, mice reconstituted with Hoxb8-FL cells carrying the conditional integrated proviruses showed significantly reduced overall survival rates compared to controls (**Figure 18a**). Their median survival was reduced to 21 weeks in contrast to control mice, which were alive and appeared healthy until the final analysis time point (40 weeks after the transplant). The analysis of sick mice reconstituted with Hoxb8-FL cells transduced with conditional *Bcl6* and *c-MYC* revealed tumorous lymphoid structures spread throughout the body (**Figure 18b**). FACS characterization demonstrated a predominance of B220<sup>+</sup> THY1.1<sup>high</sup> B cells in these structures (**Figure 18c**). Although I only detected THY1.1<sup>high</sup> B cells in the analyzed lymphoid tumors, in the spleen of the same mice THY1.1<sup>+</sup>, thCD2<sup>+</sup> and double positive B cells could be detected indicating the persistence of all transplanted cell populations *in vivo*. As my conditional expression model depended on Cre-activation and I utilized the Cy1cre-carrying HoxB8FL line in my experiments, I expected the oncogene-induction to be limited to (class-

switched) GCB cells. Surprisingly, phenotypic analysis showed that THY1.1<sup>high</sup> B cells were devoid of GCB markers and were negative for the GFP reporter for Cre-mediated recombination (R26-LSL-Cas9-GFP). On the other hand, Hoxb8-FL derived GFP<sup>+</sup> GCB cells were detectable in the spleens of these mice, indicating that the Hoxb8FL-derived cells are in principle capable to form GCBs and activate Cy1cre-mediated recombination. All the analyzed tumorous structures had diminished IgM and IgD expression, although there was one sample characterized by high expression of IgM (**Figure 18c**). Overall, my results indicate the induction of mature pre-GCB cell lymphoma through this experimental setup.

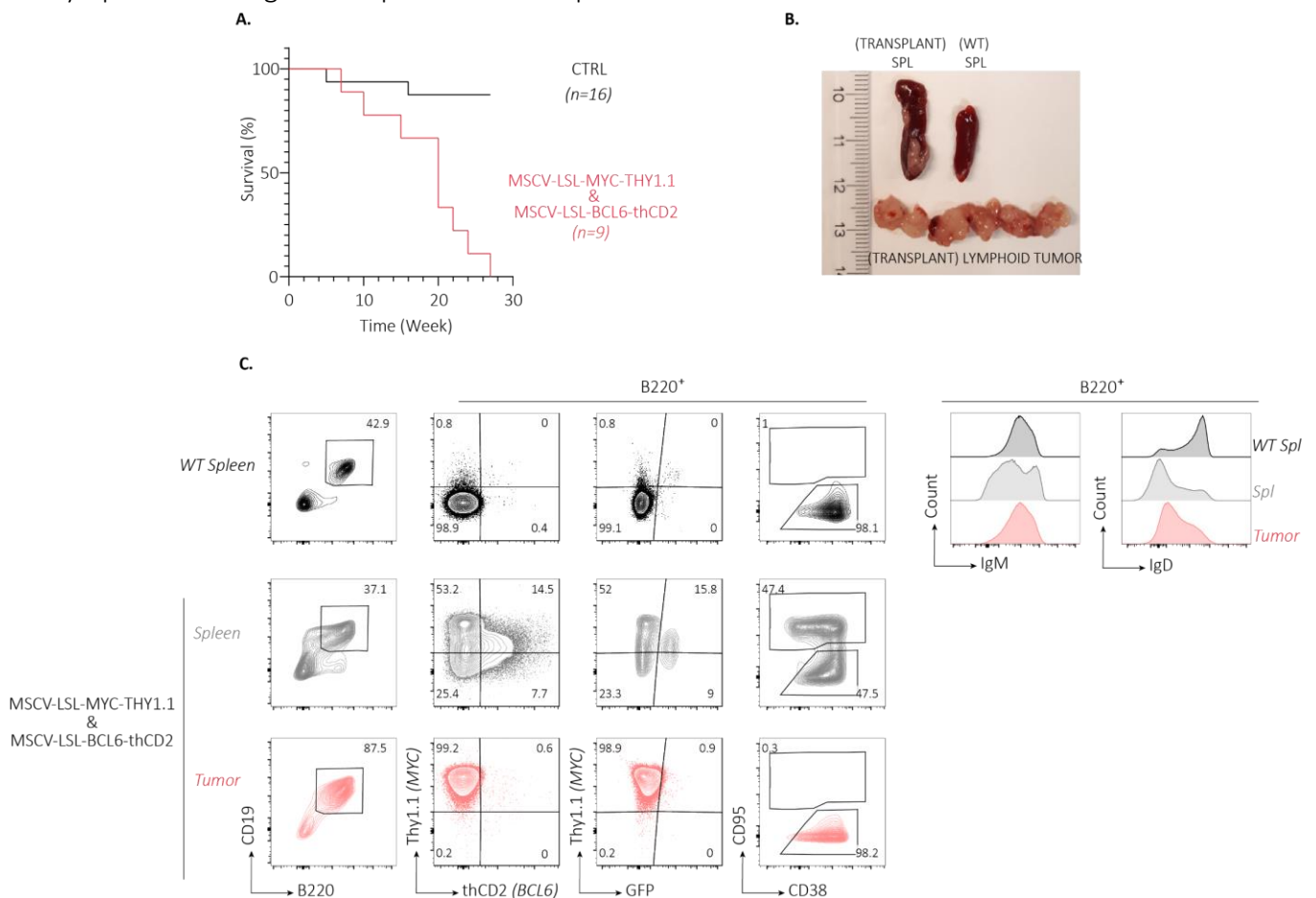


**Figure 18: Integrated provirus-mediated c-MYC expression in VavP-Bcl2 Hoxb8-FL adoptive transfer model drives mature B-cell lymphomas**

**A)** Kaplan–Meier survival curves of mice transplanted with VavP-Bcl2 Cy1cre LSL-Cas9-GFP Hoxb8-FL cells either in the absence (CTRL n=16) or presence (n=9) of MSCV-LSL-MYC-THY1.1 & MCV-LSL-BCL6-thCD2 conditional integrated proviruses. Data represent one experiment. **B)** Representative images of spleen and lymphoid tumor observed in the sick mice transplanted with VavP-Bcl2 Cy1cre LSL-Cas9-GFP Hoxb8-FL cells that were transduced with the conditional expression vectors. A spleen from a WT mouse is shown for reference. **C)** Example of pre-GCB tumors observed in 75% (3/4) of all analyzed mice that are reconstituted with Hoxb8-FL cells carrying integrated MSCV-LSL-MYC-THY1.1 & MCV-LSL-BCL6-thCD2 conditional proviruses. Representative FACS plots of B cells (B220<sup>+</sup> CD19<sup>+</sup>), germinal center B cells (GCB, B220<sup>+</sup> CD95<sup>high</sup> CD38<sup>low</sup>), and naïve-B cells (B220<sup>+</sup> CD95<sup>low</sup> CD38<sup>high</sup>) in the spleen and lymphoid tumor of the sick mouse transplanted with VavP-Bcl2 Cy1cre LSL-Cas9-GFP Hoxb8-FLs carrying the conditional expression vectors. THY1.1, thCD2, GFP, IgM and IgD expressions are depicted on B220<sup>+</sup> cells. WT mouse spleen is shown for reference. Numbers in quadrants indicate percentages.

## 4. DISCUSSION

### 4.1. The VavP-*Bcl2* Hoxb8-FL System to Investigate Regulators of GCB cells and GC Derived B-Cell Lymphomas *In vivo*

Blood cancers, including lymphomas, leukemias, and myelomas arise from neoplastic transformation of immune cells. NHL represent the most common hematological malignancy type. Importantly, the germinal center derived mature B cell lymphomas DLBCL and FL are most prevalent amongst all NHL cases reaching up to 40% and 25%, respectively (Perry et al., 2016). In the treatment of these germinal center derived lymphomas, besides classical approaches including chemotherapy and depletion of mature B cells with anti-CD20 antibodies (i.e. rituximab and obinutuzumab), the use of novel agents including immunomodulators (i.e. lenalidomide), BCL2-inhibitors (i.e. venetoclax), phosphoinositide 3-kinase (PI3K) inhibitors (i.e. umbralisib, duvelisib) (Casulo, 2019) has been implemented. Even though these treatments improved the life expectancies of lymphoma patients, many of them develop resistance to therapies and eventually disease relapses (Casulo, 2019) (Lowry & Linch, 2013) (Klener & Klanova, 2020) . Therefore, we need to improve our understanding of the biology of these still devastating diseases including the molecular and genetic changes that occur in malignant clones, as well as the evolution of these clones throughout disease progression. The ultimate goal of fundamental lymphoma research is to help improving stratification of patients and to lay the groundwork for developing novel effective treatments. Large-scale genomic sequencing studies revealed the molecular complexity of these lymphomas and yielded a plethora of lymphoma-associated genetic aberrations whose roles in tumorigenesis needs to be investigated (Pasqualucci, Trifonov, et al., 2011) (Okosun et al., 2014) (Bödör et al., 2013) (Cheung et al., 2009) (Schwaenen et al., 2009) (Li et al., 2014) (Küppers & Stevenson, 2018) (Devan et al., 2018). For example, phylogenetic trees constructed by paired longitudinal analysis of FL and transformed FL patients' mutations showed the clonal dynamics of the disease and identified lymphoma-addictive alterations of the chromatin modifiers KMT2D and CREBBP as well as of the immune modulator TNFRSF14. Similarly, genes involved in the JAK-STAT signaling pathway

(*SOCS1*, *STAT6*) or in the BCR/NF- $\kappa$ B signaling pathway (*MYD88*, *TNFAIP3*, *BCL10*, *CARD11*, *CD79B*) were identified among the targets of recurrent mutations (Okosun et al., 2014).

Functional studies mostly conducted in immortalized transformed cell lines and transgenic mouse models enabled assigning of some of these alterations as tumor suppressors or oncogenes (Donnou et al., 2012) (Ramezani-Rad & Rickert, 2017) (Flümann et al., 2020) (Mossadegh-Keller et al., 2021) (Meyer et al., 2021). Given the recent advances in genome editing techniques (CRISPR-mediated gene knockout, gene knock-in, transcriptional activation/inactivation, base editing, ectopic expression of genes using various viral delivery systems, etc.), studying gene functions has become more convenient. These technologies facilitate gene targeting and allow the induction of precise genetic alterations in cells as well as in animal models (Hsu et al., 2014) (Tschaharganeh et al., 2016) (Adli, 2018) (Anzalone et al., 2020) with unprecedented speed and in dramatically increased throughput. Primary cells, which retain the features of their tissue of origin, are good resources for research addressing organ and tissue physiology and for monitoring the direct consequences of simple genetic perturbations. However, due to their restricted lifespan in culture conditions, primary cells and tissues are difficult to use in experimental settings that require introducing, selecting and sustaining complex genetic modifications. Establishment of immortalized lymphoma cell lines and their characterization via exome and RNA sequencing highly contributed to lymphoma studies (Drexler, 2011) (Drexler et al., 2016) (Quentmeier et al., 2019). However, even though these cell lines can provide an unlimited source of cell material for the investigation of relevant biological factors through gene editing, they are still limited in the information they provide in the absence of an intact microenvironment (Khurana & Ansell, 2020) (Schneider et al., 2017). Moreover, stably immortalized transformed cell lines usually contain a large number of mutagenic alterations and adaptation to the tissue culture environment. This may bring about an unnatural complexity complicating the interpretation of loss and gain of function studies of individual investigated genes (Carter & Shieh, 2010). Alternatively, *in vivo* approaches, in which mouse models containing specific tumor-associated engineered genetic perturbations permit investigating molecular mechanisms of disease development as well as the role of the microenvironment, can provide more comprehensive information. Genome editing technologies

expedited the generation of new mouse strains containing diverse alterations including knockouts, knock-ins, and translocations enormously. Nevertheless, combining multiple transgenic alleles in compound mutant experimental animals in order to reflect and assess the multi-hit nature of cancers requires several breeding steps and the maintenance of large animal cohorts, which accounts for high costs and longer establishment times of the disease models. Adding additional genetic alterations to existing complex compound mutant mice can then take more than a year to complete.

Considering the limitations of the current experimental resources, with this project I aimed to establish a new adoptive transfer-based model system where mature B-cell biology can be studied *in vivo* to unveil novel regulators of GC derived lymphomas and to investigate mechanisms of clonal evolution in B cells.

In my approach, by using conditionally immortalized hematopoietic progenitors, I aimed to culture mouse progenitor cells sufficiently long to perform complex gene editing procedures *in vitro* followed by assessing the functional consequences of the induced alterations *in vivo* by transplanting them into recipient mice. As these cells are generated from primary tissue, they should be devoid of unintended mutations, in contrast to lymphoma cell lines. Moreover, their *in vivo* reconstitution and differentiation potential would enable them to pass through all the normal physiological steps of B-cell development and maturation in the presence of intact microenvironments thereby ensuring a closer recapitulation of the natural biological processes. Previously, Redecke and colleagues characterized the myeloid and lymphoid differentiation ability of conditionally immortalized Hoxb8-FL progenitor cells *in vitro* and *in vivo* (Redecke et al., 2013). Importantly, they showed that upon adoptive transfer of Hoxb8-FL cells into lethally irradiated mice, Hoxb8-FL derived B-cell subsets (i.e. B-cell progenitors, transitional, follicular, and marginal zone B cells) can be detected in bone marrow, blood, and peripheral lymphoid organs. Furthermore, Redecke and co-workers also reported that antigen-specific class-switched antibodies can be found in the serum of Hoxb8-FL reconstituted animals after immunization, indicating that Hoxb8-FL derived B cells can generate functional plasma cells.

Based on these data, for studying germinal center B cell biology and programming them for lymphomagenesis, I generated Hoxb8-FL cell pools from VavP-*Bcl2* transgenic mice, which spontaneously develop germinal center hyperplasia and are used to study FL (Egle et al., 2004). Additionally, to enable gene targeting by CRISPR/Cas9 *in vivo* at distinct B-cell developmental stages, I derived Hoxb8-FL cells from VavP-*Bcl2* mice crossed to different B-cell stage-specific Cre-recombinase strains (*Mb1cre*, *CD19cre*, *Cy1cre*) together with the Cre-activatable Cas9-knock-in mouse line (R26-LSL-Cas9-eGFP). R26-LSL-Cas9-eGFP mice were previously used to establish CRISPR-based knockout models *in vivo*, also in hematological systems where myeloid or lymphoid cells were conditionally targeted for induction of knockouts *in vivo* (Platt et al., 2014) (Chow et al., 2017) (Ye et al., 2017) (Laidlaw et al., 2020).

Furthermore, to identify novel modulators of germinal center lymphomas, I performed unbiased, genome-wide *in vivo* transposon screens in VavP-Bcl2 mice. In this approach, I employed conditional *PiggyBac* transposon mutagenesis together with CD19Cre to introduce transposon-mobilization starting at early B cell development. Hoxb8-FL cell pools that I generated from these mice can be adoptively transferred to reveal BCL2-collaborating alterations in lymphoma development. This approach can eliminate the extensive breeding steps to bring in the four genetic components of my transposon screen. Importantly, they can also allow to integrate further founder alterations of lymphomas (i.e., inactivation of KMT2D, CREBBP, HVEM) *in vitro*, to identify other relevant accompanying hits of the disease *in vivo*.

#### **4.2. Gene Editing in Hoxb8-FL Cells**

Following the generation of the Hoxb8-FL cell pools, I established and optimized gene-editing protocols in these cells. Since viral delivery systems are highly useful for genetic engineering, I initially tested viral transduction of Hoxb8-FL cells and observed very high infection efficiencies using retroviral and lentiviral expression vectors. This enables me to deliver genes of interest for gain of function studies or to facilitate further modification of cells through ectopic expression of other gene-editing components. For example, by transduction of Cas9-expressing Hoxb8-FL cells with retroviral sgRNA-expressing vectors, I could achieve > 90% gene disruption in bulk populations. Previously, other research groups also utilized viral mediated CRISPR-knockouts in

Hoxb8 cells by transducing them with a Cas9-sgRNA double expressor vector or by two-step transduction of Cas9 and sgRNA vectors (i.e., transducing cells with the Cas9 expression vector, selecting high-level Cas9-expressing single cell clones, and infecting them with the sgRNA expression vector) (Grajkowska et al., 2017) (Leithner et al., 2018) (Khojraty et al., 2021). In my approach, similar to the study of Hammerschmidt and colleagues, I generated Hoxb8-FL cells from the constitutively Cas9-expressing R26-Cas9-GFP mice, which ensures ubiquitous Cas9 expression in all cells and therefore helps to bypass single-cell cloning step which might introduce biases due to the cellular heterogeneity of bulk progenitors (Hammerschmidt et al., 2018) . Similarly, low viral titers, which are caused by the large cargo size of Cas9-sgRNA double expression vectors, can be overcome in this way (Graham & Root, 2015). In addition, I demonstrated that through the use of multiplexing CRISPR vectors, various loci can be targeted simultaneously in Hoxb8-FLs. In my approach, to test the applicability of multiplexing, I designed a dual sgRNA-expressing retroviral vector. In Hoxb8-FL cells, this vector enabled the robust generation of double knockout cells. However, a slight reduction in editing levels was observed when an sgRNA was expressed from the 5' proximal hU6-sgRNA cassette of the vector compared to the 3' site, which might be caused by positional effects or transcriptional interference (Shearwin et al., 2005) (McCarty et al., 2020). Therefore, in the future, for multiplex editing with this viral vector, the sgRNAs with the lower targeting efficiencies should be cloned into the 3' proximal hU6-sgRNA cassette if equal editing efficiencies between the two vector-encoded sgRNAs are desired.

As alternative to viral delivery systems in the generation of genetic perturbations, I systematically optimized the transfection of CRISPR components (sgRNAs, Cas9, and RNPs) into Hoxb8-FL cells using the Neon® electroporator. By testing electroporation of sgRNAs into stably Cas9-expressing Hoxb8-FLs, I was able to determine the optimal buffer and electroporation condition for these cells. Combination of buffer T with program 2 (P2: 1600 V-10 ms-3 pulses), which was previously reported to be the optimal program for primary human HSPCs in the Neon® electroporator, provided the most efficient strategy for gene ablation while maintaining high cell viability (Gundry et al., 2016). By applying the same conditions, I showed that near-complete gene depletion could be achieved with the use of pre-complexed RNPs upon

electroporation of Hoxb8-FLs lacking genetically encoded Cas9. Furthermore, in my optimizations, I determined the minimum RNP amount required for an efficient knockout while avoiding potential off-target effects that might be caused by the excess use of the RNA-guided Cas9 (Fu et al., 2013). I also showed that addition of single-stranded non-homologous DNA oligos (electroporation enhancer) can greatly improve the gene-editing efficiencies of RNPs, especially with suboptimal sgRNAs, while decreasing the required total amount of RNPs required per reaction, as shown by other studies as well (Richardson et al., 2016) (Jacobi et al., 2017) (Shapiro et al., 2020). Overall, with the optimizations developed herein, I implemented efficient RNP-mediated CRISPR editing in Hoxb8-FL cells. Importantly, as my RNP protocols permit very efficient gene knockout, they can eliminate the need for transgenic marker selection or enrichment steps. Moreover, electroporation of cells with RNP complexes provides temporally limited presence of Cas9, as RNPs degrade over time, as early as 24 h after the transfection (Kim et al., 2014). Therefore, compared to viral systems, the delivery of RNPs can reduce the off-target effect that might be caused by the prolonged expression of CRISPR elements (Hendel et al., 2015) (Cameron et al., 2017) (Vakulskas et al., 2018). Similarly, by avoiding the expression of immunogenic Cas9 and other immunogenic components of the viral vector systems in cells, transient RNP delivery greatly reduces the risk of being targeted by immune recognition of these foreign antigens in *in vivo adoptive*-transfer experiments (Dubrot et al., 2021). I also showed that electroporating Hoxb8-FL cells in a single reaction with two RNPs directed to different genes can result in double-knockout cells accounting for more than half of the entire population. Successful RNP multiplexing in Hoxb8-FL cells can eliminate the necessity for sequential gene targeting and expand the gene editing applications such as induction of targeted deletions or chromosomal translocations. For example, Jeong and colleagues could investigate the clonal selection and expansion in acute leukemias by implementing t(9;11) translocations in human blood HSPCs via RNPs (Jeong et al., 2019). Similar to this study, in the future, highly frequent chromosomal deletions (6q, 1p36, 16p13) or translocations (t(2;18), t(8;14), t(3;14)) of germinal center derived lymphomas can be studied in detail using this system to understand their roles in disease pathogenesis (Xian et al., 2020) (Fangazio et al., 2015) (Oricchio et al., 2011).

To broaden the flexible use of established targeting methods, I tested gene knockout in Hoxb8-FL cell pools lacking genetically encoded Cas9 via split delivery of CRISPR components. As previously discussed by Ting and colleagues, electroporation of Cas9 alone into sgRNA-expressing cells, which is highly desirable for screening approaches, significantly diminishes the total editing efficiencies compared to electroporation of pre-complexed RNPs. To overcome this problem, I tested the applicability of Guide Swap in Hoxb8-FL cells (Ting et al., 2018). Via Guide Swap experiments, I showed that in Hoxb8-FL cells previously transduced with a retroviral sgRNA vector electroporation of Cas9-precomplexed with non-targeting sgRNAs led to successful and efficient knockout of the retrovirally expressed sgRNA-targeted gene. Moreover, since pre-complexing of Cas9 with sgRNAs increases the overall Cas9 uptake into the cells, I reasoned that instead of non-targeting sgRNAs, I could use commercially available and cheaper non-homologous single-stranded DNA oligos, which were reported to facilitate the uptake of RNP molecules into the cells during electroporation (Jacobi et al., 2017). In fact, I demonstrated that the addition of non-homologous single-stranded DNA oligonucleotides during the Cas9 electroporation of transduced cells rescued the editing levels comparable to those achieved with non-targeting sgRNA-loaded RNP complexes. Furthermore, I found that combining non-homologous single-stranded DNA oligonucleotides with non-targeting sgRNA precomplexed Cas9 does not further improve the total editing efficiencies, implying that they exert their enhancement effect via a similar mechanism. Importantly, the applicability of this flexible, economic, combinatory model can enable the implementation of CRISPR knockout screens in Hoxb8-FL cells even in the absence of genetically encoded Cas9 expression when pooled sgRNA libraries are provided via viral transduction (Shifrut et al., 2018) (Humes et al., 2021).

Furthermore, to study the effects of somatic mutations detected in patients, to generate reporter genes for tracking expression regulation temporally and spatially, and to insert genetic components of other experimental tools used to study gene functionality (i.e., loxP sites, peptide tags, TetO cassette), I established CRISPR/Cas9-mediated homology recombination-based gene editing protocols in Hoxb8-FL cells.

By adapting the GFP-BFP conversion assay, which was developed by Glaser and colleagues to simultaneously quantify HDR or NHEJ resulted genetic alterations in different cell lines, I showed the efficient knock-in of point mutations in Hoxb8-FLs (Glaser et al., 2016). Similarly, efficient substitution of the CD45.2 variant to CD45.1 confirmed that efficient HDR-mediated knock-ins can be achieved also in endogenous loci of these cells. In these experiments, next-generation sequencing of the targeted loci can be employed to verify the sequence identity of the induced alterations. Moreover, generating single-cell clones from the gene-converted cells and sequencing the targeted regions in these clones can reveal the mono- or bi-allelic conversion status of the cells. Overall, robust conversion of GFP to BFP and CD45.2 to CD45.1 provided the proof of concept for efficient CRISPR/Cas9 mediated single amino acid substitutions in Hoxb8-FLs and pointed out successful induction of the HDR repair pathway in these cells. In future experiments, during the introduction of specific alterations in other genes (i.e. lymphoma related mutations), I can also integrate these FACS-identifiable conversion systems via multiplexing to enrich the knock-in-containing populations. Previously, it was shown that cells that display HDR-mediated gene editing in one locus are more likely to contain HDR-mediated gene editing in other loci when they are independently targeted at the same time (Shy et al., 2016) (Agudelo et al., 2017) (Yan et al., 2020). Based on this observation, in the past years, to facilitate the selection of clones with the desired change, "DNA repair outcome-reporters" were employed in knock-in experiments as they enable enrichment of HDR-experienced cells (Certo et al., 2011) (Mitzelfelt et al., 2017) (Coelho et al., 2018) (Standage-Beier et al., 2019) (Yan et al., 2020) (Janssen et al., 2019) (Budagyan & Chernoff, 2021). In this line, in my future experiments, knock-in positive cells harboring the desired modification (not detectable by FACS) can be enriched from bulk edited populations by utilizing CD45.2 or GFP conversion assays in parallel.

After demonstrating the remarkably efficient single amino acid conversions in Hoxb8-FL cells, I modified my knock-in protocol further to bring larger DNA fragments into cells by replacing the ssODN donor templates electroporation step with the transduction of recombinant AAV donor vectors, as they are good vehicles for the transfer of large DNA cargoes (Yang et al., 2013) (Martin et al., 2019) (Ngoc Tung Tran et al., 2019). Other groups previously used this approach to achieve CRISPR/Cas9-mediated gene insertions in human and mouse progenitor cells via

transduction of rAAV-6 and rAAV-DJ donor vectors after introduction of DNA double-strand breaks at the genomic target locus via RNP electroporation (Bak & Porteus, 2017) (Bak et al., 2017) (Bak et al., 2018) (Dever et al., 2016) (Charlesworth et al., 2018) (Ngoc Tung Tran et al., 2019). Tran and colleagues demonstrated that compared to rAAV-6 donor templates, using rAAV-DJ donor templates results in a greater frequency of HDR-mediated knock-in events in mouse HSPCs. Based on this finding, as Hoxb8-FL cells are derived from mouse HSPCs, I established a protocol with rAAV-DJ donor templates and was able to demonstrate the efficient integration of a 0.8 kb fluorescence reporter into the *Actb* locus. In the study of Tran et al., mouse HSPCs that were edited *ex vivo* by this experimental setup were shown to fully reconstitute all mature immune cell lineages after transplantation into irradiated recipients, although a slight reduction in the engraftment of AAV-infected cells compared to only RNP-transfected cells was observed (Ngoc Tung Tran et al., 2019). Although I anticipate efficient *in vivo* differentiation of rAAV-DJ gene manipulated Hoxb8FL cells, addressing the question will be essential to test in future experiments. Moreover, to further optimize the HDR-mediated gene knock-in protocols in Hoxb8-FLs, integrase-deficient lentiviral vectors (IDLVs) can also be implemented as repair template donors in alternative to AAVs since they would eliminate the laborious AAV production protocol and allow to benefit from the high lentiviral transduction efficiencies of Hoxb8-FL cells (Cornu & Cathomen, 2007) (Janssen et al., 2019) (Chan et al., 2020). Overall, the effective implementation of these knock-in methods will allow me to examine the role of specific mutations discovered in lymphoma sequencing studies more accurately, as well as enable to modify cells to follow molecular changes more precisely.

Finally, as a part of my Hoxb8-FL modification strategies, I developed protocols to induce Cre-mediated DNA recombination *in vitro* at the progenitor state in cells that carry loxP site-flanked DNA segments. Electroporation of Cre mRNA or transduction of Cre recombinase protein fused to a TAT domain into Hoxb8-FL cells resulted in efficient recombination of loxP-sites and enabled the expression of target genes upon deletion of a loxP-flanked stop cassette *in vitro*. Utilizing these *in vitro* Cre-delivery methods will enable me to expand my Hoxb8-FL cell pool repertoires without the need to breed loxP-carrying conditional transgenic animals with a Cre-deleter strain (i.e., Mx1-Cre) to obtain Cre-recombined Hoxb8FL cell pools. Previously, Velasco-Hernandez and

colleagues studied the functions of genes in hematopoiesis via *ex vivo* TAT-Cre treatment of murine HSPCs in *in vivo* transfer experiments as an alternative to employing the Mx1cre-deleter strain (Velasco-Hernandez et al., 2016). Although only the short-term (15 day) reconstitution efficiencies of TAT-Cre treated HSPCs were examined in their study, the observation of preserved hematopoietic reconstitution of these cells can support the idea that TAT-Cre treated Hoxb8-FL cells can maintain their *in vivo* reconstitution potential after the *in vitro* delivery of the protein. Therefore, in the future, these Hoxb8-FL cells can be used in *in vivo* transfer experiments to investigate the role of genes starting at early hematopoietic developmental stages.

#### **4.3. Introduction of Lymphoma-Predisposing Genetic Alterations in VavP-Bcl2 Hoxb8-FL cells by CRISPR/Cas9**

Following the establishment of different gene editing protocols in Hoxb8-FLs, I was able to introduce lymphoma-related genetic perturbations into these cells. *KMT2D*, an epigenetic regulator recurrently mutated in follicular lymphoma patients, became a major interest for me to target in BCL2 overexpressing Hoxb8-FL cells as it is an early founder hit in lymphomagenesis (Morin et al., 2011) (Pasqualucci, Trifonov, et al., 2011) (Okosun et al., 2014) (Zhang et al., 2015) (Green et al., 2015). Since *KMT2D* alterations are reported to result in inactivation, I utilized a CRISPR/Cas9-mediated knockout strategy to inactivate *KMT2D* for further investigations. After electroporation or viral expression of my designed sgRNAs in Hoxb8-FL cell pools, I obtained a decent proportion of cells carrying a spectrum of indels in the targeted regions of *Kmt2d*. However, given the immense size of the gene (42 kb) and several different alternative transcripts rising from the locus, I considered generating targeted deletions in *Kmt2d* by combining different sgRNA pairs. Multiplexing of selected sgRNA pairs generated Hoxb8-FL cells with deletions in the gene locus spanning up to 31 kb. Moreover, further single-cell cloning of bulk cells enabled me to select mono-or bi-allelic deleted clones, which can eventually allow me to study the contribution of both mono-and bi-allelic truncating *KMT2D* mutations observed in lymphoma patients (Zhang et al., 2015). Importantly, because frequently detected mutations of *KMT2D* in FL were reported to impair the H3K4 methyltransferase activity of the protein, targeting only the C-terminal with this method can provide a precise approach to study the role of the SET

methyltransferase domain of KMT2D in lymphoma development (Pasqualucci, Trifonov, et al., 2011) (Morin et al., 2011) (Zhang et al., 2015). Also, in the future, it would be reassuring to show the loss of protein by Western blot (or SET domain inactivation by methyltransferase activity assays) in the targeted cells, as this would provide the ultimate proof for the CRISPR/Cas9-mediated inactivation of KMT2D. Furthermore, as an alternative to this deletion approach, my established CRISPR-mediated knock-in protocols can be utilized to generate conditional reactivatable KMT2D-deficient founder progenitor cells by targeting a stop cassette with a fluorescence reporter to the 5' of the gene. This strategy would allow both inactivation of the gene and enrichment of the targeted cells by fluorescence selection. Then, one could study the effects of KMT2D re-activation in lymphoma. Finally, thanks to long-term culturing capacity of the Hoxb8-FL system, additional genetic alterations on the established KMT2D-deficient VavP-Bcl2 Hoxb8-FL cell pools can be introduced to investigate the role of collaborating lesions in follicular lymphoma. For example, elucidating the cooperative role of mutations detected in chromatin modifying genes (KMT2D, CREBBP, EZH2) would be very interesting to determine the essential biological mechanisms that lymphoma cells rely on during the progression and can help to illuminate the reasons for the observed strong dependencies between these epigenetic regulators (Pasqualucci et al., 2014) (Green, 2018).

Of the other highly mutated FL genes, I targeted in VavP-*Bcl2* Hoxb8-FLs the immune modulator, *TNFRSF14* (*HVEM*), whose loss of function is attributed to increased lymphomagenesis (Boice et al., 2016) (Mintz et al., 2019). Through viral expression of sgRNAs targeting the early exons of HVEM, I could achieve efficient knockout of TNFRSF14. One technical advantage of targeting this gene were its relatively high levels of expression in Hoxb8-FL cells and therefore easy detection by FACS, as this allows me to FACS-purify and work with the pure knockout progenitor populations in the subsequent experiment steps. The study of Mintz and colleagues demonstrated that HVEM deficiency in B cells reshapes the microenvironment through the BTLA axis, characterized by constant, augmented Tfh signaling in the germinal centers, which in turn leads to the accumulation of BCL2 overexpressing pre-malignant B cells when HVEM deficiency is combined with BCL2 overexpression in B cells (Mintz et al., 2019). In a similar direction, BCL2-transgenic mouse models already highlighted the importance of enhanced T cell help in follicular

lymphoma development; while only B cell-restricted BCL2 expressing E $\mu$ -Bcl2 transgenic mice do not develop FL, VavP-Bcl2 transgenic mice, which were shown to have an increased frequency of helper T cells due to the induced BCL2 expression also in the T cell compartment, develop FL in 50% of aged mice (Strasser et al., 1993) (Egle et al., 2004). In this regard, acquisition of HVEM mutations could be a crucial step for FL development, as HVEM-deficient B cells remodel their microenvironment to receive enhanced T cell help. Also, according to sequencing studies, KMT2D and HVEM mutations are described as early clonal events and stay stable throughout the progression. Therefore, it would be interesting to highlight their relation to each other; for example, whether one mutation preconditions the acquisition of the other and whether a sequential acquisition of KMT2D and HVEM mutations in a particular order is critical for the evolution of FL (Okosun et al., 2014). Therefore, testing the effect of HVEM inactivation together with KMT2D silencing, especially in B cell-restricted BCL2 expressing mouse models, could unveil the natural evolution steps of follicular lymphoma by eliminating the artificially inflated presence of BCL2-overexpressing T follicular helper cells and therefore T cell help present in the VavP-BCL2 transgenic mouse model.

#### **4.4. The VavP-Bcl2 Hoxb8-FL Adoptive Transfer Model: A Novel System for Studying GCB Cells and GC derived B-Cell Lymphomas**

After establishing efficient gene editing protocols in Hoxb8-FL cells, I generated many independent BCL2-expressing Hoxb8-FL cell pools of different genotypes. As a next step, I validated their potential to serve as a novel *in vivo* model to identify, interrogate and validate molecular mediators of GCB cells and GC derived B cell lymphomas.

Initially, I showed that upon adoptive transfer of VavP-Bcl2 Hoxb8-FL cells together with B-cell deficient bone marrow cells into lethally irradiated mice, Hoxb8-FL derived myeloid and lymphoid cells can be detected in the blood of transplanted mice by day 10. At early time points of the reconstitution, Hoxb8-FL derived myeloid cells constituted a major proportion of the blood cells, and they drastically decreased within a week. As myeloid cells generally exhibit a short life span, their only transient presence in the blood following reconstitution, as also shown by the study of Redecke and colleagues, is an anticipated feature of the *in vivo* differentiation

wave of the transferred Hoxb8-FL progenitors (Janssen et al., 2016) (Redecke et al., 2013). On the other hand, Hoxb8-FL derived B cells, which I showed to be present as early as 10 days after transfer, persisted continuously throughout all analysis time points, which spanned over 6 months. By day 20, a small proportion of Hoxb8-FL derived T cells could be detected in the blood of mice reconstituted with one of the VavP-Bcl2 Hoxb8-FL lines demonstrating preserved T cell potential, and the population showed a minor rise over time. Overall, the *in vivo* differentiation of VavP-Bcl2 Hoxb8-FL progenitor cells into mature myeloid and lymphoid cells showed similar differentiation dynamics compared to that of WT Hoxb8-FL progenitors described by Redecke et al. (Redecke et al., 2013). However, it is crucial to highlight the variability that I observed in the multilineage potential of the generated VavP-Bcl2 Hoxb8-FL lines. Upon *in vivo* transplantation, all generated cell lines were able to robustly induce differentiation into myeloid compartments. In contrast, the reconstitution efficiency of Hoxb8-FL-derived lymphoid cells was highly dependent on the particular cell pool that was used. Even though most of the tested cell pools were diminished in their T cell reconstitution potential, one VavP-Bcl2 Hoxb8-FL line (among the 7 tested lines) efficiently gave rise to T cells and Hoxb8-FL derived mature CD4+ and CD8+ T cells were consistently detected in the secondary lymphoid organs. Interestingly, the majority of the transplanted VavP-Bcl2 Hoxb8-FL pools were capable efficiently produce B cell progenitors *in vivo*, although one of the tested lines had significantly reduced B cell potential *in vivo*. Therefore, for future experiments, it will be important to test the differentiation potential of the newly generated Hoxb8-FL pools prior to extensive manipulation for functional *in vivo* assays. Testing the capacities of cell pools can be performed by transplanting newly generated cells into recipient mice. Alternatively, *in vitro* lineage differentiation assays should be implemented and their results correlated to the *in vivo* differentiation potential of individual Hoxb8-FL cell pools. If *in vitro* results reliably predict *in vivo* differentiation behavior, Hoxb8-FL pools should be characterized and assessed for their differentiation capacities *in vitro*. For example, from every new line, a number of single cell clones can be selected for *in vitro* differentiation into myeloid, B, and T cells to estimate the progeny capabilities of the lines based on the calculated *in vitro* percentages (Redecke et al., 2013). Differences observed in the progeny potential of the Hoxb8-FL lines might be resulting from their cell of origin. I use reproducible parameters and protocols to generate these cell Hoxb8FL cell pools, which are reported to generally resemble the LMMP

progenitor state. Nevertheless, it is possible that during the transduction of unfractionated bulk bone marrow cells, depending on the availability or number of distinct (but somewhat similar) progenitor cell types, different proportions of multipotent progenitor (MPP) populations (MPP1-5) of the Lin<sup>-</sup> c-Kit<sup>+</sup> compartment are conditionally immortalized to form the respective Hoxb8-FL cell pool (Lai and Kondo, 2006; Iwasaki and Akashi, 2007; Cheng et al., 2020). As distinct MPP populations have different potentials to form lymphoid and myeloid cells, in the future approaches to enrich and transduce the MPP4 fraction, which is reported to have the highest potential to become lymphoid progeny, can be tested to enhance the likelihood of generating Hoxb8-FL lines with high lymphoid potential (Pietras et al., 2015) (Sommerkamp et al., 2021) .

Since my ultimate goal was to study GCB cell biology and tumorigenesis using my *in vivo* VavP-*Bcl2* Hoxb8-FL adoptive transfer system, I characterized the B cell compartment of the reconstituted mice in detail. Analysis of secondary lymphoid organs revealed that this model gives rise to all mature B cell subsets, including FOB, MZB, and, importantly, GCB cells. Interestingly, even though BCL2-expressing T cells were absent in this model, already one month after the transplant a sizeable GCB cell population could be identified. Furthermore, BCL2<sup>+</sup> plasma cells could also be detected at large proportions in all secondary lymphoid tissues and in the bone marrow as well. Remarkably, the proportion of mature B cell populations (including GCBs and PCs) in the lymphoid organs of the recipients of VavP-Bcl2 Hoxb8-FL cells was highly similar to that of VavP-*Bcl2* transgenic control animals. The striking spontaneous generation of large numbers of GCB cells and PC cells in the absence of immunization highlights the promising potential of the VavP-*Bcl2* Hoxb8-FL transplant system to study germinal center dynamics and lymphomagenesis. The indolent nature of FL is reflected in the VavP-*Bcl2* mouse model as tumor development mostly occurs at older ages (>6 months). Therefore, the sustained presence of VavP-*Bcl2* Hoxb8-FL derived B cells in my transplant model was also a crucial aspect to check. Even after 8 months, all mature B cell subsets were stably present in my aged cohorts, suggesting that the time-frame required for the indolent transformation of germinal center B cells could be achieved by this model.

Before targeting lymphoma relevant candidate alterations in my VavP-*Bcl2* Hoxb8-FL adoptive transfer system, I tested whether retrovirally transduced Hoxb8-FL cells expressing a THY1.1

reporter could develop and persist in the transplanted mice. Spike-in experiments that I conducted by mixing THY1.1<sup>+</sup> infected cells with non-infected cells at different ratios showed that the initial spike ratios of the *in vitro* culture were well preserved in the Hoxb8-FL derived B cells in the reconstituted mice even after months. This indicates that retrovirally infected THY1.1<sup>+</sup> Hoxb8FL-derived cells are not negatively or positively selected *in vivo*. Therefore, in the future this system can be employed to track the impact of induced genetic changes on the evolution of the targeted B cells.

To facilitate CRISPR-mediated gene knockouts *in vivo* at distinct B cell developmental stages via conditional Cas9 expression, I generated different Cre-carrying cell pools. One of the pools generated in this effort was a VavP-Bcl2 Cy1cre LSL-Cas9-GFP Hoxb8-FL preparation to conditionally knockout genes in GCB cells. Remarkably, a high proportion of GFP-expressing GCB cells and PCs in lymphoid organs could be detected after the adoptive transfer, indicating efficient Cy1-Cre mediated deletion of the loxP-flanked stop cassette in class switched GCB cells *in vivo*. In the future, this conditional targeting system could enable *in vivo* CRISPR-knockout screens in germinal center B cells to identify mediators of GCB-PC cell differentiation and lymphomagenesis. For example, in FL patients, in addition to the most frequent translocation of t(14;18), secondary genomic aberrations including large chromosomal deletions are commonly detected (Mohamed et al., 2001). These large genomic regions may cover (multiple) tumor suppressors. In order to determine whether relevant tumor suppressors are present in these lesions, functional approaches, including unbiased genetic screens, can be conducted. For instance, in up to 30% of FL patients chromosome 6q deletions are observed and associated with poor outcomes (Oricchio et al., 2017) (Cheung et al., 2009). Oricchio and colleagues (2011 and 2017) identified two FL-related tumor suppressor genes located in this chromosomal region: ephrin receptor A7 (EPHA7) and SESTRIN1 by targeting 6q-genes with a pooled shRNA library in a murine pro-B cell line and validating them *in vivo* using lymphoma mouse models (Oricchio et al., 2011) (Oricchio et al., 2017). In the future, I can employ the VavP-Bcl2 Hoxb8-FL transfer model to conduct *in vivo* CRISPR screens using pooled sgRNA libraries: This will allow me to assess several putative regulators at once in the presence of an intact microenvironment. Moreover, the fact that my model enables the cell type as well as differentiation stage specific

introduction of genetic alterations is a considerable step forward compared to panhematopoietic shRNA-mediated gene silencing. In addition to screens, the transfer model can also be employed for in depth validation studies in a model in which only B cells carry the BCL2 transgene, which more closely reflects human FL compared to VavP-Bcl2tg mice.

Furthermore, I wanted to adapt this conditional targeting system not only to inactivate candidate tumor suppressors but also to overexpress lymphoma-associated proto-oncogenes *in vivo*. MYC and BCL6, two important germinal center regulators, are frequently involved in germinal center derived malignancies and are considered potent oncogenes especially in aggressive forms of lymphoma including tFL, DLBCL, and double-hit/triple-hit lymphomas (Kridel et al., 2015) (Godfrey et al., 2019). The combination of alterations affecting the expression of BCL2, MYC and BCL6 is associated with a poor prognosis in patients (Johnson et al., 2009) (Xia & Zhang, 2020). To study the effects of the activation of these oncogenic targets in the germinal center, I generated Cre-inducible retroviral MYC- and BCL6-expression constructs carrying the THY1.1 or thCD2 surface markers to identify transduced cells, respectively (Turner et al., 2010) (Shoumariyeh et al., 2020). VavP-Bcl2 Cy1cre LSL-Cas9-GFP Hoxb8-FL cells, transduced with conditional BCL6 and MYC expression vectors, were adoptively transferred and the recipient mice were monitored. Mice reconstituted with the conditional expression vectors showed a significant reduction in survival rates and had lymphoid tumors consisting of B cells expressing high levels of THY1.1, indicating a synergistic MYC & BCL2 mediated malignant transformation of B cells. However, these malignant B cells did not show signs of a germinal center surface phenotype or of having passed through the germinal center: some were IgM positive and others generally lacked surface Ig expression and none showed signs of Cre-mediated recombination of the R26-LSL-Cas9-GFP locus, as they were without exception GFP negative. The phenotype that I observed resembled the lymph node-inhabiting pre-B/B cell lymphomas of the Eμ-*bcl2/myc* transgenic mouse model described in the study of Strasser and colleagues, in 1990 (Strasser et al., 1990). Overall, these observations may indicate a possible leaky MYC expression from the conditional retroviral vector in the absence of Cre-mediated recombination. Cre-independent expression of the highly aggressive proto-oncogene MYC in early B cells might lead to transformation of developing B cells and the occurrence of pre-GC B cell tumors before the

transformation of GCB cells through conditional MYC/BCL6 activation can take place. A study by Shoumariyeh and colleagues reported surprising differences regarding the altered leakiness of similar retroviral conditional expression constructs depending on the loxP-flanked Stop sequence, which supports this hypothesis (Shoumariyeh et al., 2020). In this line, analyzing the genomic DNA of these tumors to assess excision of the stop cassette might give hints about the leakiness of my constructs. In the future, instead of these translational stop cassette-carrying conditional expression vectors, other transgene expression vectors designed to drive the expression of the transgene of interest only after Cre-mediated uni-directional inversion, could be used. This approach eliminates the problem of leakiness given the reverse orientation of the transgene of interest in the expression vector and has been validated in a model of MYC overexpression with concomitant p53 knock-down (Schnütgen et al., 2003) (Stern et al., 2008) (Yau et al., 2013).

#### **4.5. Contribution of the Established Model System and Potential Pitfalls with Alternative Solutions**

To dissect the role of genes in GC biology and lymphoma development *in vivo*, primarily two techniques were employed up to now. One approach involves the generation of murine models by breeding transgenic animals carrying the desired mutations. This requires the availability or establishment of mouse strains with the target mutations, complex breeding steps to achieve final experimental genotypes and the necessity of maintaining breeding cohorts continuously. In comparison to the breeding-based establishment of transgenic mouse models, my (VavP-*Bcl2*) Hoxb8-FL transfer system allows integration of the desired mutations much faster via utilization of the above-described genetic tools. The new model bypasses many expensive and complex breeding steps.

A second approach previously employed to study lymphoma biology in mouse models involves *in vitro* manipulation and adoptive transfer of primary hematopoietic stem and progenitor cells (BM or fetal liver progenitor cells), similar to my Hoxb8-FL system. In this approach, however, in contrast to Hoxb8-FLs, the limited culture duration of primary stem and progenitor cells restricts the time-frame and therefore possibilities to introduce multiple different mutations and to

select for the cells carrying the desired induced genetic changes. Overall, this restricts the number and diversity of genetic alterations that can be investigated. Until now, investigation of follicular lymphoma regulators via transfer of progenitor cells involved the transduction of VavP-*Bcl2* progenitor cells with constitutively active shRNA-expression vectors for knocking down the respective target genes (Ortega-Molina et al., 2015) (Oricchio et al., 2011) (Boice et al., 2016) (Ortega-Molina et al., 2019). Even though this strategy has served as an important and valuable methodology, it carries some pitfalls, such as the incomplete knockouts afforded by the use of shRNA vectors. Although some studies implemented CRISPR/Cas9-based gene targeting strategies in primary mouse progenitors to study gene functions in B cells *in vivo*, this approach can still be challenging. This is especially the case when multiple mutations have to be combined or more sophisticated gene knock-in to be implemented, as those may require longer times in culture to introduce or select for the desired changes (LaFleur et al., 2019) (Laidlaw et al., 2020) (Duan et al., 2021). The Hoxb8-FL adoptive transfer system can overcome these issues since these cells can be cultured over long periods of time to achieve a high genetic complexity through introduced modifications. Another pitfall stems from the use of constitutively expressed shRNA or overexpression vectors since modified progenitors reconstitute the entire hematopoietic system of the transplanted mice, and this leads to the presence of the induced alterations not only in B cells but also in the other blood lineages, including T and myeloid cells. As a result, relating the observed phenotypes to causally to genetically modified B cells can become more difficult (Mintz et al., 2019). I can overcome this problem by using my established B-cell specific conditional Hoxb8-FL lines, which provide Cre-mediated spatial and temporal control over the induced alterations.

Few Hoxb8-FL cell preparations have *in vivo* T cell differentiation capacity, an observation also made by Redecke and colleagues. In comparison with VavP-Bcl2tg mice, this might impede lymphoma development in my adoptive transfer system, since reconstituted mice in which B cells are the only long-lived immune lineage overexpressing BCL2 lack the lymphomagenic microenvironment generated by the excessive number of BCL2-expressing T helper cells of the VavP-*Bcl2* model (Egle et al., 2004). In this regard, the VavP-*Bcl2* Hoxb8-FL adoptive-transfer model might resemble the B cell lineage-restricted BCL2 over-expressing E $\mu$ -*Bcl2* transgenic

mice, that do not develop follicular lymphomas in the absence of other mutations (Strasser et al., 1993) (Meyer et al., 2021). On the other hand, this feature of my system can serve as a favorable alternative strategy to define the natural developmental stages of FL. Essential relevant FL-defining genetic alterations (i.e. inactivation of *Tnfrsf14*, *Kmt2d*) may, when introduced into BCL2-overexpressing B cells, naturally trigger the formation of a protumorigenic microenvironment in place of artificially induced enhanced T cell help through the genetically encoded pan-hematopoietic BCL2 overexpression of the VavP-Bcl2 model (Kridel et al., 2012). Therefore, the adoptive transfer model with additional FL-defining mutations may better reflect the natural progression steps of FL. In addition, human FL is thought to be triggered by a singular or rare translocation in proB cells and the subsequent expansion of mature B cells derived from these progenitors, which then acquire additional mutations. Also, this aspect is better modelled by a single wave of differentiating Hoxb8-FL cells, instead of the life-long production of Bcl2tg B cells in the other models. On the other hand, when it becomes necessary to identify the effect of induced alterations in B cells in the presence of BCL2-overexpressing T and myeloid cells, this limitation can be easily overcome by exchanging the B cell-deficient supportive BM cells (*Mb1-Cre<sup>i/i</sup>*) with B cell-deficient BCL2-overexpressing supportive bone marrow (VavP-Bcl2 *Mb1-Cre<sup>i/i</sup>*). Therefore, by simple adaptations of the transfer model, E $\mu$ -*Bcl2* or VavP-*Bcl2* transgenic lines can be easily recapitulated in my model. Furthermore, this modular system also allows me to functionally investigate the interplay between the microenvironment and tumor cells, for example by using T-cell deficient or myeloid-deficient supportive BM cells.

Another potential pitfall of my VavP-*Bcl2* *Hoxb8-FL* adoptive transfer system might be caused by the limited self-renewal capacity of Hoxb8-FL cells *in vivo*. These cells highly resemble lymphoid-primed multipotent progenitor LMPP cells, and therefore, they have diminished self-renewal capacity compared to HSCs (Redecke et al., 2013) (Kucinski et al., 2020). As a result, after the *in vivo* transfer of cells, there is only a transient wave of mature blood cell production and differentiation, which does not fully recapitulate the transgenic mouse models or BM chimeras in which mature B cell production is continuous throughout life. However, it is likely that additional integration of critical lymphoma-defining mutations in addition to BCL2 overexpression may suffice to eliminate the necessity for continuous cell generation and trigger

malignant transformation even in a single differentiation wave. Furthermore, as alluded to above, the adoptive transfer system reflects the ontogeny of human FL much better compared to the endogenous transgenic mice.

Here, I demonstrate the potential of the Hoxb8-FL-based adoptive transfer system to model human FL and other lymphoid malignancies characterized by BCL2 overexpression. Similarly, the generation of Hoxb8-FL cells carrying hallmark genetic alterations of other lymphomas and diseases (CyclinD1 in mantle cell lymphoma, MyD88L265P in Waldenström Macroglobulinemia, TCL1 in chronic lymphocytic leukemia) can expand the scope of the adoptive transfer model (Wang et al., 2009) (Treon et al., 2012) (Bichi et al., 2002).

To my knowledge, the VavP-*Bcl2* Hoxb8-FL adoptive transfer system is the first study employing Hoxb8-FL cells to systematically study B cell differentiation and function since it was first described by the group of Hans Häcker (Redecke et al., 2013). Given the technical and modular advantages of the system and my established gene-targeting strategies, I believe it can constitute a valuable *in vivo* approach to model the genetic complexity and clonal evolution of B-cell lymphomas in particular because it allows dissecting the roles of the microenvironment.

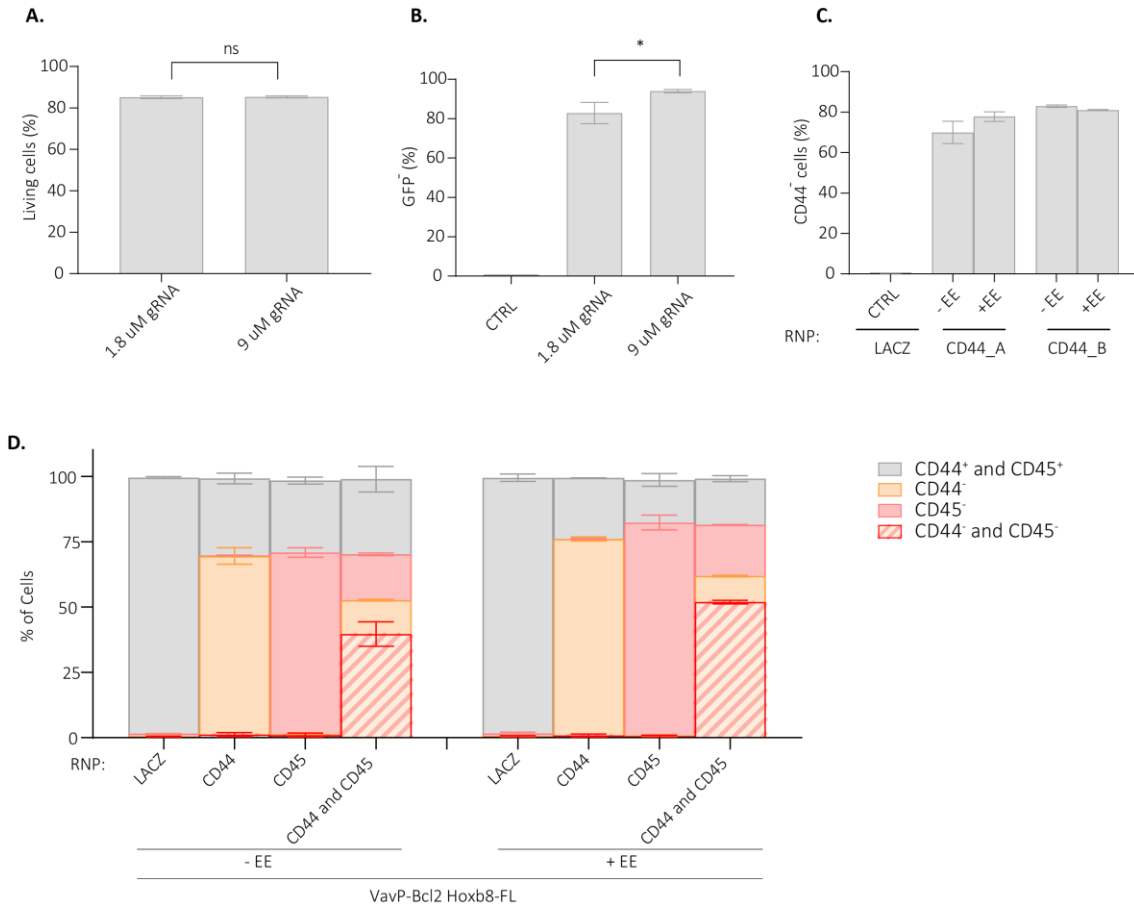
## 5. SUPPLEMENTARY MATERIAL

| Hoxb8-FL line name             | Genotype  | Cre-induction | Line-ID | <i>In vivo</i> reconstitution: |
|--------------------------------|---|---------------|---------|--------------------------------|
| VavP-Bcl2                      | <i>VavP-Bcl2 tg</i>                                     | -             | Line-1  | Myeloid and B                  |
|                                |   |               | Line-2  | Myeloid, B and T               |
| VavP-Bcl2 CD19cre LSL-Cas9-GFP | <i>VavP-Bcl2 CD19crei/wt R26-LSL-Cas9-eGFP i/wt</i>     | pro/pre-B     | Line-3  | Myeloid                        |
|                                |   |               | Line-4  | N.T.                           |
| VavP-Bcl2 Mb1cre LSL-Cas9-GFP  | <i>VavP-Bcl2 Mb1crei/wt R26-LSL-Cas9-eGFPi/wt</i>       | pro-B         | Line-5  | N.T.                           |
| VavP-Bcl2 Cy1cre LSL-Cas9-GFP  | <i>VavP-Bcl2 Cy1crei/wt R26-LSL-Cas9-eGFP i/wt</i>      | GCB           | Line-6  | Myeloid and B                  |
|                                |   |               | Line-7  | Myeloid and B                  |
|                                |   |               | Line-8  | N.T.                           |
| VavP-Bcl2 LSL-Cas9-GFP         | <i>VavP-Bcl2 R26-LSL-Cas9-eGFPi/wt</i>                  | -             | Line-9  | Myeloid and B                  |
| VavP-Bcl2 LSL-PB ATP           | <i>VavP-Bcl2 R26-LSL-PBi/wt ATP2-H32 tg</i>             | -             | Line-10 | N.T.                           |
|                                |   |               | Line-11 | N.T.                           |
| VavP-Bcl2 CD19cre LSL-PB ATP   | <i>VavP-Bcl2 CD19crei/wt R26-LSL-PBi/wt ATP2-H32 tg</i> | pro/pre-B     | Line-12 | Myeloid and B                  |
|                                |   |               | Line-13 | Myeloid and B                  |
| WT                             | <i>C57BL/6N</i>   | -             | Line-14 | N.T.                           |
| Cas9-GFP                       | <i>R26-Cas9-P2A-eGFP</i>                                | -             | Line-15 | N.T.                           |

N.T.: Generated line's *in vivo* reconstitution potential not tested.

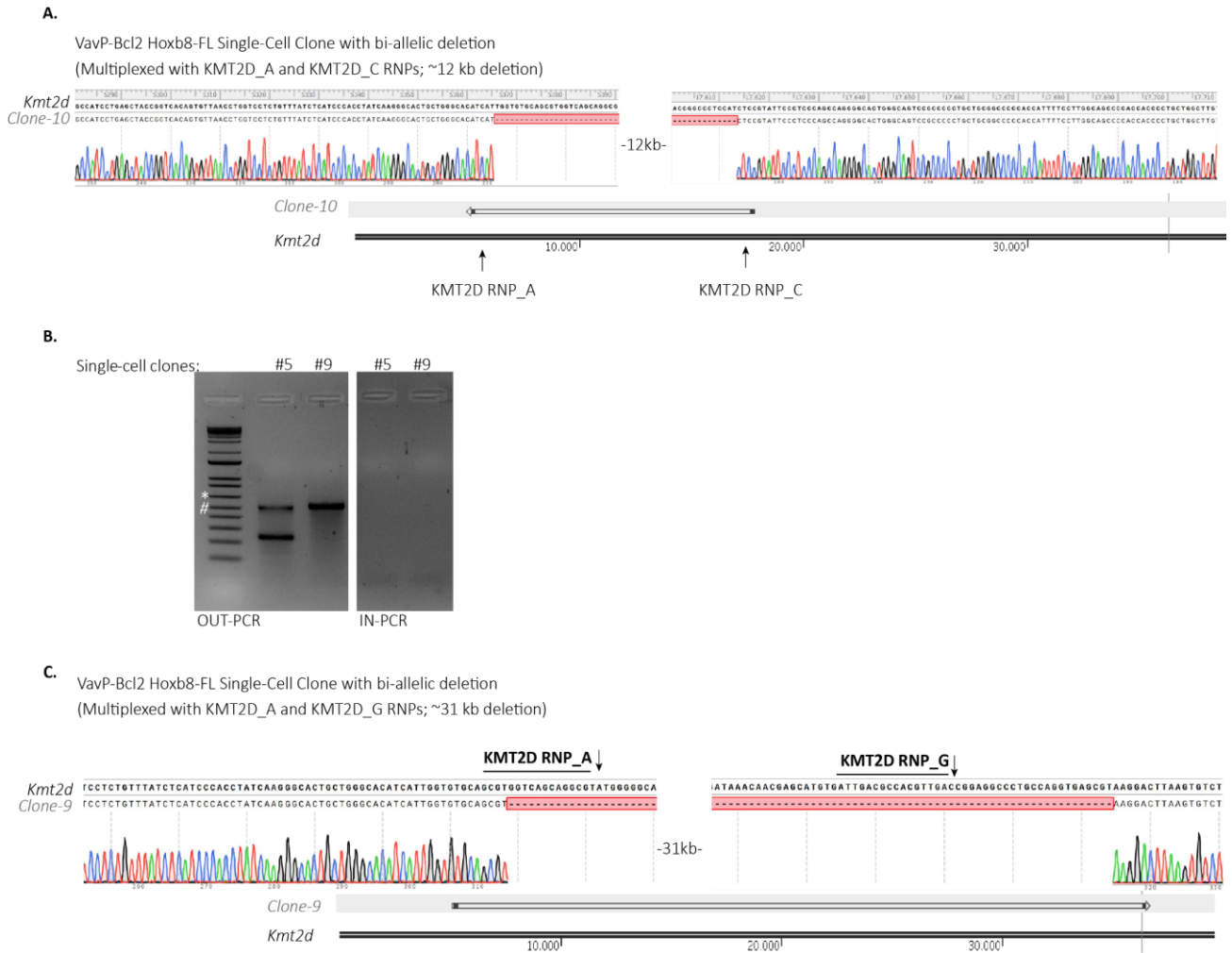
### Supplementary Table. 1. Summary of the generated Hoxb8-FL cell lines

The table reports the genotype of mice used for the generation of Hoxb8-FL lines. The *in vivo* reconstitution potential of the lines into myeloid (CD11b<sup>+</sup>) and lymphoid subsets (B cells B220<sup>+</sup>; T cells TCRβ<sup>+</sup>) is listed if they are tested by the adoptive transfer of cells into recipient mice.



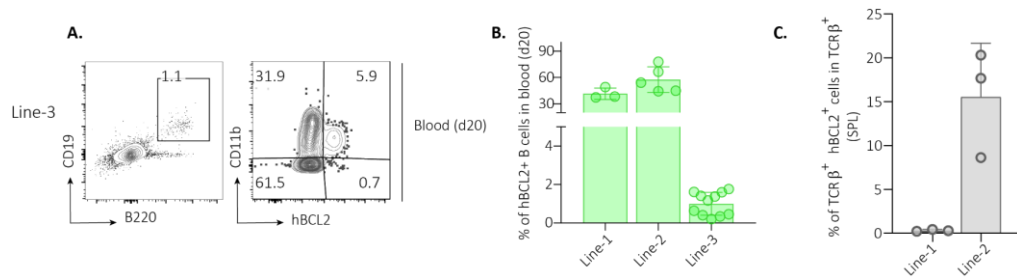
**Supplementary Figure 1: Optimization of Hoxb8-FL electroporation conditions**

**A)** Flow cytometry–based viability (PF840<sup>+</sup>) assessment in Cas9-GFP Hoxb8-FL cells; 48 hours after electroporation with 1.8  $\mu$ M or 9  $\mu$ M GFP-targeting (GFP) crRNA:tracrRNA gRNA complexes (n=2-5, mean $\pm$ SD). Two-tailed Student’s t-test (ns P > 0.05). **B)** Flow cytometry–based assessment of GFP gene editing in Cas9-GFP Hoxb8-FL cells; 48 hours after electroporation with control (LACZ) or GFP-targeting (GFP) crRNA:tracrRNA gRNA complexes (n=2-4, mean $\pm$ SD). Two-tailed Student’s t-test (\*P < 0.05). **C)** Flow cytometry–based assessment of CD44 gene editing in VavP-Bcl2 Hoxb8-FL cells 4 days after electroporation with RNPs. Control (LACZ) or CD44-targeting (CD44\_A or CD44\_B) RNPs were precomplexed at the determined optimum 1:0.8 gRNA:Cas9 molar and electroporated into cells in the presence or absence of the electroporation enhancer (EE) (n=2-5, mean $\pm$ SD). **D)** Flow cytometry–based assessment of CD44 and CD45 gene editing in VavP-Bcl2 Hoxb8-FL cells 2 days after electroporation with RNPs. Control (LACZ), CD44-targeting (CD44\_A) or CD45-targeting (CD45) RNPs were precomplexed individually and electroporated into cells singularly or in combination in the presence or absence of EE (n=2, mean $\pm$ SD).



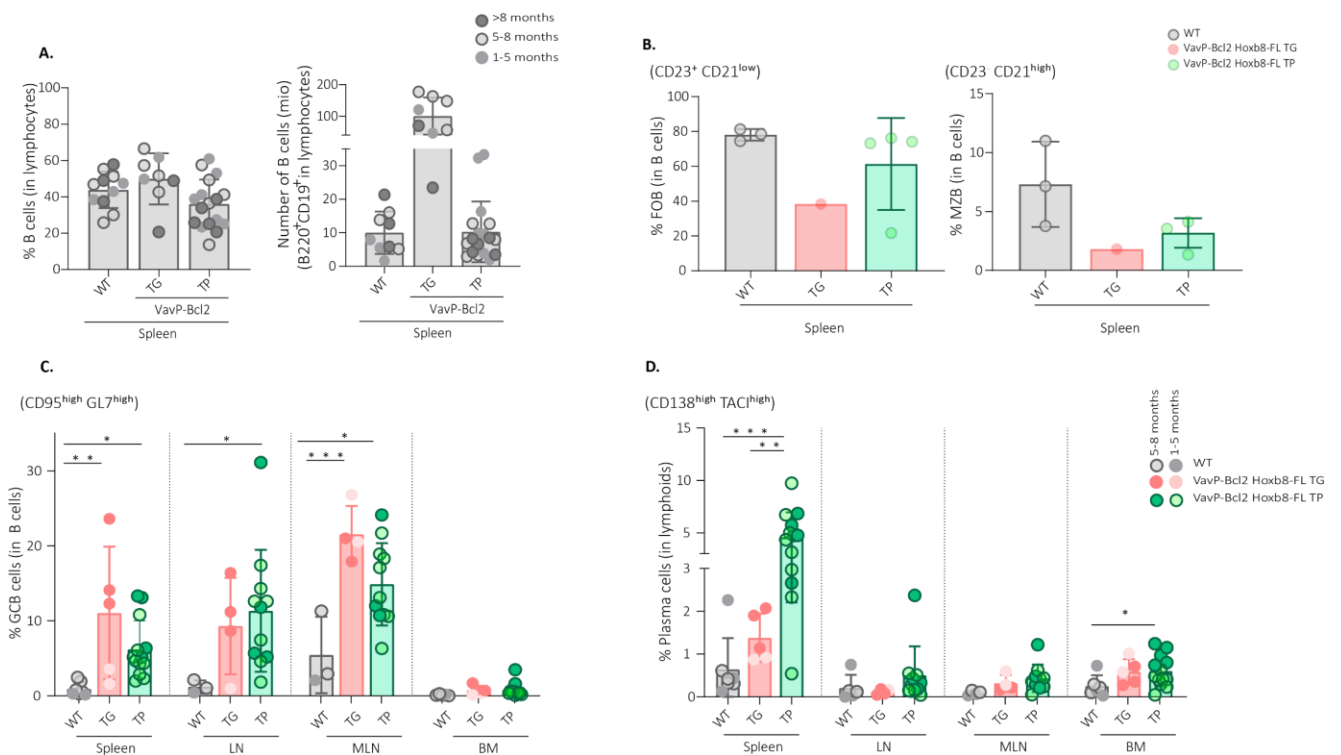
**Supplementary Figure 2: Kmt2d locus-deletions in VavP-Bcl2 Hoxb8-FL cells via RNP multiplexing**

**A)** Sanger-sequencing chromatogram of a single-cell clone (Clone-10) identified with a bi-allelic deletion band in the 12 kb-deletion condition (co-electroporation of KMT2D\_A and KMT2D\_C RNPs). Sequencing data aligned to the *Kmt2d* genomic sequence and the homozygous deletion region covering the 12 kb area was represented with the red line. **B)** Representative gel image of in- and out-PCRs identifying the *Kmt2d* deletion status of VavP-Bcl2 Hoxb8-FL single-cell clones that were generated from KMT2D\_A and KMT2D\_G RNPs' multiplexing (~31 kb deletion). For out-PCR the primer pair PP2 and for in-PCR the primer pair PP7 was used. # corresponds to the 500 bp-band and \* corresponds to the 650 bp-band in the ladder. **C)** Sanger-sequencing chromatogram of a single-cell clone (Clone-9) identified with a bi-allelic deletion band in the 31 kb-deletion condition (co-electroporation of KMT2D\_A and KMT2D\_G RNPs). Sequencing data aligned to the *Kmt2d* genomic sequence and the homozygous deletion region covering the 31 kb area was represented with the red line.



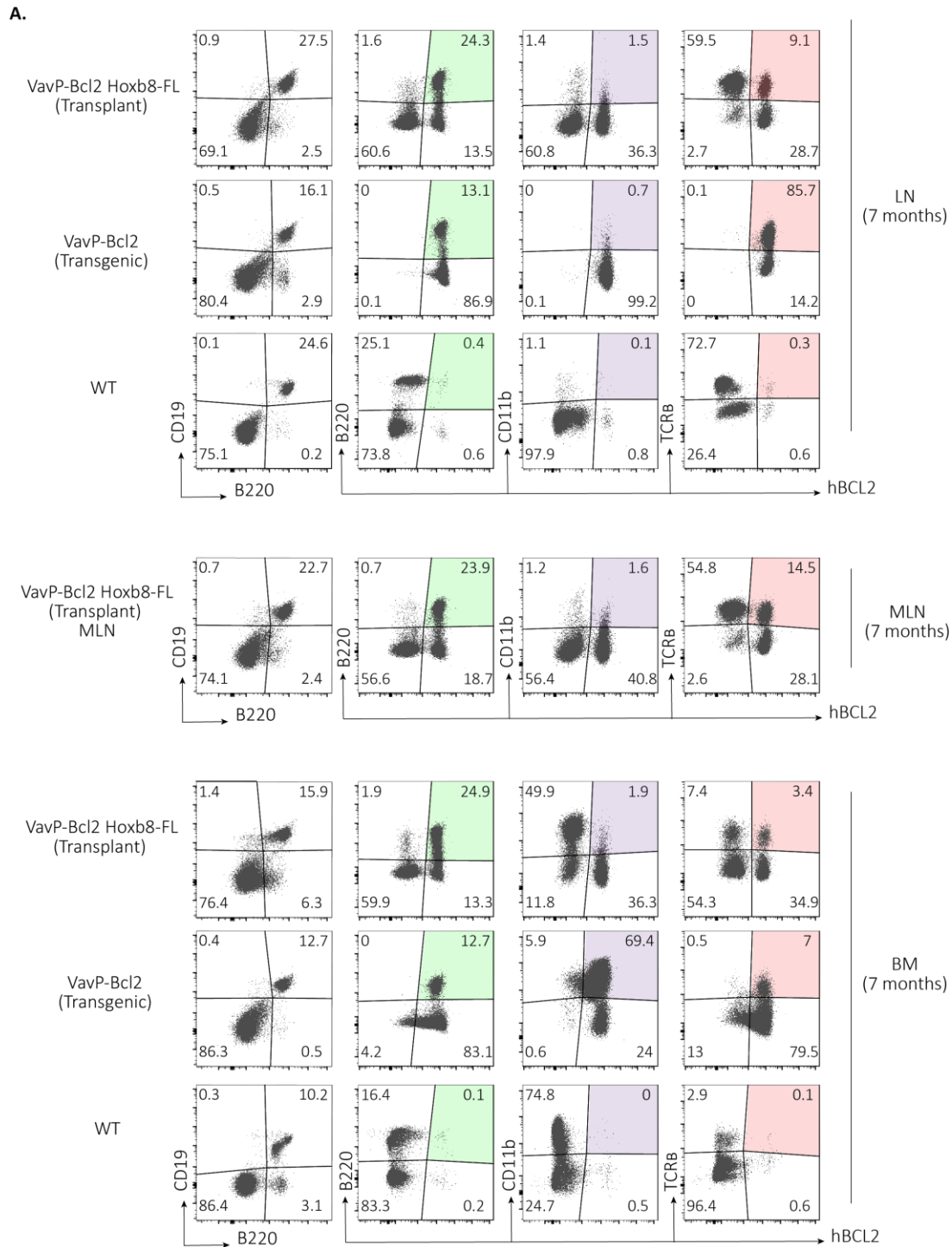
**Supplementary Figure 3: Adoptive transfer of VavP-Bcl2 Hoxb8-FL cells**

**A)** Representative FACS plots of hBCL2, B220 and CD19 expression in peripheral blood of lethally irradiated mice transplanted with VavP-Bcl2 Hoxb8-FL Line-3 (20 days after the transplantation). Numbers in quadrants indicate percentages. Plots are representative of data obtained from eleven mice transferred with VavP-Bcl2 Hoxb8-FL Line-3. Data are representative of 3 experiments. **B)** Percentage of hBCL2<sup>+</sup> B (B220<sup>+</sup>) cells in the peripheral blood of lethally irradiated mice transplanted with VavP-Bcl2 Hoxb8-FL Line-1, Line-2 or Line-3. (n=2-11, mean±SD). **C)** Percentage of hBCL2<sup>+</sup> T (TCRβ<sup>+</sup>) cells among the total T cells in the spleens of lethally irradiated mice transplanted with VavP-Bcl2 Hoxb8-FL Line-1 or Line-2 (3-4 months after the transplantation) (n=3 for each line, mean±SD).



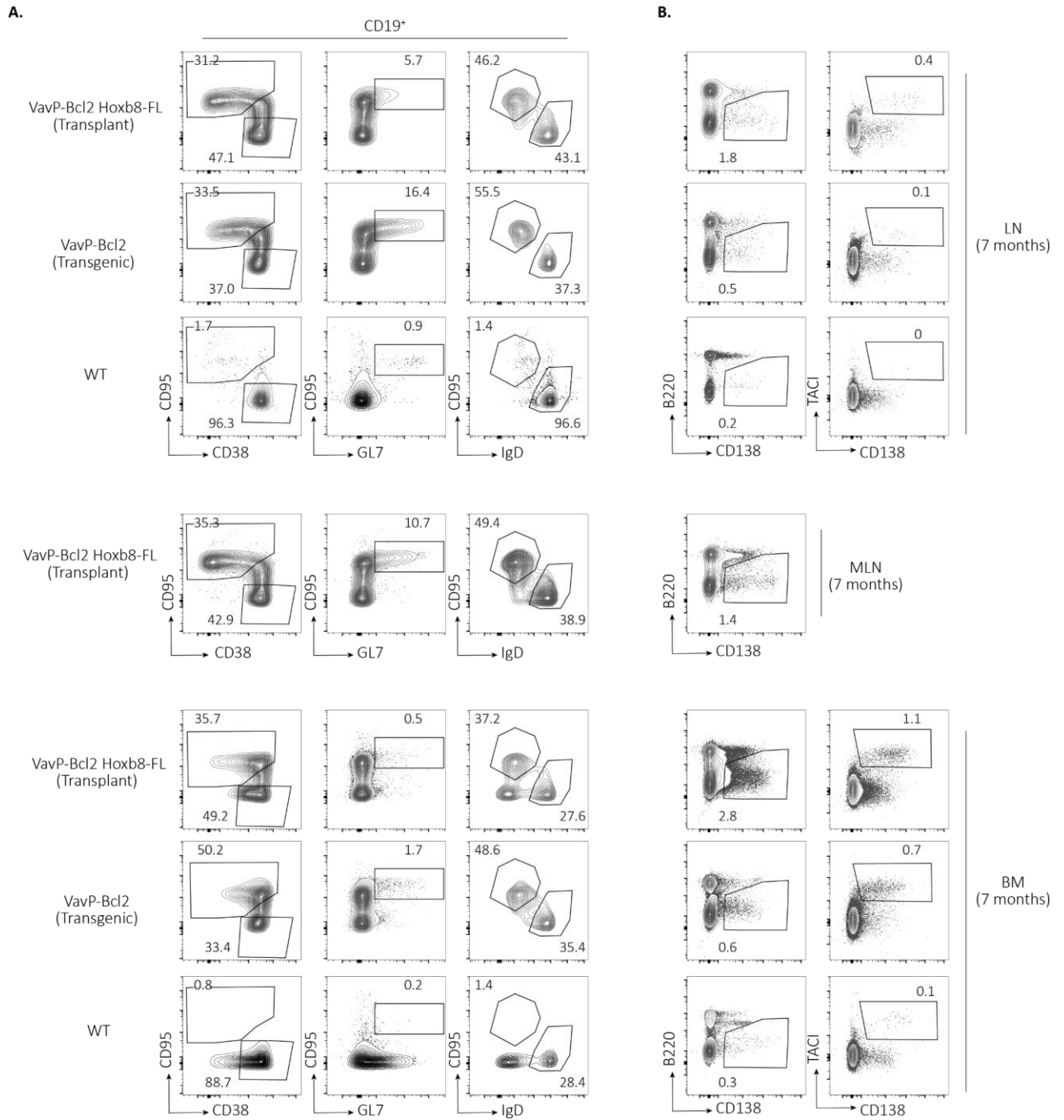
**Supplementary Figure 4: Adoptive transfer of VavP-Bcl2 Hoxb8-FL cells and ensuing B-cell differentiation *in vivo***

**A)** Percentage and number of B cells (B220<sup>+</sup> CD19<sup>+</sup>) and in the spleen of mice transplanted with VavP-Bcl2 Hoxb8-FL cells (TP), untreated control WT and VavP-Bcl2 Hoxb8-FL transgenic (TG) mice. (n ≥ 2 for each time-interval, mean±SD). Four independent VavP-Bcl2 Hoxb8-FL cell lines were tested. Data are representative of 6 experiments. **B)** Percentage of marginal zone B (MZB, B220<sup>+</sup> AA4.1<sup>-</sup> CD23<sup>-</sup> CD21<sup>high</sup>) and follicular B (FOB, B220<sup>+</sup> AA4.1<sup>-</sup> CD23<sup>+</sup> CD21<sup>low</sup>) cells in spleen of mice transplanted with VavP-Bcl2 Hoxb8-FL cells (TP), untreated control WT and VavP-Bcl2 Hoxb8-FL transgenic (TG) mice. (n=1 for VavP-Bcl2 Hoxb8-FL transgenic (TG) n ≥ 2 for the rest, mean±SD). **C)** Percentage of germinal center B cells (GCB, CD19<sup>+</sup> CD95<sup>+</sup> GL7<sup>+</sup>) in spleen, lymph nodes (LN), mesenteric lymph nodes (MLN) and BM of mice transplanted with VavP-Bcl2 Hoxb8-FL cells (TP), untreated control WT and VavP-Bcl2 Hoxb8-FL transgenic (TG) mice. (n ≥ 2 for each time-interval, mean±SD) Sidak's multiple comparisons test comparing all conditions to each other (\*P < 0.05, \*\*P < 0.01, \*\*\*P ≤ 0.001). Data are representative of 5 experiments. **D)** Percentage of plasma cells (PC, TAC1<sup>high</sup> CD138<sup>+</sup>) in spleen, lymph nodes (LN), mesenteric lymph nodes (MLN) and bone marrow (BM) of mice transplanted with VavP-Bcl2 Hoxb8-FL cells (TP), untreated control WT and VavP-Bcl2 Hoxb8-FL transgenic (TG) mice. Samples are pregated on CD45.2<sup>+</sup> cells. (n ≥ 2 for each time-interval, mean±SD) Sidak's multiple comparisons test comparing all conditions to each other (\*P < 0.05, \*\*P < 0.01, \*\*\*P ≤ 0.001). Data are representative of 5 experiments.



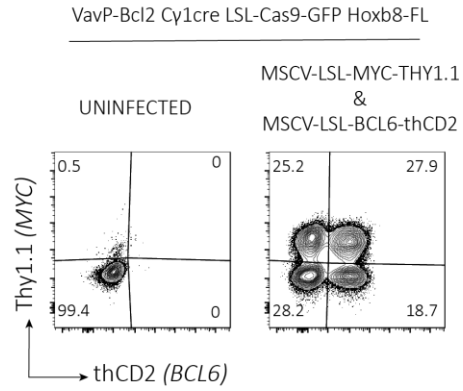
**Supplementary Figure 5: Adoptive transfer of VavP-Bcl2 Hoxb8-FL cells and *in vivo* differentiation**

Representative FACS plots of hBCL2 expression in lymph nodes (LN), mesenteric lymph nodes (MLN) and bone marrow (BM) of lethally irradiated mice transplanted (TP) with VavP-Bcl2 Hoxb8-FL cells (7 months after the transplantation). Samples are pregated on CD45.2<sup>+</sup> cells. Numbers in quadrants indicate percentages. Plots are representative of data obtained from four mice transferred with one of the two independent VavP-Bcl2 Hoxb8-FL cell lines. Tissue from untreated control mice (WT) and from transgenic (TG) VavP-Bcl2 mice were used for comparison. B cells (B220<sup>+</sup> CD19<sup>+</sup>), myeloid cells (CD11b<sup>+</sup>) and T cells (TCRβ<sup>+</sup>). Data are representative of 3 experiments (Analysis up to 10 months).



**Supplementary Figure 6: Adoptive transfer of VavP-Bcl2 Hoxb8-FL cells and ensuing B-cell differentiation in LN, MLN, BM**

**A)** Representative FACS plots of germinal center B cells (GCB, CD19<sup>+</sup> CD95<sup>high</sup> CD38<sup>low</sup> /CD95<sup>+</sup> GL7<sup>+</sup> /CD95<sup>+</sup> IgD<sup>+</sup>) and naive-B (CD19<sup>+</sup> CD95<sup>-</sup> CD38<sup>+</sup> /CD95<sup>-</sup> IgD<sup>+</sup>) cells in lymph nodes (LN), mesenteric lymph nodes (MLN) and bone marrow (BM), 7 months after the transplantation (TP) of VavP-Bcl2 Hoxb8-FL cells. Four independent VavP-Bcl2 Hoxb8-FL cell lines were tested. Numbers in quadrants indicate percentages. Data are representative of 5-7 experiments. (Analysis up to 10 months). **B)** Representative FACS plots of plasma cells (PC, B220<sup>low</sup> CD138<sup>high</sup>) in lymph nodes (LN), mesenteric lymph nodes (MLN) and bone marrow (BM), 7 months after the transplantation (TP) of VavP-Bcl2 Hoxb8-FL cells. Samples are pregated on CD45.2<sup>+</sup> cells. Four independent VavP-Bcl2 Hoxb8-FL cell lines were tested. Numbers in quadrants indicate percentages. Data are representative of 5-7 experiments. (Analysis up to 10 months).



**Supplementary Figure 7: Transduction of VavP-Bcl2 Cγ1cre LSL-Cas9-GFP Hoxb8-FL Cells with Retroviral Vectors for the Conditional Expression of c-MYC and BCL6**

Representative FACS plots of VavP-Bcl2 Cγ1cre LSL-Cas9-GFP Hoxb8-FL cells transduced with the retroviruses for conditional expression of c-MYC (MSCV-LSL-MYC-THY1.1) and BCL6 (MSCV-LSL-BCL6-thCD2). Hoxb8-FL cells were infected with two retroviral vectors together, then singly or doubly transduced cells are identified by the expression of Thy1.1 and thCD2 markers via FACS.

## 6. REFERENCES

- Adams, J. M., Harris, A. W., Pinkert, C. A., Corcoran, L. M., Alexander, W. S., Cory, S., Palmiter, R. D., & Brinster, R. L. (1985). The c-myc oncogene driven by immunoglobulin enhancers induces lymphoid malignancy in transgenic mice. *Nature*, *318*(6046), 533-538. <https://doi.org/10.1038/318533a0>
- Adli, M. (2018). The CRISPR tool kit for genome editing and beyond. *Nature Communications*, *9*(1), 1911. <https://doi.org/10.1038/s41467-018-04252-2>
- Adolfsson, J., Månsson, R., Buza-Vidas, N., Hultquist, A., Liuba, K., Jensen, C. T., Bryder, D., Yang, L., Borge, O. J., Thoren, L. A., Anderson, K., Sitnicka, E., Sasaki, Y., Sigvardsson, M., & Jacobsen, S. E. (2005). Identification of Flt3+ lympho-myeloid stem cells lacking erythro-megakaryocytic potential a revised road map for adult blood lineage commitment. *Cell*, *121*(2), 295-306. <https://doi.org/10.1016/j.cell.2005.02.013>
- Agudelo, D., Durringer, A., Bozoyan, L., Huard, C. C., Carter, S., Loehr, J., Synodinou, D., Drouin, M., Salsman, J., Dellaire, G., Laganière, J., & Doyon, Y. (2017). Marker-free coselection for CRISPR-driven genome editing in human cells. *Nat Methods*, *14*(6), 615-620. <https://doi.org/10.1038/nmeth.4265>
- Akasaka, T., Lossos, I. S., & Levy, R. (2003). BCL6 gene translocation in follicular lymphoma: a harbinger of eventual transformation to diffuse aggressive lymphoma. *Blood*, *102*(4), 1443-1448. <https://doi.org/10.1182/blood-2002-08-2482>
- Anzalone, A. V., Koblan, L. W., & Liu, D. R. (2020). Genome editing with CRISPR–Cas nucleases, base editors, transposases and prime editors. *Nature Biotechnology*, *38*(7), 824-844. <https://doi.org/10.1038/s41587-020-0561-9>
- Araf, S., Wang, J., Korfi, K., Pangault, C., Kotsiou, E., Rio-Machin, A., Rahim, T., Heward, J., Clear, A., Iqbal, S., Davies, J. K., Johnson, P., Calaminici, M., Montoto, S., Auer, R., Chelala, C., Gribben, J. G., Graham, T. A., Fest, T., Fitzgibbon, J., & Okosun, J. (2018). Genomic profiling reveals spatial intra-tumor heterogeneity in follicular lymphoma. *Leukemia*, *32*(5), 1261-1265. <https://doi.org/10.1038/s41375-018-0043-y>
- Armitage, J., Gascoyne, R., Lunning, M., & Cavalli, F. (2017). Non-Hodgkin lymphoma. *The Lancet*, *390*. [https://doi.org/10.1016/S0140-6736\(16\)32407-2](https://doi.org/10.1016/S0140-6736(16)32407-2)
- Bajaj, J., Hamilton, M., Shima, Y., Chambers, K., Spinler, K., Van Nostrand, E. L., Yee, B. A., Blue, S. M., Chen, M., Rizzeri, D., Chuah, C., Oehler, V. G., Broome, H. E., Sasik, R., Scott-Browne, J., Rao, A., Yeo, G. W., & Reya, T. (2020). An in vivo genome-wide CRISPR screen identifies the RNA-binding protein Stauf2 as a key regulator of myeloid leukemia. *Nature Cancer*, *1*(4), 410-422. <https://doi.org/10.1038/s43018-020-0054-2>
- Bak, R. O., Dever, D. P., & Porteus, M. H. (2018). CRISPR/Cas9 genome editing in human hematopoietic stem cells. *Nat Protoc*, *13*(2), 358-376. <https://doi.org/10.1038/nprot.2017.143>
- Bak, R. O., Dever, D. P., Reinisch, A., Cruz Hernandez, D., Majeti, R., & Porteus, M. H. (2017). Multiplexed genetic engineering of human hematopoietic stem and progenitor cells using CRISPR/Cas9 and AAV6. *Elife*, *6*. <https://doi.org/10.7554/eLife.27873>
- Bak, R. O., & Porteus, M. H. (2017). CRISPR-Mediated Integration of Large Gene Cassettes Using AAV Donor Vectors. *Cell reports*, *20*(3), 750-756. <https://doi.org/10.1016/j.celrep.2017.06.064>
- Barneda-Zahonero, B., Roman-Gonzalez, L., Collazo, O., Mahmoudi, T., & Parra, M. (2012). Epigenetic Regulation of B Lymphocyte Differentiation, Transdifferentiation, and Reprogramming. *Comparative and Functional Genomics*, *2012*, 564381. <https://doi.org/10.1155/2012/564381>
- Basilico, S., Wang, X., Kennedy, A., Tzelepis, K., Giotopoulos, G., Kinston, S. J., Quiros, P. M., Wong, K., Adams, D. J., Carnevalli, L. S., Huntly, B. J. P., Vassiliou, G. S., Calero-Nieto,

- F. J., & Göttgens, B. (2020). Dissecting the early steps of MLL induced leukaemogenic transformation using a mouse model of AML. *Nat Commun*, 11(1), 1407. <https://doi.org/10.1038/s41467-020-15220-0>
- Bichi, R., Shinton, S. A., Martin, E. S., Koval, A., Calin, G. A., Cesari, R., Russo, G., Hardy, R. R., & Croce, C. M. (2002). Human chronic lymphocytic leukemia modeled in mouse by targeted TCL1 expression. *Proc Natl Acad Sci U S A*, 99(10), 6955-6960. <https://doi.org/10.1073/pnas.102181599>
- Bischin, A. M., Dorer, R., & Aboulafia, D. M. (2017). Transformation of Follicular Lymphoma to a High-Grade B-Cell Lymphoma With MYC and BCL2 Translocations and Overlapping Features of Burkitt Lymphoma and Acute Lymphoblastic Leukemia: A Case Report and Literature Review. *Clin Med Insights Blood Disord*, 10, 1179545x17692544. <https://doi.org/10.1177/1179545x17692544>
- Bödör, C., Grossmann, V., Popov, N., Okosun, J., O'Riain, C., Tan, K., Marzec, J., Araf, S., Wang, J., Lee, A. M., Clear, A., Montoto, S., Matthews, J., Iqbal, S., Rajnai, H., Rosenwald, A., Ott, G., Campo, E., Rimsza, L. M., Smeland, E. B., Chan, W. C., Braziel, R. M., Staudt, L. M., Wright, G., Lister, T. A., Elemento, O., Hills, R., Gribben, J. G., Chelala, C., Matolcsy, A., Kohlmann, A., Haferlach, T., Gascoyne, R. D., & Fitzgibbon, J. (2013). EZH2 mutations are frequent and represent an early event in follicular lymphoma. *Blood*, 122(18), 3165-3168. <https://doi.org/10.1182/blood-2013-04-496893>
- Boice, M., Salloum, D., Mourcin, F., Sanghvi, V., Amin, R., Oricchio, E., Jiang, M., Mottok, A., Denis-Lagache, N., Ciriello, G., Tam, W., Teruya-Feldstein, J., de Stanchina, E., Chan, W. C., Malek, S. N., Ennishi, D., Brentjens, R. J., Gascoyne, R. D., Cogné, M., Tarte, K., & Wendel, H. G. (2016). Loss of the HVEM Tumor Suppressor in Lymphoma and Restoration by Modified CAR-T Cells. *Cell*, 167(2), 405-418.e413. <https://doi.org/10.1016/j.cell.2016.08.032>
- Brinkman, E. K., Chen, T., Amendola, M., & van Steensel, B. (2014). Easy quantitative assessment of genome editing by sequence trace decomposition. *Nucleic acids research*, 42(22), e168-e168. <https://doi.org/10.1093/nar/gku936>
- Budagyan, K., & Chernoff, J. (2021). A Facile Method to Engineer Mutant Kras Alleles in an Isogenic Cell Background. *Methods Mol Biol*, 2262, 323-334. [https://doi.org/10.1007/978-1-0716-1190-6\\_20](https://doi.org/10.1007/978-1-0716-1190-6_20)
- Bunin, A., Sisirak, V., Ghosh, H. S., Grajkowska, L. T., Hou, Z. E., Miron, M., Yang, C., Ceribelli, M., Uetani, N., Chaperot, L., Plumas, J., Hendriks, W., Tremblay, M. L., Häcker, H., Staudt, L. M., Green, P. H., Bhagat, G., & Reizis, B. (2015). Protein Tyrosine Phosphatase PTPRS Is an Inhibitory Receptor on Human and Murine Plasmacytoid Dendritic Cells. *Immunity*, 43(2), 277-288. <https://doi.org/10.1016/j.immuni.2015.07.009>
- Cabal-Hierro, L., van Galen, P., Prado, M. A., Higby, K. J., Togami, K., Mowery, C. T., Paulo, J. A., Xie, Y., Cejas, P., Furusawa, T., Bustin, M., Long, H. W., Sykes, D. B., Gygi, S. P., Finley, D., Bernstein, B. E., & Lane, A. A. (2020). Chromatin accessibility promotes hematopoietic and leukemia stem cell activity. *Nat Commun*, 11(1), 1406. <https://doi.org/10.1038/s41467-020-15221-z>
- Cai, Z., Zhang, L., Cao, M., Wang, Y., Wang, F., Bian, W., Zhai, S., & Wang, X. (2020). Generation of a Murine Model for c-MYC and BCL2 Co-expression B Cell Lymphomas. *Frontiers in oncology*, 10, 1007-1007. <https://doi.org/10.3389/fonc.2020.01007>
- Cameron, P., Fuller, C. K., Donohoue, P. D., Jones, B. N., Thompson, M. S., Carter, M. M., Gradia, S., Vidal, B., Garner, E., Slorach, E. M., Lau, E., Banh, L. M., Lied, A. M., Edwards, L. S., Settle, A. H., Capurso, D., Llaca, V., Deschamps, S., Cigan, M., Young, J. K., & May, A. P. (2017). Mapping the genomic landscape of CRISPR–Cas9 cleavage. *Nature Methods*, 14(6), 600-606. <https://doi.org/10.1038/nmeth.4284>

- Carbone, A., Roulland, S., Gloghini, A., Younes, A., von Keudell, G., López-Guillermo, A., & Fitzgibbon, J. (2019). Follicular lymphoma. *Nature Reviews Disease Primers*, 5(1), 83. <https://doi.org/10.1038/s41572-019-0132-x>
- Carter, M., & Shieh, J. C. (2010). Chapter 13 - Cell Culture Techniques. In M. Carter & J. C. Shieh (Eds.), *Guide to Research Techniques in Neuroscience* (pp. 281-296). Academic Press. <https://doi.org/https://doi.org/10.1016/B978-0-12-374849-2.00013-6>
- Carthew, R. W., & Sontheimer, E. J. (2009). Origins and Mechanisms of miRNAs and siRNAs. *Cell*, 136(4), 642-655. <https://doi.org/10.1016/j.cell.2009.01.035>
- Casola, S., Cattoretti, G., Uyttersprot, N., Koralov, S. B., Seagal, J., Hao, Z., Waisman, A., Egert, A., Ghitza, D., & Rajewsky, K. (2006). Tracking germinal center B cells expressing germ-line immunoglobulin gamma1 transcripts by conditional gene targeting. *Proc Natl Acad Sci U S A*, 103(19), 7396-7401. <https://doi.org/10.1073/pnas.0602353103>
- these cells
- Casulo, C. (2019). How I manage patients with follicular lymphoma. *Br J Haematol*, 186(4), 513-523. <https://doi.org/10.1111/bjh.16011>
- Casulo, C., Burack, W. R., & Friedberg, J. W. (2015). Transformed follicular non-Hodgkin lymphoma. *Blood*, 125(1), 40-47. <https://doi.org/10.1182/blood-2014-04-516815>
- Cattoretti, G., Pasqualucci, L., Ballon, G., Tam, W., Nandula, S. V., Shen, Q., Mo, T., Murty, V. V., & Dalla-Favera, R. (2005). Deregulated BCL6 expression recapitulates the pathogenesis of human diffuse large B cell lymphomas in mice. *Cancer Cell*, 7(5), 445-455. <https://doi.org/10.1016/j.ccr.2005.03.037>
- Certo, M. T., Ryu, B. Y., Annis, J. E., Garibov, M., Jarjour, J., Rawlings, D. J., & Scharenberg, A. M. (2011). Tracking genome engineering outcome at individual DNA breakpoints. *Nat Methods*, 8(8), 671-676. <https://doi.org/10.1038/nmeth.1648>
- Chan, W., Gottschalk, R. A., Yao, Y., Pomerantz, J. L., & Germain, R. N. (2020). Efficient Immune Cell Genome Engineering with Improved CRISPR Editing Tools. *bioRxiv*, 2020.2002.2013.947002. <https://doi.org/10.1101/2020.02.13.947002>
- Chapeau, E. A., Gembarska, A., Durand, E. Y., Mandon, E., Estadieu, C., Romanet, V., Wiesmann, M., Tiedt, R., Lehar, J., de Weck, A., Rad, R., Barys, L., Jeay, S., Ferretti, S., Kauffmann, A., Sutter, E., Grevot, A., Moulin, P., Murakami, M., Sellers, W. R., Hofmann, F., & Jensen, M. R. (2017). Resistance mechanisms to TP53-MDM2 inhibition identified by in vivo piggyBac transposon mutagenesis screen in an Arf<sup>-/-</sup> mouse model. *Proceedings of the National Academy of Sciences*, 201620262. <https://doi.org/10.1073/pnas.1620262114>
- Charlesworth, C. T., Camarena, J., Cromer, M. K., Vaidyanathan, S., Bak, R. O., Carte, J. M., Potter, J., Dever, D. P., & Porteus, M. H. (2018). Priming Human Repopulating Hematopoietic Stem and Progenitor Cells for Cas9/sgRNA Gene Targeting. *Molecular therapy. Nucleic acids*, 12, 89-104. <https://doi.org/10.1016/j.omtn.2018.04.017>
- Chen, S., Sanjana, N. E., Zheng, K., Shalem, O., Lee, K., Shi, X., Scott, D. A., Song, J., Pan, J. Q., Weissleder, R., Lee, H., Zhang, F., & Sharp, P. A. (2015). Genome-wide CRISPR screen in a mouse model of tumor growth and metastasis. *Cell*, 160(6), 1246-1260. <https://doi.org/10.1016/j.cell.2015.02.038>
- Cheng, H., Zheng, Z., & Cheng, T. (2020). New paradigms on hematopoietic stem cell differentiation. *Protein Cell*, 11(1), 34-44. <https://doi.org/10.1007/s13238-019-0633-0>
- Cheung, K.-J. J., Shah, S. P., Steidl, C., Johnson, N., Relander, T., Telenius, A., Lai, B., Murphy, K. P., Lam, W., Al-Tourah, A. J., Connors, J. M., Ng, R. T., Gascoyne, R. D., & Horsman, D. E. (2009). Genome-wide profiling of follicular lymphoma by array comparative genomic hybridization reveals prognostically significant DNA copy number imbalances. *Blood*, 113(1), 137-148. <https://doi.org/10.1182/blood-2008-02-140616>
- Chow, R. D., & Chen, S. (2018). Cancer CRISPR Screens *In Vivo*. *Trends in Cancer*, 4(5), 349-358. <https://doi.org/10.1016/j.trecan.2018.03.002>

- Chow, R. D., Guzman, C. D., Wang, G., Schmidt, F., Youngblood, M. W., Ye, L., Errami, Y., Dong, M. B., Martinez, M. A., Zhang, S., Renauer, P., Bilguvar, K., Gunel, M., Sharp, P. A., Zhang, F., Platt, R. J., & Chen, S. (2017). AAV-mediated direct in vivo CRISPR screen identifies functional suppressors in glioblastoma. *Nat Neurosci*, *20*(10), 1329-1341. <https://doi.org/10.1038/nn.4620>
- Coelho, M. A., Li, S., Pane, L. S., Firth, M., Ciotta, G., Wrigley, J. D., Cuomo, M. E., Maresca, M., & Taylor, B. J. M. (2018). BE-FLARE: a fluorescent reporter of base editing activity reveals editing characteristics of APOBEC3A and APOBEC3B. *BMC Biology*, *16*(1), 150. <https://doi.org/10.1186/s12915-018-0617-1>
- Collier, L. S., Carlson, C. M., Ravimohan, S., Dupuy, A. J., & Largaespada, D. A. (2005). Cancer gene discovery in solid tumours using transposon-based somatic mutagenesis in the mouse. *Nature*, *436*(7048), 272-276. <https://doi.org/10.1038/nature03681>
- Cornu, T. I., & Cathomen, T. (2007). Targeted genome modifications using integrase-deficient lentiviral vectors. *Mol Ther*, *15*(12), 2107-2113. <https://doi.org/10.1038/sj.mt.6300345>
- De Silva, N. S., & Klein, U. (2015). Dynamics of B cells in germinal centres. *Nat Rev Immunol*, *15*(3), 137-148. <https://doi.org/10.1038/nri3804>
- Dent, A. L., Shaffer, A. L., Yu, X., Allman, D., & Staudt, L. M. (1997). Control of inflammation, cytokine expression, and germinal center formation by BCL-6. *Science*, *276*(5312), 589-592. <https://doi.org/10.1126/science.276.5312.589>
- Devan, J., Janikova, A., & Mraz, M. (2018). New concepts in follicular lymphoma biology: From BCL2 to epigenetic regulators and non-coding RNAs. *Seminars in Oncology*, *45*(5), 291-302. <https://doi.org/https://doi.org/10.1053/j.seminoncol.2018.07.005>
- Dever, D. P., Bak, R. O., Reinisch, A., Camarena, J., Washington, G., Nicolas, C. E., Pavel-Dinu, M., Saxena, N., Wilkens, A. B., Mantri, S., Uchida, N., Hendel, A., Narla, A., Majeti, R., Weinberg, K. I., & Porteus, M. H. (2016). CRISPR/Cas9  $\beta$ -globin gene targeting in human haematopoietic stem cells. *Nature*, *539*(7629), 384-389. <https://doi.org/10.1038/nature20134>
- Ding, S., Wu, X., Li, G., Han, M., Zhuang, Y., & Xu, T. (2005). Efficient transposition of the piggyBac (PB) transposon in mammalian cells and mice. *Cell*, *122*(3), 473-483. <https://doi.org/10.1016/j.cell.2005.07.013>
- Doench, J. G., Fusi, N., Sullender, M., Hegde, M., Vaimberg, E. W., Donovan, K. F., Smith, I., Tothova, Z., Wilen, C., Orchard, R., Virgin, H. W., Listgarten, J., & Root, D. E. (2016). Optimized sgRNA design to maximize activity and minimize off-target effects of CRISPR-Cas9. *Nat Biotechnol*, *34*(2), 184-191. <https://doi.org/10.1038/nbt.3437>
- Dong, Y., Li, H., Zhao, L., Koopman, P., Zhang, F., & Huang, J. X. (2019). Genome-Wide Off-Target Analysis in CRISPR-Cas9 Modified Mice and Their Offspring. *G3 (Bethesda)*, *9*(11), 3645-3651. <https://doi.org/10.1534/g3.119.400503>
- Donnou, S., Galand, C., Touitou, V., Sautès-Fridman, C., Fabry, Z., & Fisson, S. (2012). Murine models of B-cell lymphomas: promising tools for designing cancer therapies. *Adv Hematol*, *2012*, 701704. <https://doi.org/10.1155/2012/701704>
- Dorshkind, K., & Rawlings, D. J. (2018). Chapter 20 - B-Cell Development. In R. Hoffman, E. J. Benz, L. E. Silberstein, H. E. Heslop, J. I. Weitz, J. Anastasi, M. E. Salama, & S. A. Abutalib (Eds.), *Hematology (Seventh Edition)* (pp. 210-220). Elsevier. <https://doi.org/https://doi.org/10.1016/B978-0-323-35762-3.00020-2>
- Doudna, J. A., & Charpentier, E. (2014). Genome editing. The new frontier of genome engineering with CRISPR-Cas9. *Science*, *346*(6213), 1258096. <https://doi.org/10.1126/science.1258096>
- Drexler, H. G. (2011). Establishment and culture of leukemia-lymphoma cell lines. *Methods Mol Biol*, *731*, 181-200. [https://doi.org/10.1007/978-1-61779-080-5\\_16](https://doi.org/10.1007/978-1-61779-080-5_16)

- Drexler, H. G., Eberth, S., Nagel, S., & MacLeod, R. A. F. (2016). Malignant hematopoietic cell lines: in vitro models for double-hit B-cell lymphomas. *Leukemia & Lymphoma*, 57(5), 1015-1020. <https://doi.org/10.3109/10428194.2015.1108414>
- Duan, L., Liu, D., Chen, H., Mintz, M. A., Chou, M. Y., Kotov, D. I., Xu, Y., An, J., Laidlaw, B. J., & Cyster, J. G. (2021). Follicular dendritic cells restrict interleukin-4 availability in germinal centers and foster memory B cell generation. *Immunity*, 54(10), 2256-2272.e2256. <https://doi.org/10.1016/j.immuni.2021.08.028>
- Dubrot, J., Lane-Reticker, S. K., Kessler, E. A., Ayer, A., Mishra, G., Wolfe, C. H., Zimmer, M. D., Du, P. P., Mahapatra, A., Ockerman, K. M., Davis, T. G. R., Kohnle, I. C., Pope, H. W., Allen, P. M., Olander, K. E., Iracheta-Vellve, A., Doench, J. G., Haining, W. N., Yates, K. B., & Manguso, R. T. (2021). In vivo screens using a selective CRISPR antigen removal lentiviral vector system reveal immune dependencies in renal cell carcinoma. *Immunity*, 54(3), 571-585.e576. <https://doi.org/10.1016/j.immuni.2021.01.001>
- Egle, A., Harris, A. W., Bath, M. L., O'Reilly, L., & Cory, S. (2004). VavP-Bcl2 transgenic mice develop follicular lymphoma preceded by germinal center hyperplasia. *Blood*, 103(6), 2276-2283. <https://doi.org/10.1182/blood-2003-07-2469>
- Eisen, H. N. (2014). Affinity enhancement of antibodies: how low-affinity antibodies produced early in immune responses are followed by high-affinity antibodies later and in memory B-cell responses. *Cancer Immunol Res*, 2(5), 381-392. <https://doi.org/10.1158/2326-6066.Cir-14-0029>
- Elbashir, S. M., Harborth, J., Lendeckel, W., Yalcin, A., Weber, K., & Tuschl, T. (2001). Duplexes of 21-nucleotide RNAs mediate RNA interference in cultured mammalian cells. *Nature*, 411(6836), 494-498. <https://doi.org/10.1038/35078107>
- Fajrial, A. K., He, Q. Q., Wirusanti, N. I., Slansky, J. E., & Ding, X. (2020). A review of emerging physical transfection methods for CRISPR/Cas9-mediated gene editing. *Theranostics*, 10(12), 5532-5549. <https://doi.org/10.7150/thno.43465>
- Fangazio, M., Pasqualucci, L., & Dalla-Favera, R. (2015). Chromosomal Translocations in B Cell Lymphomas. In J. D. Rowley, M. M. Le Beau, & T. H. Rabbitts (Eds.), *Chromosomal Translocations and Genome Rearrangements in Cancer* (pp. 157-188). Springer International Publishing. [https://doi.org/10.1007/978-3-319-19983-2\\_9](https://doi.org/10.1007/978-3-319-19983-2_9)
- Ferlay, J., Colombet, M., Soerjomataram, I., Mathers, C., Parkin, D. M., Piñeros, M., Znaor, A., & Bray, F. (2019). Estimating the global cancer incidence and mortality in 2018: GLOBOCAN sources and methods. *Int J Cancer*, 144(8), 1941-1953. <https://doi.org/10.1002/ijc.31937>
- Fire, A., Albertson, D., Harrison, S. W., & Moerman, D. G. (1991). Production of antisense RNA leads to effective and specific inhibition of gene expression in *C. elegans* muscle. *Development*, 113(2), 503-514.
- Fire, A., Xu, S., Montgomery, M. K., Kostas, S. A., Driver, S. E., & Mello, C. C. (1998). Potent and specific genetic interference by double-stranded RNA in *Caenorhabditis elegans*. *Nature*, 391(6669), 806-811. <https://doi.org/10.1038/35888>
- Flümman, R., Nieper, P., Reinhardt, H. C., & Knittel, G. (2020). New murine models of aggressive lymphoma. *Leukemia & Lymphoma*, 61(4), 788-798. <https://doi.org/10.1080/10428194.2019.1691200>
- Friedrich, M. J., Rad, L., Bronner, I. F., Strong, A., Wang, W., Weber, J., Mayho, M., Ponstingl, H., Engleitner, T., Grove, C., Pfaus, A., Saur, D., Cadiñanos, J., Quail, M. A., Vassiliou, G. S., Liu, P., Bradley, A., & Rad, R. (2017). Genome-wide transposon screening and quantitative insertion site sequencing for cancer gene discovery in mice. *Nat Protoc*, 12(2), 289-309. <https://doi.org/10.1038/nprot.2016.164>
- Fu, Y., Foden, J. A., Khayter, C., Maeder, M. L., Reyon, D., Joung, J. K., & Sander, J. D. (2013). High-frequency off-target mutagenesis induced by CRISPR-Cas nucleases in human cells. *Nat Biotechnol*, 31(9), 822-826. <https://doi.org/10.1038/nbt.2623>

- Gaj, T., Ojala, D. S., Ekman, F. K., Byrne, L. C., Limsirichai, P., & Schaffer, D. V. (2017). In vivo genome editing improves motor function and extends survival in a mouse model of ALS. *Science Advances*, 3(12), eaar3952. <https://doi.org/10.1126/sciadv.aar3952>
- Glaser, A., McColl, B., & Vadolas, J. (2016). GFP to BFP Conversion: A Versatile Assay for the Quantification of CRISPR/Cas9-mediated Genome Editing. *Molecular therapy. Nucleic acids*, 5(7), e334-e334. <https://doi.org/10.1038/mtna.2016.48>
- Godfrey, J. K., Nabhan, C., Karrison, T., Kline, J. P., Cohen, K. S., Bishop, M. R., Stadler, W. M., Karmali, R., Venugopal, P., Rapoport, A. P., & Smith, S. M. (2019). Phase 1 study of lenalidomide plus dose-adjusted EPOCH-R in patients with aggressive B-cell lymphomas with deregulated MYC and BCL2. *Cancer*, 125(11), 1830-1836. <https://doi.org/10.1002/cncr.31877>
- Govindarajah, V., Lee, J. M., Solomon, M., Goddard, B., Nayak, R., Nattamai, K., Geiger, H., Salomonis, N., Cancelas, J. A., & Reynaud, D. (2020). FOXO activity adaptation safeguards the hematopoietic stem cell compartment in hyperglycemia. *Blood Adv*, 4(21), 5512-5526. <https://doi.org/10.1182/bloodadvances.2020001826>
- Graf, R., Li, X., Chu, V. T., & Rajewsky, K. (2019). sgRNA Sequence Motifs Blocking Efficient CRISPR/Cas9-Mediated Gene Editing. *Cell Rep*, 26(5), 1098-1103.e1093. <https://doi.org/10.1016/j.celrep.2019.01.024>
- Graham, D. B., & Root, D. E. (2015). Resources for the design of CRISPR gene editing experiments. *Genome biology*, 16, 260. <https://doi.org/10.1186/s13059-015-0823-x>
- Grajkowska, L. T., Ceribelli, M., Lau, C. M., Warren, M. E., Tiniakou, I., Nakandakari Higa, S., Bunin, A., Haecker, H., Mirny, L. A., Staudt, L. M., & Reizis, B. (2017). Isoform-Specific Expression and Feedback Regulation of E Protein TCF4 Control Dendritic Cell Lineage Specification. *Immunity*, 46(1), 65-77. <https://doi.org/10.1016/j.immuni.2016.11.006>
- Green, M. R. (2018). Chromatin modifying gene mutations in follicular lymphoma. *Blood*, 131(6), 595-604. <https://doi.org/10.1182/blood-2017-08-737361>
- Green, M. R., Kihira, S., Liu, C. L., Nair, R. V., Salari, R., Gentles, A. J., Irish, J., Stehr, H., Vicente-Dueñas, C., Romero-Camarero, I., Sanchez-Garcia, I., Plevritis, S. K., Arber, D. A., Batzoglou, S., Levy, R., & Alizadeh, A. A. (2015). Mutations in early follicular lymphoma progenitors are associated with suppressed antigen presentation. *Proceedings of the National Academy of Sciences*, 201501199. <https://doi.org/10.1073/pnas.1501199112>
- Gundry, M. C., Brunetti, L., Lin, A., Mayle, A. E., Kitano, A., Wagner, D., Hsu, J. I., Hoegenauer, K. A., Rooney, C. M., Goodell, M. A., & Nakada, D. (2016). Highly Efficient Genome Editing of Murine and Human Hematopoietic Progenitor Cells by CRISPR/Cas9. *Cell Rep*, 17(5), 1453-1461. <https://doi.org/10.1016/j.celrep.2016.09.092>
- Hamey, F. K., Nestorowa, S., Kinston, S. J., Kent, D. G., Wilson, N. K., & Göttgens, B. (2017). Reconstructing blood stem cell regulatory network models from single-cell molecular profiles. *Proceedings of the National Academy of Sciences*, 114(23), 5822-5829. <https://doi.org/10.1073/pnas.1610609114>
- Hammerschmidt, S. I., Werth, K., Rothe, M., Galla, M., Permanyer, M., Patzer, G. E., Bubke, A., Frenk, D. N., Selich, A., Lange, L., Schambach, A., Bošnjak, B., & Förster, R. (2018). CRISPR/Cas9 Immunoengineering of Hoxb8-Immortalized Progenitor Cells for Revealing CCR7-Mediated Dendritic Cell Signaling and Migration Mechanisms in vivo. *Front Immunol*, 9, 1949. <https://doi.org/10.3389/fimmu.2018.01949>
- Han, D., Hong, Y., Mai, X., Hu, Q., Lu, G., Duan, J., Xu, J., Si, X., & Zhang, Y. (2019). Systematical study of the mechanistic factors regulating genome dynamics in vivo by CRISPRs. *J Mol Cell Biol*, 11(11), 1018-1020. <https://doi.org/10.1093/jmcb/mjz074>
- Hendel, A., Bak, R. O., Clark, J. T., Kennedy, A. B., Ryan, D. E., Roy, S., Steinfeld, I., Lunstad, B. D., Kaiser, R. J., Wilkens, A. B., Bacchetta, R., Tsalenko, A., Dellinger, D., Bruhn, L., & Porteus, M. H. (2015). Chemically modified guide RNAs enhance CRISPR-Cas

- genome editing in human primary cells. *Nature Biotechnology*, 33(9), 985-989. <https://doi.org/10.1038/nbt.3290>
- Hobeika, E., Thiemann, S., Storch, B., Jumaa, H., Nielsen, P. J., Pelanda, R., & Reth, M. (2006). Testing gene function early in the B cell lineage in mb1-cre mice. *Proc Natl Acad Sci U S A*, 103(37), 13789-13794. <https://doi.org/10.1073/pnas.0605944103>
- Horie, K., Kuroiwa, A., Ikawa, M., Okabe, M., Kondoh, G., Matsuda, Y., & Takeda, J. (2001). Efficient chromosomal transposition of a *Tc1*-like transposon *Sleeping Beauty* in mice. *Proceedings of the National Academy of Sciences*, 98(16), 9191-9196. <https://doi.org/10.1073/pnas.161071798>
- Hsiao, T., Maures, T., Waite, K., Yang, J., Kelso, R., Holden, K., & Stoner, R. (2018). Inference of CRISPR Edits from Sanger Trace Data. *bioRxiv*, 251082. <https://doi.org/10.1101/251082>
- Hsu, P. D., Lander, E. S., & Zhang, F. (2014). Development and applications of CRISPR-Cas9 for genome engineering. *Cell*, 157(6), 1262-1278. <https://doi.org/10.1016/j.cell.2014.05.010>
- Huang, W., Medeiros, L. J., Lin, P., Wang, W., Tang, G., Khoury, J., Konoplev, S., Yin, C. C., Xu, J., Oki, Y., & Li, S. (2018). MYC/BCL2/BCL6 triple hit lymphoma: a study of 40 patients with a comparison to MYC/BCL2 and MYC/BCL6 double hit lymphomas. *Mod Pathol*, 31(9), 1470-1478. <https://doi.org/10.1038/s41379-018-0067-x>
- Humes, D., Rainwater, S., & Overbaugh, J. (2021). The TOP vector: a new high-titer lentiviral construct for delivery of sgRNAs and transgenes to primary T cells. *Mol Ther Methods Clin Dev*, 20, 30-38. <https://doi.org/10.1016/j.omtm.2020.10.020>
- Ivics, Z., Hackett, P. B., Plasterk, R. H., & Izsvák, Z. (1997). Molecular reconstruction of *Sleeping Beauty*, a *Tc1*-like transposon from fish, and its transposition in human cells. *Cell*, 91(4), 501-510. [https://doi.org/10.1016/s0092-8674\(00\)80436-5](https://doi.org/10.1016/s0092-8674(00)80436-5)
- Jacob, J., Kelsoe, G., Rajewsky, K., & Weiss, U. (1991). Intraclonal generation of antibody mutants in germinal centres. *Nature*, 354(6352), 389-392. <https://doi.org/10.1038/354389a0>
- Jacobi, A. M., Rettig, G. R., Turk, R., Collingwood, M. A., Zeiner, S. A., Quadros, R. M., Harms, D. W., Bonthuis, P. J., Gregg, C., Ohtsuka, M., Gurumurthy, C. B., & Behlke, M. A. (2017). Simplified CRISPR tools for efficient genome editing and streamlined protocols for their delivery into mammalian cells and mouse zygotes. *Methods*, 121-122, 16-28. <https://doi.org/10.1016/j.ymeth.2017.03.021>
- Janssen, J. M., Chen, X., Liu, J., & Gonçalves, M. (2019). The Chromatin Structure of CRISPR-Cas9 Target DNA Controls the Balance between Mutagenic and Homology-Directed Gene-Editing Events. *Molecular therapy. Nucleic acids*, 16, 141-154. <https://doi.org/10.1016/j.omtn.2019.02.009>
- Janssen, W. J., Bratton, D. L., Jakubzick, C. V., & Henson, P. M. (2016). Myeloid Cell Turnover and Clearance. *Microbiology spectrum*, 4(6), 10.1128/microbiolspec.MCHD-0005-2015. <https://doi.org/10.1128/microbiolspec.MCHD-0005-2015>
- Jeong, J., Jager, A., Domizi, P., Pavel-Dinu, M., Gojenola, L., Iwasaki, M., Wei, M. C., Pan, F., Zehnder, J. L., Porteus, M. H., Davis, K. L., & Cleary, M. L. (2019). High-efficiency CRISPR induction of t(9;11) chromosomal translocations and acute leukemias in human blood stem cells. *Blood Adv*, 3(19), 2825-2835. <https://doi.org/10.1182/bloodadvances.2019000450>
- Jinek, M., Chylinski, K., Fonfara, I., Hauer, M., Doudna, J. A., & Charpentier, E. (2012). A Programmable Dual-RNA-Guided DNA Endonuclease in Adaptive Bacterial Immunity. *Science*, 337(6096), 816-821. <https://doi.org/10.1126/science.1225829>
- Johnson, N. A., Al-Tourah, A., Brown, C. J., Connors, J. M., Gascoyne, R. D., & Horsman, D. E. (2008). Prognostic significance of secondary cytogenetic alterations in follicular

- lymphomas. *Genes, Chromosomes and Cancer*, 47(12), 1038-1048. <https://doi.org/https://doi.org/10.1002/gcc.20606>
- Johnson, N. A., Savage, K. J., Ludkovski, O., Ben-Neriah, S., Woods, R., Steidl, C., Dyer, M. J., Siebert, R., Kuruvilla, J., Klasa, R., Connors, J. M., Gascoyne, R. D., & Horsman, D. E. (2009). Lymphomas with concurrent BCL2 and MYC translocations: the critical factors associated with survival. *Blood*, 114(11), 2273-2279. <https://doi.org/10.1182/blood-2009-03-212191>
- Joung, J. K., & Sander, J. D. (2013). TALENs: a widely applicable technology for targeted genome editing. *Nat Rev Mol Cell Biol*, 14(1), 49-55. <https://doi.org/10.1038/nrm3486>
- Kapur, S., & Levin, M. B. (2014). Transformation of follicular lymphoma to double hit B-cell lymphoma causing hypercalcemia in a 69-year-old female: a case report and review of the literature. *Case Rep Hematol*, 2014, 619760. <https://doi.org/10.1155/2014/619760>
- Kennedy, R., & Klein, U. (2019). A T Cell-B Cell Tumor-Suppressive Axis in the Germinal Center. *Immunity*, 51(2), 204-206. <https://doi.org/10.1016/j.immuni.2019.07.006>
- Khan, A. A., Betel, D., Miller, M. L., Sander, C., Leslie, C. S., & Marks, D. S. (2009). Transfection of small RNAs globally perturbs gene regulation by endogenous microRNAs. *Nat Biotechnol*, 27(6), 549-555. <https://doi.org/10.1038/nbt.1543>
- Khoyratty, T. E., Ai, Z., Ballesteros, I., Eames, H. L., Mathie, S., Martín-Salamanca, S., Wang, L., Hemmings, A., Willemsen, N., von Werz, V., Zehrer, A., Walzog, B., van Grinsven, E., Hidalgo, A., & Udalova, I. A. (2021). Distinct transcription factor networks control neutrophil-driven inflammation. *Nature Immunology*, 22(9), 1093-1106. <https://doi.org/10.1038/s41590-021-00968-4>
- Khurana, A., & Ansell, S. M. (2020). Role of Microenvironment in Non-Hodgkin Lymphoma: Understanding the Composition and Biology. *Cancer J*, 26(3), 206-216. <https://doi.org/10.1097/ppo.0000000000000446>
- Kim, S., Kim, D., Cho, S. W., Kim, J., & Kim, J. S. (2014). Highly efficient RNA-guided genome editing in human cells via delivery of purified Cas9 ribonucleoproteins. *Genome Res*, 24(6), 1012-1019. <https://doi.org/10.1101/gr.171322.113>
- Kirkling, M. E., Cytlak, U., Lau, C. M., Lewis, K. L., Resteu, A., Khodadadi-Jamayran, A., Siebel, C. W., Salmon, H., Merad, M., Tsirigos, A., Collin, M., Bigley, V., & Reizis, B. (2018). Notch Signaling Facilitates In Vitro Generation of Cross-Presenting Classical Dendritic Cells. *Cell Rep*, 23(12), 3658-3672.e3656. <https://doi.org/10.1016/j.celrep.2018.05.068>
- Klener, P., & Klanova, M. (2020). Drug Resistance in Non-Hodgkin Lymphomas. *Int J Mol Sci*, 21(6). <https://doi.org/10.3390/ijms21062081>
- Koike-Yusa, H., Li, Y., Tan, E. P., Velasco-Herrera Mdel, C., & Yusa, K. (2014). Genome-wide recessive genetic screening in mammalian cells with a lentiviral CRISPR-guide RNA library. *Nat Biotechnol*, 32(3), 267-273. <https://doi.org/10.1038/nbt.2800>
- Kool, J., & Berns, A. (2009). High-throughput insertional mutagenesis screens in mice to identify oncogenic networks. *Nat Rev Cancer*, 9(6), 389-399. <https://doi.org/10.1038/nrc2647>
- Kool, J., Uren, A. G., Martins, C. P., Sie, D., de Ridder, J., Turner, G., van Uitert, M., Matentzoglou, K., Lagcher, W., Krimpenfort, P., Gadiot, J., Pritchard, C., Lenz, J., Lund, A. H., Jonkers, J., Rogers, J., Adams, D. J., Wessels, L., Berns, A., & van Lohuizen, M. (2010). Insertional mutagenesis in mice deficient for p15Ink4b, p16Ink4a, p21Cip1, and p27Kip1 reveals cancer gene interactions and correlations with tumor phenotypes. *Cancer research*, 70(2), 520-531. <https://doi.org/10.1158/0008-5472.CAN-09-2736>
- Kopf, A., Renkawitz, J., Hauschild, R., Girkontaite, I., Tedford, K., Merrin, J., Thorn-Seshold, O., Trauner, D., Häcker, H., Fischer, K. D., Kiermaier, E., & Sixt, M. (2020). Microtubules control cellular shape and coherence in amoeboid migrating cells. *J Cell Biol*, 219(6). <https://doi.org/10.1083/jcb.201907154>
- Kovalchuk, A. L., Qi, C. F., Torrey, T. A., Taddesse-Heath, L., Feigenbaum, L., Park, S. S., Gerbitz, A., Klobeck, G., Hoertnagel, K., Polack, A., Bornkamm, G. W., Janz, S., &

- Morse, H. C., 3rd. (2000). Burkitt lymphoma in the mouse. *J Exp Med*, 192(8), 1183-1190. <https://doi.org/10.1084/jem.192.8.1183>
- Kridel, R., Mottok, A., Farinha, P., Ben-Neriah, S., Ennishi, D., Zheng, Y., Chavez, E. A., Shulha, H. P., Tan, K., Chan, F. C., Boyle, M., Meissner, B., Telenius, A., Sehn, L. H., Marra, M. A., Shah, S. P., Steidl, C., Connors, J. M., Scott, D. W., & Gascoyne, R. D. (2015). Cell of origin of transformed follicular lymphoma. *Blood*, 126(18), 2118-2127. <https://doi.org/10.1182/blood-2015-06-649905>
- Kridel, R., Sehn, L. H., & Gascoyne, R. D. (2012). Pathogenesis of follicular lymphoma. *J Clin Invest*, 122(10), 3424-3431. <https://doi.org/10.1172/jci63186>
- Kucinski, I., Wilson, N. K., Hannah, R., Kinston, S. J., Cauchy, P., Lenaerts, A., Grosschedl, R., & Göttgens, B. (2020). Interactions between lineage-associated transcription factors govern haematopoietic progenitor states. *Embo j*, 39(24), e104983. <https://doi.org/10.15252/embj.2020104983>
- Küppers, R., & Dalla-Favera, R. (2001). Mechanisms of chromosomal translocations in B cell lymphomas. *Oncogene*, 20(40), 5580-5594. <https://doi.org/10.1038/sj.onc.1204640>
- Küppers, R., & Stevenson, F. K. (2018). Critical influences on the pathogenesis of follicular lymphoma. *Blood*, 131(21), 2297-2306. <https://doi.org/10.1182/blood-2017-11-764365>
- Kuriakose, J., Redecke, V., Guy, C., Zhou, J., Wu, R., Ippagunta, S. K., Tillman, H., Walker, P. D., Vogel, P., & Häcker, H. (2019). Patrolling monocytes promote the pathogenesis of early lupus-like glomerulonephritis. *J Clin Invest*, 129(6), 2251-2265. <https://doi.org/10.1172/jci125116>
- LaFleur, M. W., Nguyen, T. H., Coxe, M. A., Yates, K. B., Trombley, J. D., Weiss, S. A., Brown, F. D., Gillis, J. E., Coxe, D. J., Doench, J. G., Haining, W. N., & Sharpe, A. H. (2019). A CRISPR-Cas9 delivery system for in vivo screening of genes in the immune system. *Nature Communications*, 10(1), 1668. <https://doi.org/10.1038/s41467-019-09656-2>
- Laidlaw, B. J., Duan, L., Xu, Y., Vazquez, S. E., & Cyster, J. G. (2020). The transcription factor Hhex cooperates with the corepressor Tle3 to promote memory B cell development. *Nat Immunol*, 21(9), 1082-1093. <https://doi.org/10.1038/s41590-020-0713-6>
- Lattanzi, A., Meneghini, V., Pavani, G., Amor, F., Ramadier, S., Felix, T., Antoniani, C., Masson, C., Alibeu, O., Lee, C., Porteus, M. H., Bao, G., Amendola, M., Mavilio, F., & Miccio, A. (2019). Optimization of CRISPR/Cas9 Delivery to Human Hematopoietic Stem and Progenitor Cells for Therapeutic Genomic Rearrangements. *Mol Ther*, 27(1), 137-150. <https://doi.org/10.1016/j.ymthe.2018.10.008>
- Launay, E., Pangault, C., Bertrand, P., Jardin, F., Lamy, T., Tilly, H., Tarte, K., Bastard, C., & Fest, T. (2012). High rate of TNFRSF14 gene alterations related to 1p36 region in de novo follicular lymphoma and impact on prognosis. *Leukemia*, 26(3), 559-562. <https://doi.org/10.1038/leu.2011.266>
- LeBien, T. W., & Tedder, T. F. (2008). B lymphocytes: how they develop and function. *Blood*, 112(5), 1570-1580. <https://doi.org/10.1182/blood-2008-02-078071>
- Leithner, A., Renkawitz, J., De Vries, I., Hauschild, R., Häcker, H., & Sixt, M. (2018). Fast and efficient genetic engineering of hematopoietic precursor cells for the study of dendritic cell migration. *Eur J Immunol*, 48(6), 1074-1077. <https://doi.org/10.1002/eji.201747358>
- Li, B., Clohisey, S. M., Chia, B. S., Wang, B., Cui, A., Eisenhaure, T., Schweitzer, L. D., Hoover, P., Parkinson, N. J., Nachshon, A., Smith, N., Regan, T., Farr, D., Gutmann, M. U., Bukhari, S. I., Law, A., Sangesland, M., Gat-Viks, I., Digard, P., Vasudevan, S., Lingwood, D., Dockrell, D. H., Doench, J. G., Baillie, J. K., & Hacohen, N. (2020). Genome-wide CRISPR screen identifies host dependency factors for influenza A virus infection. *Nature Communications*, 11(1), 164. <https://doi.org/10.1038/s41467-019-13965-x>
- Li, H., Kaminski, M. S., Li, Y., Yildiz, M., Ouillette, P., Jones, S., Fox, H., Jacobi, K., Saiya-Cork, K., Bixby, D., Lebovic, D., Roulston, D., Shedden, K., Sabel, M., Marentette, L.,

- Cimmino, V., Chang, A. E., & Malek, S. N. (2014). Mutations in linker histone genes HIST1H1 B, C, D, and E; OCT2 (POU2F2); IRF8; and ARID1A underlying the pathogenesis of follicular lymphoma. *Blood*, 123(10), 1487-1498. <https://doi.org/10.1182/blood-2013-05-500264>
- Li, L., Hu, S., & Chen, X. (2018). Non-viral delivery systems for CRISPR/Cas9-based genome editing: Challenges and opportunities. *Biomaterials*, 171, 207-218. <https://doi.org/10.1016/j.biomaterials.2018.04.031>
- Liang, P., Xu, Y., Zhang, X., Ding, C., Huang, R., Zhang, Z., Lv, J., Xie, X., Chen, Y., Li, Y., Sun, Y., Bai, Y., Songyang, Z., Ma, W., Zhou, C., & Huang, J. (2015). CRISPR/Cas9-mediated gene editing in human trippronuclear zygotes. *Protein Cell*, 6(5), 363-372. <https://doi.org/10.1007/s13238-015-0153-5>
- Lo Coco, F., Ye, B. H., Lista, F., Corradini, P., Offit, K., Knowles, D. M., Chaganti, R. S., & Dalla-Favera, R. (1994). Rearrangements of the BCL6 gene in diffuse large cell non-Hodgkin's lymphoma. *Blood*, 83(7), 1757-1759.
- Lohr, J. G., Stojanov, P., Lawrence, M. S., Auclair, D., Chapuy, B., Sougnez, C., Cruz-Gordillo, P., Knoechel, B., Asmann, Y. W., Slager, S. L., Novak, A. J., Dogan, A., Ansell, S. M., Link, B. K., Zou, L., Gould, J., Saksena, G., Stransky, N., Rangel-Escareño, C., Fernandez-Lopez, J. C., Hidalgo-Miranda, A., Melendez-Zajgla, J., Hernández-Lemus, E., Schwarz-Cruz y Celis, A., Imaz-Rosshandler, I., Ojesina, A. I., Jung, J., Pedamallu, C. S., Lander, E. S., Habermann, T. M., Cerhan, J. R., Shipp, M. A., Getz, G., & Golub, T. R. (2012). Discovery and prioritization of somatic mutations in diffuse large B-cell lymphoma (DLBCL) by whole-exome sequencing. *Proc Natl Acad Sci U S A*, 109(10), 3879-3884. <https://doi.org/10.1073/pnas.1121343109>
- Lowry, L., & Linch, D. (2013). Non-Hodgkin's lymphoma. *Medicine*, 41(5), 282-289. <https://doi.org/https://doi.org/10.1016/j.mpmed.2013.03.008>
- Manguso, R. T., Pope, H. W., Zimmer, M. D., Brown, F. D., Yates, K. B., Miller, B. C., Collins, N. B., Bi, K., LaFleur, M. W., Juneja, V. R., Weiss, S. A., Lo, J., Fisher, D. E., Miao, D., Van Allen, E., Root, D. E., Sharpe, A. H., Doench, J. G., & Haining, W. N. (2017). In vivo CRISPR screening identifies Ptpn2 as a cancer immunotherapy target. *Nature*, 547(7664), 413-418. <https://doi.org/10.1038/nature23270>
- Martin, R. M., Ikeda, K., Cromer, M. K., Uchida, N., Nishimura, T., Romano, R., Tong, A. J., Lemgart, V. T., Camarena, J., Pavel-Dinu, M., Sindhu, C., Wiebking, V., Vaidyanathan, S., Dever, D. P., Bak, R. O., Laustsen, A., Lesch, B. J., Jakobsen, M. R., Sebastiano, V., Nakauchi, H., & Porteus, M. H. (2019). Highly Efficient and Marker-free Genome Editing of Human Pluripotent Stem Cells by CRISPR-Cas9 RNP and AAV6 Donor-Mediated Homologous Recombination. *Cell Stem Cell*, 24(5), 821-828.e825. <https://doi.org/10.1016/j.stem.2019.04.001>
- Martins, R., Maier, J., Gorki, A. D., Huber, K. V., Sharif, O., Starkl, P., Saluzzo, S., Quattrone, F., Gawish, R., Lakovits, K., Aichinger, M. C., Radic-Sarikas, B., Lardeau, C. H., Hladik, A., Korosec, A., Brown, M., Vaahtomeri, K., Duggan, M., Kerjaschki, D., Esterbauer, H., Colinge, J., Eisenbarth, S. C., Decker, T., Bennett, K. L., Kubicek, S., Sixt, M., Superti-Furga, G., & Knapp, S. (2016). Heme drives hemolysis-induced susceptibility to infection via disruption of phagocyte functions. *Nat Immunol*, 17(12), 1361-1372. <https://doi.org/10.1038/ni.3590>
- Maul, R. W., & Gearhart, P. J. (2010). AID and somatic hypermutation. *Adv Immunol*, 105, 159-191. [https://doi.org/10.1016/s0065-2776\(10\)05006-6](https://doi.org/10.1016/s0065-2776(10)05006-6)
- McCarty, N. S., Graham, A. E., Studená, L., & Ledesma-Amaro, R. (2020). Multiplexed CRISPR technologies for gene editing and transcriptional regulation. *Nature Communications*, 11(1), 1281. <https://doi.org/10.1038/s41467-020-15053-x>
- Mehta, A., & Merkel, O. M. (2020). Immunogenicity of Cas9 Protein. *J Pharm Sci*, 109(1), 62-67. <https://doi.org/10.1016/j.xphs.2019.10.003>

- Melchers, F. (2015). Checkpoints that control B cell development. *J Clin Invest*, 125(6), 2203-2210. <https://doi.org/10.1172/jci78083>
- Mesin, L., Ersching, J., & Victora, G. D. (2016). Germinal Center B Cell Dynamics. *Immunity*, 45(3), 471-482. <https://doi.org/10.1016/j.immuni.2016.09.001>
- Meyer-Hermann, M., Mohr, E., Pelletier, N., Zhang, Y., Victora, G. D., & Toellner, K. M. (2012). A theory of germinal center B cell selection, division, and exit. *Cell Rep*, 2(1), 162-174. <https://doi.org/10.1016/j.celrep.2012.05.010>
- Meyer, S. N., Koul, S., & Pasqualucci, L. (2021). Mouse Models of Germinal Center Derived B-Cell Lymphomas. *Frontiers in Immunology*, 12, 710711-710711. <https://doi.org/10.3389/fimmu.2021.710711>
- Migliazza, A., Martinotti, S., Chen, W., Fusco, C., Ye, B. H., Knowles, D. M., Offit, K., Chaganti, R. S., & Dalla-Favera, R. (1995). Frequent somatic hypermutation of the 5' noncoding region of the BCL6 gene in B-cell lymphoma. *Proceedings of the National Academy of Sciences of the United States of America*, 92(26), 12520-12524. <https://doi.org/10.1073/pnas.92.26.12520>
- Mintz, M. A., Felce, J. H., Chou, M. Y., Mayya, V., Xu, Y., Shui, J.-W., An, J., Li, Z., Marson, A., Okada, T., Ware, C. F., Kronenberg, M., Dustin, M. L., & Cyster, J. G. (2019). The HVEM-BTLA Axis Restrains T Cell Help to Germinal Center B Cells and Functions as a Cell-Extrinsic Suppressor in Lymphomagenesis. *Immunity*, 51(2), 310-323.e317. <https://doi.org/https://doi.org/10.1016/j.immuni.2019.05.022>
- Mitzelfelt, K. A., McDermott-Roe, C., Grzybowski, M. N., Marquez, M., Kuo, C. T., Riedel, M., Lai, S., Choi, M. J., Kolander, K. D., Helbling, D., Dimmock, D. P., Battle, M. A., Jou, C. J., Tristani-Firouzi, M., Verbsky, J. W., Benjamin, I. J., & Geurts, A. M. (2017). Efficient Precision Genome Editing in iPSCs via Genetic Co-targeting with Selection. *Stem Cell Reports*, 8(3), 491-499. <https://doi.org/10.1016/j.stemcr.2017.01.021>
- Mohamed, A. N., Palutke, M., Eisenberg, L., & Al-Katib, A. (2001). Chromosomal analyses of 52 cases of follicular lymphoma with t(14;18), including blastic/blastoid variant. *Cancer Genet Cytogenet*, 126(1), 45-51. [https://doi.org/10.1016/s0165-4608\(00\)00383-6](https://doi.org/10.1016/s0165-4608(00)00383-6)
- Morin, R. D., Mendez-Lago, M., Mungall, A. J., Goya, R., Mungall, K. L., Corbett, R. D., Johnson, N. A., Severson, T. M., Chiu, R., Field, M., Jackman, S., Krzywinski, M., Scott, D. W., Trinh, D. L., Tamura-Wells, J., Li, S., Firme, M. R., Rogic, S., Griffith, M., Chan, S., Yakovenko, O., Meyer, I. M., Zhao, E. Y., Smailus, D., Moksa, M., Chittaranjan, S., Rimsza, L., Brooks-Wilson, A., Spinelli, J. J., Ben-Neriah, S., Meissner, B., Woolcock, B., Boyle, M., McDonald, H., Tam, A., Zhao, Y., Delaney, A., Zeng, T., Tse, K., Butterfield, Y., Birol, I., Holt, R., Schein, J., Horsman, D. E., Moore, R., Jones, S. J. M., Connors, J. M., Hirst, M., Gascoyne, R. D., & Marra, M. A. (2011). Frequent mutation of histone-modifying genes in non-Hodgkin lymphoma. *Nature*, 476(7360), 298-303. <https://doi.org/10.1038/nature10351>
- Morrison, S. J., & Weissman, I. L. (1994). The long-term repopulating subset of hematopoietic stem cells is deterministic and isolatable by phenotype. *Immunity*, 1(8), 661-673. [https://doi.org/10.1016/1074-7613\(94\)90037-x](https://doi.org/10.1016/1074-7613(94)90037-x)
- Mossadegh-Keller, N., Brisou, G., Beyou, A., Nadel, B., & Roulland, S. (2021). Human B Lymphomas Reveal Their Secrets Through Genetic Mouse Models [10.3389/fimmu.2021.683597]. *Frontiers in Immunology*, 12, 2033. <https://www.frontiersin.org/article/10.3389/fimmu.2021.683597>
- Noorani, I., Bradley, A., & de la Rosa, J. (2020). CRISPR and transposon in vivo screens for cancer drivers and therapeutic targets. *Genome biology*, 21(1), 204-204. <https://doi.org/10.1186/s13059-020-02118-9>
- Okosun, J., Bödör, C., Wang, J., Araf, S., Yang, C.-Y., Pan, C., Boller, S., Cittaro, D., Bozek, M., Iqbal, S., Matthews, J., Wrench, D., Marzec, J., Tawana, K., Popov, N., O'Riain, C., O'Shea, D., Carlotti, E., Davies, A., Lawrie, C. H., Matolcsy, A., Calaminici, M., Norton,

- A., Byers, R. J., Mein, C., Stupka, E., Lister, T. A., Lenz, G., Montoto, S., Gribben, J. G., Fan, Y., Grosschedl, R., Chelala, C., & Fitzgibbon, J. (2014). Integrated genomic analysis identifies recurrent mutations and evolution patterns driving the initiation and progression of follicular lymphoma. *Nature Genetics*, *46*(2), 176-181. <https://doi.org/10.1038/ng.2856>
- Okosun, J., Wolfson, R. L., Wang, J., Araf, S., Wilkins, L., Castellano, B. M., Escudero-Ibarz, L., Al Seraihi, A. F., Richter, J., Bernhart, S. H., Efeyan, A., Iqbal, S., Matthews, J., Clear, A., Guerra-Assunção, J. A., Bődör, C., Quentmeier, H., Mansbridge, C., Johnson, P., Davies, A., Strefford, J. C., Packham, G., Barrans, S., Jack, A., Du, M.-Q., Calaminici, M., Lister, T. A., Auer, R., Montoto, S., Gribben, J. G., Siebert, R., Chelala, C., Zoncu, R., Sabatini, D. M., & Fitzgibbon, J. (2016). Recurrent mTORC1-activating RRAGC mutations in follicular lymphoma. *Nature Genetics*, *48*(2), 183-188. <https://doi.org/10.1038/ng.3473>
- Oricchio, E., Ciriello, G., Jiang, M., Boice, M. H., Schatz, J. H., Heguy, A., Viale, A., de Stanchina, E., Teruya-Feldstein, J., Bouska, A., McKeithan, T., Sander, C., Tam, W., Seshan, V. E., Chan, W. C., Chaganti, R. S., & Wendel, H. G. (2014). Frequent disruption of the RB pathway in indolent follicular lymphoma suggests a new combination therapy. *J Exp Med*, *211*(7), 1379-1391. <https://doi.org/10.1084/jem.20132120>
- Oricchio, E., Katanayeva, N., Donaldson, M. C., Sungalee, S., Pasion, J. P., Béguelin, W., Battistello, E., Sanghvi, V. R., Jiang, M., Jiang, Y., Teater, M., Parmigiani, A., Budanov, A. V., Chan, F. C., Shah, S. P., Kridel, R., Melnick, A. M., Ciriello, G., & Wendel, H. G. (2017). Genetic and epigenetic inactivation of SESTRIN1 controls mTORC1 and response to EZH2 inhibition in follicular lymphoma. *Sci Transl Med*, *9*(396). <https://doi.org/10.1126/scitranslmed.aak9969>
- Oricchio, E., Nanjangud, G., Wolfe, A. L., Schatz, J. H., Mavrakis, K. J., Jiang, M., Liu, X., Bruno, J., Heguy, A., Olshen, A. B., Socci, N. D., Teruya-Feldstein, J., Weis-Garcia, F., Tam, W., Shaknovich, R., Melnick, A., Himanen, J. P., Chaganti, R. S., & Wendel, H. G. (2011). The Eph-receptor A7 is a soluble tumor suppressor for follicular lymphoma. *Cell*, *147*(3), 554-564. <https://doi.org/10.1016/j.cell.2011.09.035>
- Ortega-Molina, A., Boss, I. W., Canela, A., Pan, H., Jiang, Y., Zhao, C., Jiang, M., Hu, D., Agirre, X., Niesvizky, I., Lee, J. E., Chen, H. T., Ennishi, D., Scott, D. W., Mottok, A., Hother, C., Liu, S., Cao, X. J., Tam, W., Shaknovich, R., Garcia, B. A., Gascoyne, R. D., Ge, K., Shilatifard, A., Elemento, O., Nussenzweig, A., Melnick, A. M., & Wendel, H. G. (2015). The histone lysine methyltransferase KMT2D sustains a gene expression program that represses B cell lymphoma development. *Nat Med*, *21*(10), 1199-1208. <https://doi.org/10.1038/nm.3943>
- Ortega-Molina, A., Deleyto-Seldas, N., Carreras, J., Sanz, A., Lebrero-Fernández, C., Menéndez, C., Vandenberg, A., Fernández-Ruiz, B., Marín-Arraiza, L., de la Calle Arregui, C., Belén Plata-Gómez, A., Caleiras, E., de Martino, A., Martínez-Martín, N., Troulé, K., Piñeiro-Yáñez, E., Nakamura, N., Araf, S., Victora, G. D., Okosun, J., Fitzgibbon, J., & Efeyan, A. (2019). Oncogenic Rag GTPase signaling enhances B cell activation and drives follicular lymphoma sensitive to pharmacological inhibition of mTOR. *Nat Metab*, *1*(8), 775-789. <https://doi.org/10.1038/s42255-019-0098-8>
- Pasqualucci, L. (2019). Molecular pathogenesis of germinal center-derived B cell lymphomas. *Immunol Rev*, *288*(1), 240-261. <https://doi.org/10.1111/imr.12745>
- Pasqualucci, L., Bhagat, G., Jankovic, M., Compagno, M., Smith, P., Muramatsu, M., Honjo, T., Morse, H. C., 3rd, Nussenzweig, M. C., & Dalla-Favera, R. (2008). AID is required for germinal center-derived lymphomagenesis. *Nat Genet*, *40*(1), 108-112. <https://doi.org/10.1038/ng.2007.35>

- Pasqualucci, L., Dominguez-Sola, D., Chiarenza, A., Fabbri, G., Grunn, A., Trifonov, V., Kasper, L. H., Lerach, S., Tang, H., Ma, J., Rossi, D., Chadburn, A., Murty, V. V., Mullighan, C. G., Gaidano, G., Rabadan, R., Brindle, P. K., & Dalla-Favera, R. (2011). Inactivating mutations of acetyltransferase genes in B-cell lymphoma. *Nature*, *471*(7337), 189-195. <https://doi.org/10.1038/nature09730>
- Pasqualucci, L., Khiabanian, H., Fangazio, M., Vasishtha, M., Messina, M., Holmes, A. B., Ouillette, P., Trifonov, V., Rossi, D., Tabbò, F., Ponzoni, M., Chadburn, A., Murty, V. V., Bhagat, G., Gaidano, G., Inghirami, G., Malek, S. N., Rabadan, R., & Dalla-Favera, R. (2014). Genetics of follicular lymphoma transformation. *Cell Rep*, *6*(1), 130-140. <https://doi.org/10.1016/j.celrep.2013.12.027>
- Pasqualucci, L., Migliazza, A., Basso, K., Houldsworth, J., Chaganti, R. S., & Dalla-Favera, R. (2003). Mutations of the BCL6 proto-oncogene disrupt its negative autoregulation in diffuse large B-cell lymphoma. *Blood*, *101*(8), 2914-2923. <https://doi.org/10.1182/blood-2002-11-3387>
- Pasqualucci, L., Trifonov, V., Fabbri, G., Ma, J., Rossi, D., Chiarenza, A., Wells, V. A., Grunn, A., Messina, M., Elliot, O., Chan, J., Bhagat, G., Chadburn, A., Gaidano, G., Mullighan, C. G., Rabadan, R., & Dalla-Favera, R. (2011). Analysis of the coding genome of diffuse large B-cell lymphoma. *Nat Genet*, *43*(9), 830-837. <https://doi.org/10.1038/ng.892>
- Peitz, M., Pfannkuche, K., Rajewsky, K., & Edenhofer, F. (2002). Ability of the hydrophobic FGF and basic TAT peptides to promote cellular uptake of recombinant Cre recombinase: a tool for efficient genetic engineering of mammalian genomes. *Proc Natl Acad Sci U S A*, *99*(7), 4489-4494. <https://doi.org/10.1073/pnas.032068699>
- Perez-Pinera, P., Kocak, D. D., Vockley, C. M., Adler, A. F., Kabadi, A. M., Polstein, L. R., Thakore, P. I., Glass, K. A., Ousterout, D. G., Leong, K. W., Guilak, F., Crawford, G. E., Reddy, T. E., & Gersbach, C. A. (2013). RNA-guided gene activation by CRISPR-Cas9-based transcription factors. *Nat Methods*, *10*(10), 973-976. <https://doi.org/10.1038/nmeth.2600>
- Perry, A. M., Diebold, J., Nathwani, B. N., MacLennan, K. A., Müller-Hermelink, H. K., Bast, M., Boilesen, E., Armitage, J. O., & Weisenburger, D. D. (2016). Non-Hodgkin lymphoma in the developing world: review of 4539 cases from the International Non-Hodgkin Lymphoma Classification Project. *Haematologica*, *101*(10), 1244-1250. <https://doi.org/10.3324/haematol.2016.148809>
- Pietras, E. M., Reynaud, D., Kang, Y.-A., Carlin, D., Calero-Nieto, F. J., Leavitt, A. D., Stuart, J. M., Göttgens, B., & Passegué, E. (2015). Functionally Distinct Subsets of Lineage-Biased Multipotent Progenitors Control Blood Production in Normal and Regenerative Conditions. *Cell Stem Cell*, *17*(1), 35-46. <https://doi.org/10.1016/j.stem.2015.05.003>
- Piperno, G. M., Naseem, A., Silvestrelli, G., Amadio, R., Caronni, N., Cervantes-Luevano, K. E., Liv, N., Klumperman, J., Colliva, A., Ali, H., Graziano, F., Benaroch, P., Haecker, H., Hanna, R. N., & Benvenuti, F. (2020). Wiskott-Aldrich syndrome protein restricts cGAS/STING activation by dsDNA immune complexes. *JCI Insight*, *5*(17). <https://doi.org/10.1172/jci.insight.132857>
- Platt, R. J., Chen, S., Zhou, Y., Yim, M. J., Swiech, L., Kempton, H. R., Dahlman, J. E., Parnas, O., Eisenhaure, T. M., Jovanovic, M., Graham, D. B., Jhunjunwala, S., Heidenreich, M., Xavier, R. J., Langer, R., Anderson, D. G., Hacohen, N., Regev, A., Feng, G., Sharp, P. A., & Zhang, F. (2014). CRISPR-Cas9 knockin mice for genome editing and cancer modeling. *Cell*, *159*(2), 440-455. <https://doi.org/10.1016/j.cell.2014.09.014>
- Qi, L. S., Larson, M. H., Gilbert, L. A., Doudna, J. A., Weissman, J. S., Arkin, A. P., & Lim, W. A. (2013). Repurposing CRISPR as an RNA-guided platform for sequence-specific control of gene expression. *Cell*, *152*(5), 1173-1183. <https://doi.org/10.1016/j.cell.2013.02.022>

- Quentmeier, H., Pommerenke, C., Dirks, W. G., Eberth, S., Koeppel, M., MacLeod, R. A. F., Nagel, S., Steube, K., Uphoff, C. C., & Drexler, H. G. (2019). The LL-100 panel: 100 cell lines for blood cancer studies. *Scientific Reports*, *9*(1), 8218. <https://doi.org/10.1038/s41598-019-44491-x>
- Rad, R., Rad, L., Wang, W., Cadinanos, J., Vassiliou, G., Rice, S., Campos, L. S., Yusa, K., Banerjee, R., Li, M. A., de la Rosa, J., Strong, A., Lu, D., Ellis, P., Conte, N., Yang, F. T., Liu, P., & Bradley, A. (2010). PiggyBac transposon mutagenesis: a tool for cancer gene discovery in mice. *Science*, *330*(6007), 1104-1107. <https://doi.org/10.1126/science.1193004>
- Rad, R., Rad, L., Wang, W., Strong, A., Ponstingl, H., Bronner, I. F., Mayho, M., Steiger, K., Weber, J., Hieber, M., Veltkamp, C., Eser, S., Geumann, U., Öllinger, R., Zukowska, M., Barenboim, M., Maresch, R., Cadiñanos, J., Friedrich, M., Varela, I., Constantino-Casas, F., Sarver, A., Ten Hoeve, J., Prosser, H., Seidler, B., Bauer, J., Heikenwälder, M., Metzakopian, E., Krug, A., Ehmer, U., Schneider, G., Knösel, T., Rümmele, P., Aust, D., Grützmann, R., Pilarsky, C., Ning, Z., Wessels, L., Schmid, R. M., Quail, M. A., Vassiliou, G., Esposito, I., Liu, P., Saur, D., & Bradley, A. (2015). A conditional piggyBac transposition system for genetic screening in mice identifies oncogenic networks in pancreatic cancer. *Nat Genet*, *47*(1), 47-56. <https://doi.org/10.1038/ng.3164>
- Ramezani-Rad, P., & Rickert, R. C. (2017). Murine models of germinal center derived-lymphomas. *Current Opinion in Immunology*, *45*, 31-36. <https://doi.org/https://doi.org/10.1016/j.coi.2016.12.002>
- Ran, F. A., Hsu, P. D., Wright, J., Agarwala, V., Scott, D. A., & Zhang, F. (2013). Genome engineering using the CRISPR-Cas9 system. *Nat Protoc*, *8*(11), 2281-2308. <https://doi.org/10.1038/nprot.2013.143>
- Redecke, V., Wu, R., Zhou, J., Finkelstein, D., Chaturvedi, V., High, A. A., & Häcker, H. (2013). Hematopoietic progenitor cell lines with myeloid and lymphoid potential. *Nat Methods*, *10*(8), 795-803. <https://doi.org/10.1038/nmeth.2510>
- Renkawitz, J., Kopf, A., Stopp, J., de Vries, I., Driscoll, M. K., Merrin, J., Hauschild, R., Welf, E. S., Danuser, G., Fiolka, R., & Sixt, M. (2019). Nuclear positioning facilitates amoeboid migration along the path of least resistance. *Nature*, *568*(7753), 546-550. <https://doi.org/10.1038/s41586-019-1087-5>
- Richardson, C. D., Ray, G. J., Bray, N. L., & Corn, J. E. (2016). Non-homologous DNA increases gene disruption efficiency by altering DNA repair outcomes. *Nat Commun*, *7*, 12463. <https://doi.org/10.1038/ncomms12463>
- Rickert, R. C., Roes, J., & Rajewsky, K. (1997). B lymphocyte-specific, Cre-mediated mutagenesis in mice. *Nucleic Acids Res*, *25*(6), 1317-1318. <https://doi.org/10.1093/nar/25.6.1317>
- Roco, J. A., Mesin, L., Binder, S. C., Nefzger, C., Gonzalez-Figueroa, P., Canete, P. F., Ellyard, J., Shen, Q., Robert, P. A., Cappello, J., Vohra, H., Zhang, Y., Nowosad, C. R., Schiepers, A., Corcoran, L. M., Toellner, K. M., Polo, J. M., Meyer-Hermann, M., Victora, G. D., & Vinuesa, C. G. (2019). Class-Switch Recombination Occurs Infrequently in Germinal Centers. *Immunity*, *51*(2), 337-350.e337. <https://doi.org/10.1016/j.immuni.2019.07.001>
- Roulland, S., Lebailly, P., Roussel, G., Briand, M., Cappellen, D., Pottier, D., Hardouin, A., Troussard, X., Bastard, C., Henry-Amar, M., & Gauduchon, P. (2003). BCL-2/JH translocation in peripheral blood lymphocytes of unexposed individuals: Lack of seasonal variations in frequency and molecular features. *International Journal of Cancer*, *104*(6), 695-698. <https://doi.org/https://doi.org/10.1002/ijc.10975>
- Roulland, S., Navarro, J. M., Grenot, P., Milili, M., Agopian, J., Montpellier, B., Gauduchon, P., Lebailly, P., Schiff, C., & Nadel, B. (2006). Follicular lymphoma-like B cells in healthy

- individuals: a novel intermediate step in early lymphomagenesis. *J Exp Med*, 203(11), 2425-2431. <https://doi.org/10.1084/jem.20061292>
- Sander, S., Calado, D. P., Srinivasan, L., Köchert, K., Zhang, B., Rosolowski, M., Rodig, S. J., Holzmann, K., Stilgenbauer, S., Siebert, R., Bullinger, L., & Rajewsky, K. (2012). Synergy between PI3K signaling and MYC in Burkitt lymphomagenesis. *Cancer Cell*, 22(2), 167-179. <https://doi.org/10.1016/j.ccr.2012.06.012>
- Sanson, K. R., Hanna, R. E., Hegde, M., Donovan, K. F., Strand, C., Sullender, M. E., Vaimberg, E. W., Goodale, A., Root, D. E., Piccioni, F., & Doench, J. G. (2018). Optimized libraries for CRISPR-Cas9 genetic screens with multiple modalities. *Nature Communications*, 9(1), 5416. <https://doi.org/10.1038/s41467-018-07901-8>
- Schmitz, R., Wright, G. W., Huang, D. W., Johnson, C. A., Phelan, J. D., Wang, J. Q., Roulland, S., Kasbekar, M., Young, R. M., Shaffer, A. L., Hodson, D. J., Xiao, W., Yu, X., Yang, Y., Zhao, H., Xu, W., Liu, X., Zhou, B., Du, W., Chan, W. C., Jaffe, E. S., Gascoyne, R. D., Connors, J. M., Campo, E., Lopez-Guillermo, A., Rosenwald, A., Ott, G., Delabie, J., Rimsza, L. M., Tay Kuang Wei, K., Zelenetz, A. D., Leonard, J. P., Bartlett, N. L., Tran, B., Shetty, J., Zhao, Y., Soppet, D. R., Pittaluga, S., Wilson, W. H., & Staudt, L. M. (2018). Genetics and Pathogenesis of Diffuse Large B-Cell Lymphoma. *N Engl J Med*, 378(15), 1396-1407. <https://doi.org/10.1056/NEJMoa1801445>
- Schneider, G., Schmidt-Supprian, M., Rad, R., & Saur, D. (2017). Tissue-specific tumorigenesis: context matters. *Nature Reviews Cancer*, 17(4), 239-253. <https://doi.org/10.1038/nrc.2017.5>
- Schnütgen, F., Doerflinger, N., Calléja, C., Wendling, O., Chambon, P., & Ghyselinck, N. B. (2003). A directional strategy for monitoring Cre-mediated recombination at the cellular level in the mouse. *Nat Biotechnol*, 21(5), 562-565. <https://doi.org/10.1038/nbt811>
- Schuler, F., Afreen, S., Manzl, C., Häcker, G., Erlacher, M., & Villunger, A. (2019). Checkpoint kinase 1 is essential for fetal and adult hematopoiesis. *EMBO Rep*, 20(8), e47026. <https://doi.org/10.15252/embr.201847026>
- Schüler, F., Dölken, L., Hirt, C., Kiefer, T., Berg, T., Fusch, G., Weitmann, K., Hoffmann, W., Fusch, C., Janz, S., Rabkin, C. S., & Dölken, G. (2009). Prevalence and frequency of circulating t(14;18)-MBR translocation carrying cells in healthy individuals. *Int J Cancer*, 124(4), 958-963. <https://doi.org/10.1002/ijc.23958>
- Schwaenen, C., Viardot, A., Berger, H., Barth, T. F., Bentink, S., Döhner, H., Enz, M., Feller, A. C., Hansmann, M. L., Hummel, M., Kestler, H. A., Klapper, W., Kreuz, M., Lenze, D., Loeffler, M., Möller, P., Müller-Hermelink, H. K., Ott, G., Rosolowski, M., Rosenwald, A., Ruf, S., Siebert, R., Spang, R., Stein, H., Truemper, L., Lichter, P., Bentz, M., & Wessendorf, S. (2009). Microarray-based genomic profiling reveals novel genomic aberrations in follicular lymphoma which associate with patient survival and gene expression status. *Genes Chromosomes Cancer*, 48(1), 39-54. <https://doi.org/10.1002/gcc.20617>
- Shalem, O., Sanjana, N. E., Hartenian, E., Shi, X., Scott, D. A., Mikkelsen, T., Heckl, D., Ebert, B. L., Root, D. E., Doench, J. G., & Zhang, F. (2014). Genome-scale CRISPR-Cas9 knockout screening in human cells. *Science*, 343(6166), 84-87. <https://doi.org/10.1126/science.1247005>
- Shapiro, J., Iancu, O., Jacobi, A. M., McNeill, M. S., Turk, R., Rettig, G. R., Amit, I., Tovin-Recht, A., Yakhini, Z., Behlke, M. A., & Hendel, A. (2020). Increasing CRISPR Efficiency and Measuring Its Specificity in HSPCs Using a Clinically Relevant System. *Mol Ther Methods Clin Dev*, 17, 1097-1107. <https://doi.org/10.1016/j.omtm.2020.04.027>
- Shearwin, K. E., Callen, B. P., & Egan, J. B. (2005). Transcriptional interference--a crash course. *Trends in genetics : TIG*, 21(6), 339-345. <https://doi.org/10.1016/j.tig.2005.04.009>

- Shifrut, E., Carnevale, J., Tobin, V., Roth, T. L., Woo, J. M., Bui, C. T., Li, P. J., Diolaiti, M. E., Ashworth, A., & Marson, A. (2018). Genome-wide CRISPR Screens in Primary Human T Cells Reveal Key Regulators of Immune Function. *Cell*, *175*(7), 1958-1971.e1915. <https://doi.org/10.1016/j.cell.2018.10.024>
- Shoumariyeh, K., Schneider, N., Poggio, T., Veratti, P., Ehrenfeld, S., Redhaber, D. M., Khan, R., Pfeifer, D., Klingeberg, C., Kreutmair, S., Rudelius, M., Quintanilla-Martinez, L., Fend, F., Illert, A. L., Duyster, J., & Miething, C. (2020). A novel conditional NPM-ALK-driven model of CD30+ T-cell lymphoma mediated by a translational stop cassette. *Oncogene*, *39*(9), 1904-1913. <https://doi.org/10.1038/s41388-019-1058-1>
- Shy, B. R., MacDougall, M. S., Clarke, R., & Merrill, B. J. (2016). Co-incident insertion enables high efficiency genome engineering in mouse embryonic stem cells. *Nucleic Acids Res*, *44*(16), 7997-8010. <https://doi.org/10.1093/nar/gkw685>
- Sommerkamp, P., Romero-Mulero, M. C., Narr, A., Ladel, L., Hustin, L., Schönberger, K., Renders, S., Altamura, S., Zeisberger, P., Jäcklein, K., Klimmeck, D., Rodriguez-Fraticelli, A., Camargo, F. D., Perié, L., Trumpp, A., & Cabezas-Wallscheid, N. (2021). Mouse multipotent progenitor 5 cells are located at the interphase between hematopoietic stem and progenitor cells. *Blood*, *137*(23), 3218-3224. <https://doi.org/10.1182/blood.2020007876>
- Standage-Beier, K., Tekel, S. J., Brookhouser, N., Schwarz, G., Nguyen, T., Wang, X., & Brafman, D. A. (2019). A transient reporter for editing enrichment (TREE) in human cells. *Nucleic Acids Res*, *47*(19), e120. <https://doi.org/10.1093/nar/gkz713>
- Stern, P., Astrof, S., Erkeland, S. J., Schustak, J., Sharp, P. A., & Hynes, R. O. (2008). A system for Cre-regulated RNA interference in vivo. *Proc Natl Acad Sci U S A*, *105*(37), 13895-13900. <https://doi.org/10.1073/pnas.0806907105>
- Strasser, A., Harris, A. W., Bath, M. L., & Cory, S. (1990). Novel primitive lymphoid tumours induced in transgenic mice by cooperation between myc and bcl-2. *Nature*, *348*(6299), 331-333. <https://doi.org/10.1038/348331a0>
- Strasser, A., Harris, A. W., & Cory, S. (1993). E mu-bcl-2 transgene facilitates spontaneous transformation of early pre-B and immunoglobulin-secreting cells but not T cells. *Oncogene*, *8*(1), 1-9.
- Sungalee, S., Mamessier, E., Morgado, E., Grégoire, E., Brohawn, P. Z., Morehouse, C. A., Jouve, N., Monvoisin, C., Menard, C., Debroas, G., Faroudi, M., Mechin, V., Navarro, J. M., Drevet, C., Eberle, F. C., Chasson, L., Baudimont, F., Mancini, S. J., Tellier, J., Picquenot, J. M., Kelly, R., Vineis, P., Ruminy, P., Chetaille, B., Jaffe, E. S., Schiff, C., Hardwigsen, J., Tice, D. A., Higgs, B. W., Tarte, K., Nadel, B., & Roulland, S. (2014). Germinal center reentries of BCL2-overexpressing B cells drive follicular lymphoma progression. *J Clin Invest*, *124*(12), 5337-5351. <https://doi.org/10.1172/jci72415>
- Ting, P. Y., Parker, A. E., Lee, J. S., Trussell, C., Sharif, O., Luna, F., Federe, G., Barnes, S. W., Walker, J. R., Vance, J., Gao, M. Y., Klock, H. E., Clarkson, S., Russ, C., Miraglia, L. J., Cooke, M. P., Boitano, A. E., McNamara, P., Lamb, J., Schmedt, C., & Snead, J. L. (2018). Guide Swap enables genome-scale pooled CRISPR-Cas9 screening in human primary cells. *Nat Methods*, *15*(11), 941-946. <https://doi.org/10.1038/s41592-018-0149-1>
- Tran, N. T., Sommermann, T., Graf, R., Trombke, J., Pempe, J., Petsch, K., Kühn, R., Rajewsky, K., & Chu, V. T. (2019). Efficient CRISPR/Cas9-Mediated Gene Knockin in Mouse Hematopoietic Stem and Progenitor Cells. *Cell reports*, *28*(13), 3510-3522.e3515. <https://doi.org/10.1016/j.celrep.2019.08.065>
- Tran, N. T., Sommermann, T., Graf, R., Trombke, J., Pempe, J., Petsch, K., Kühn, R., Rajewsky, K., & Chu, V. T. (2019). Efficient CRISPR/Cas9-Mediated Gene Knockin in Mouse Hematopoietic Stem and Progenitor Cells. *Cell Rep*, *28*(13), 3510-3522.e3515. <https://doi.org/10.1016/j.celrep.2019.08.065>

- Treon, S. P., Xu, L., Yang, G., Zhou, Y., Liu, X., Cao, Y., Sheehy, P., Manning, R. J., Patterson, C. J., Tripsas, C., Arcaini, L., Pinkus, G. S., Rodig, S. J., Sohani, A. R., Harris, N. L., Laramie, J. M., Skifter, D. A., Lincoln, S. E., & Hunter, Z. R. (2012). MYD88 L265P somatic mutation in Waldenström's macroglobulinemia. *N Engl J Med*, 367(9), 826-833. <https://doi.org/10.1056/NEJMoa1200710>
- Tschaharganeh, D. F., Lowe, S. W., Garippa, R. J., & Livshits, G. (2016). Using CRISPR/Cas to study gene function and model disease in vivo. *The FEBS journal*, 283(17), 3194-3203. <https://doi.org/10.1111/febs.13750>
- Turner, V. M., Gardam, S., & Brink, R. (2010). Lineage-specific transgene expression in hematopoietic cells using a Cre-regulated retroviral vector. *J Immunol Methods*, 360(1-2), 162-166. <https://doi.org/10.1016/j.jim.2010.06.007>
- Urnov, F. D., Rebar, E. J., Holmes, M. C., Zhang, H. S., & Gregory, P. D. (2010). Genome editing with engineered zinc finger nucleases. *Nat Rev Genet*, 11(9), 636-646. <https://doi.org/10.1038/nrg2842>
- Vakulskas, C. A., Dever, D. P., Rettig, G. R., Turk, R., Jacobi, A. M., Collingwood, M. A., Bode, N. M., McNeill, M. S., Yan, S., Camarena, J., Lee, C. M., Park, S. H., Wiebking, V., Bak, R. O., Gomez-Ospina, N., Pavel-Dinu, M., Sun, W., Bao, G., Porteus, M. H., & Behlke, M. A. (2018). A high-fidelity Cas9 mutant delivered as a ribonucleoprotein complex enables efficient gene editing in human hematopoietic stem and progenitor cells. *Nature Medicine*, 24(8), 1216-1224. <https://doi.org/10.1038/s41591-018-0137-0>
- Van den Plas, D., Ponsaerts, P., Van Tendeloo, V., Van Bockstaele, D. R., Berneman, Z. N., & Merregaert, J. (2003). Efficient removal of LoxP-flanked genes by electroporation of Cre-recombinase mRNA. *Biochem Biophys Res Commun*, 305(1), 10-15. [https://doi.org/10.1016/s0006-291x\(03\)00669-7](https://doi.org/10.1016/s0006-291x(03)00669-7)
- van Lohuizen, M., Verbeek, S., Scheijen, B., Wientjens, E., van der Gulden, H., & Berns, A. (1991). Identification of cooperating oncogenes in E mu-myc transgenic mice by provirus tagging. *Cell*, 65(5), 737-752. [https://doi.org/10.1016/0092-8674\(91\)90382-9](https://doi.org/10.1016/0092-8674(91)90382-9)
- Velasco-Hernandez, T., Säwén, P., Bryder, D., & Cammenga, J. (2016). Potential Pitfalls of the Mx1-Cre System: Implications for Experimental Modeling of Normal and Malignant Hematopoiesis. *Stem Cell Reports*, 7(1), 11-18. <https://doi.org/10.1016/j.stemcr.2016.06.002>
- Viau, M., & Zouali, M. (2005). B-lymphocytes, innate immunity, and autoimmunity. *Clinical Immunology*, 114(1), 17-26. <https://doi.org/https://doi.org/10.1016/j.clim.2004.08.019>
- Vilela, J., Rohaim, M. A., & Munir, M. (2020). Application of CRISPR/Cas9 in Understanding Avian Viruses and Developing Poultry Vaccines. *Frontiers in cellular and infection microbiology*, 10, 581504-581504. <https://doi.org/10.3389/fcimb.2020.581504>
- von Gamm, M., Schaub, A., Jones, A. N., Wolf, C., Behrens, G., Lichti, J., Essig, K., Macht, A., Pircher, J., Ehrlich, A., Davari, K., Chauhan, D., Busch, B., Wurst, W., Feederle, R., Feuchtinger, A., Tschöp, M. H., Friedel, C. C., Hauck, S. M., Sattler, M., Geerloff, A., Hornung, V., Heissmeyer, V., Schulz, C., Heikenwalder, M., & Glasmacher, E. (2019). Immune homeostasis and regulation of the interferon pathway require myeloid-derived Regnase-3. *J Exp Med*, 216(7), 1700-1723. <https://doi.org/10.1084/jem.20181762>
- Wang, G. G., Calvo, K. R., Pasillas, M. P., Sykes, D. B., Häcker, H., & Kamps, M. P. (2006). Quantitative production of macrophages or neutrophils ex vivo using conditional Hoxb8. *Nat Methods*, 3(4), 287-293. <https://doi.org/10.1038/nmeth865>
- Wang, M., Sun, L., Qian, J., Han, X., Zhang, L., Lin, P., Cai, Z., & Yi, Q. (2009). Cyclin D1 as a universally expressed mantle cell lymphoma-associated tumor antigen for immunotherapy. *Leukemia*, 23(7), 1320-1328. <https://doi.org/10.1038/leu.2009.19>
- Wang, T., Wei, J. J., Sabatini, D. M., & Lander, E. S. (2014). Genetic Screens in Human Cells Using the CRISPR-Cas9 System. *Science*, 343(6166), 80-84. <https://doi.org/10.1126/science.1246981>

- Wang, T., Yu, H., Hughes, N. W., Liu, B., Kendirli, A., Klein, K., Chen, W. W., Lander, E. S., & Sabatini, D. M. (2017). Gene Essentiality Profiling Reveals Gene Networks and Synthetic Lethal Interactions with Oncogenic Ras. *Cell*, 168(5), 890-903.e815. <https://doi.org/10.1016/j.cell.2017.01.013>
- Wartewig, T., Kurgys, Z., Keppler, S., Pechloff, K., Hameister, E., Öllinger, R., Maresch, R., Buch, T., Steiger, K., Winter, C., Rad, R., & Ruland, J. (2017). PD-1 is a haploinsufficient suppressor of T cell lymphomagenesis. *Nature*, 552(7683), 121-125. <https://doi.org/10.1038/nature24649>
- Weber, J., de la Rosa, J., Grove, C. S., Schick, M., Rad, L., Baranov, O., Strong, A., Pfaus, A., Friedrich, M. J., Engleitner, T., Lersch, R., Öllinger, R., Grau, M., Menendez, I. G., Martella, M., Kohlhofer, U., Banerjee, R., Turchaninova, M. A., Scherger, A., Hoffman, G. J., Hess, J., Kuhn, L. B., Ammon, T., Kim, J., Schneider, G., Unger, K., Zimber-Strobl, U., Heikenwälder, M., Schmidt-Suppran, M., Yang, F., Saur, D., Liu, P., Steiger, K., Chudakov, D. M., Lenz, G., Quintanilla-Martinez, L., Keller, U., Vassiliou, G. S., Cadiñanos, J., Bradley, A., & Rad, R. (2019). PiggyBac transposon tools for recessive screening identify B-cell lymphoma drivers in mice. *Nature Communications*, 10(1), 1415. <https://doi.org/10.1038/s41467-019-09180-3>
- Webster, P., Dawes, J. C., Dewchand, H., Takacs, K., Iadarola, B., Bolt, B. J., Caceres, J. J., Kaczor, J., Dharmalingam, G., Dore, M., Game, L., Adejumo, T., Elliott, J., Naresh, K., Karimi, M., Rekopoulou, K., Tan, G., Paccanaro, A., & Uren, A. G. (2018). Subclonal mutation selection in mouse lymphomagenesis identifies known cancer loci and suggests novel candidates. *Nat Commun*, 9(1), 2649. <https://doi.org/10.1038/s41467-018-05069-9>
- Xia, Y., & Zhang, X. (2020). The Spectrum of MYC Alterations in Diffuse Large B-Cell Lymphoma. *Acta Haematol*, 143(6), 520-528. <https://doi.org/10.1159/000505892>
- Xian, R. R., Xie, Y., Haley, L. M., Yonescu, R., Pallavajjala, A., Pittaluga, S., Jaffe, E. S., Duffield, A. S., McCall, C. M., Gheith, S. M. F., & Gocke, C. D. (2020). CREBBP and STAT6 co-mutation and 16p13 and 1p36 loss define the t(14;18)-negative diffuse variant of follicular lymphoma. *Blood Cancer J*, 10(6), 69. <https://doi.org/10.1038/s41408-020-0335-0>
- Yamamoto, R., Wilkinson, A. C., & Nakauchi, H. (2018). Changing concepts in hematopoietic stem cells. *Science*, 362(6417), 895-896. <https://doi.org/10.1126/science.aat7873>
- Yan, N., Sun, Y., Fang, Y., Deng, J., Mu, L., Xu, K., Mymryk, J. S., & Zhang, Z. (2020). A Universal Surrogate Reporter for Efficient Enrichment of CRISPR/Cas9-Mediated Homology-Directed Repair in Mammalian Cells. *Molecular therapy. Nucleic acids*, 19, 775-789. <https://doi.org/10.1016/j.omtn.2019.12.021>
- Yang, H., Wang, H., Shivalila, C. S., Cheng, A. W., Shi, L., & Jaenisch, R. (2013). One-step generation of mice carrying reporter and conditional alleles by CRISPR/Cas-mediated genome engineering. *Cell*, 154(6), 1370-1379. <https://doi.org/10.1016/j.cell.2013.08.022>
- Yang, L., Bryder, D., Adolfsson, J., Nygren, J., Månsson, R., Sigvardsson, M., & Jacobsen, S. E. (2005). Identification of Lin(-)Sca1(+)kit(+)CD34(+)Flt3- short-term hematopoietic stem cells capable of rapidly reconstituting and rescuing myeloablated transplant recipients. *Blood*, 105(7), 2717-2723. <https://doi.org/10.1182/blood-2004-06-2159>
- Yau, I. W., Cato, M. H., Jellusova, J., Hurtado de Mendoza, T., Brink, R., & Rickert, R. C. (2013). Censoring of self-reactive B cells by follicular dendritic cell-displayed self-antigen. *J Immunol*, 191(3), 1082-1090. <https://doi.org/10.4049/jimmunol.1201569>
- Ye, B., Liu, B., Yang, L., Huang, G., Hao, L., Xia, P., Wang, S., Du, Y., Qin, X., Zhu, P., Wu, J., Sakaguchi, N., Zhang, J., & Fan, Z. (2017). Suppression of SRCAP chromatin remodelling complex and restriction of lymphoid lineage commitment by Pcid2. *Nature Communications*, 8(1), 1518. <https://doi.org/10.1038/s41467-017-01788-7>

- Ye, B. H., Cattoretti, G., Shen, Q., Zhang, J., Hawe, N., de Waard, R., Leung, C., Nouri-Shirazi, M., Orazi, A., Chaganti, R. S., Rothman, P., Stall, A. M., Pandolfi, P. P., & Dalla-Favera, R. (1997). The BCL-6 proto-oncogene controls germinal-centre formation and Th2-type inflammation. *Nat Genet*, *16*(2), 161-170. <https://doi.org/10.1038/ng0697-161>
- Ye, B. H., Lista, F., Lo Coco, F., Knowles, D. M., Offit, K., Chaganti, R. S., & Dalla-Favera, R. (1993). Alterations of a zinc finger-encoding gene, BCL-6, in diffuse large-cell lymphoma. *Science*, *262*(5134), 747-750. <https://doi.org/10.1126/science.8235596>
- Yoshida, S., Kaneita, Y., Aoki, Y., Seto, M., Mori, S., & Moriyama, M. (1999). Identification of heterologous translocation partner genes fused to the BCL6 gene in diffuse large B-cell lymphomas: 5'-RACE and LA - PCR analyses of biopsy samples. *Oncogene*, *18*(56), 7994-7999. <https://doi.org/10.1038/sj.onc.1203293>
- Zhang, J., Dominguez-Sola, D., Hussein, S., Lee, J. E., Holmes, A. B., Bansal, M., Vlasevska, S., Mo, T., Tang, H., Basso, K., Ge, K., Dalla-Favera, R., & Pasqualucci, L. (2015). Disruption of KMT2D perturbs germinal center B cell development and promotes lymphomagenesis. *Nat Med*, *21*(10), 1190-1198. <https://doi.org/10.1038/nm.3940>

## ACKNOWLEDGMENT

I would like to start by thanking my mentor, Prof. Marc Schmidt-Supprian, for his fantastic guidance, endless support, and generous understanding during all these years. I am sincerely grateful to him as he has provided the perfect environment to focus on science and follow the questions that I have been interested in since day one. It has been a unique chance and continuous excitement to discuss and do science together. His positive attitude, solution-oriented approach, and avant-garde scientific personality have always been a source of inspiration for me. As an example of his endless genuine support, I would like to recall the time when our ancient veteran irradiation machine got broken and particularly thank him for his by-any-means solutions, which kept me motivated even under loss of function circumstances.

Particular thanks to my thesis advisory committee members, Prof. Florian Bassermann and Prof. Roland Rad, for their time, guidance, and constant encouragement. I am grateful to Prof. Roland Rad for giving me the opportunity to integrate the piggyBac transposon screen in my project. It was a privilege to inherit the tools from the developer. Moreover, I am also thankful to him for welcoming me into their animal protocol. All the *in vivo* results of this project could be achieved with this help. Also, I was lucky to work with their group members, Olga Baranov, Anja Pfaus, and Ria Spallek, on various parts of this project.

Besides, I would like to thank Markus Tschurtschenthaler for providing the LSL-Cas9-GFP mice kindly. I would like to thank Prof. Martin Turner and David Turner for their contributions to the project with the sgRNA construct and the library. I am grateful to Ritu Mishra for FASC-sorter introductions. I thank animal care takers of the animal facility, especially Christian Herrler for their assistance. I am grateful to the SFB 1243 organization and particularly its graduate program coordinator Elizabeth Schroeder for her constant support, care and efforts.

I would like to express my sincere gratitude to all the members of the AG Schmidt-Supprian. It has been one of my biggest chances to be surrounded by this diverse group of extremely friendly and talented multicultural people. I absolutely enjoyed our time together and appreciated their continuous support.

I would like to specially thank Vera Wanat, Claudia Mugler, and Jasmin Schröder for their extremely careful, helpful, and beautiful work on genotyping PCRs and other experiments. In the

past year, the support of Monika Mittermeier in the mouse house was so valuable and greatly appreciated. Also, their kindness, willingness to help, and constant positive attitudes have been extremely fruitful. I would like to thank Julia Knogler for her help in preparing the library screen samples.

I would particularly thank Laura Kraus, who has greatly supported the PiggyBac transposon project with her contribution. Her ready-for-help attitude has been greatly appreciated, and it was very fun to work side by side. I would like to thank my neighbour, Valeria Soberon, for her (non-)science talks and sincere encouragement since the beginning of the journey; it meant a lot. I would like to thank Sabine Helmrath, Sabrina Bortoluzzi, and Carina Steinecke for their lively scientific discussions, support, and friendships in all these years. I am very thankful to Francisco Osorio Barrios, Daniel Kovacs, Lena Osswald, Fatemeh Mohagheghi, Vanessa Gölling, Gonul Seyhan, Kasia Jopek, Ricarda Trapp, Hyunju Oh for their help in various ways and uplifting positive vibes.

I would like to thank Mauricio Ruiz and Rebecca Hardman Carter whom I had the pleasure to supervise. It has been extremely exciting and satisfying to work with such motivated and bright students, and I have enjoyed improving the parts of the project with them.

Besides the work, I would like to thank Prof. Esther Zanin and Prof. Tamara Mikeladze-Dvali for their valuable teachings, discussions, and genuine support. I send my sincere thanks to all my friends Bacolar and particularly science geek ones; Gizem Gunes and Umut Kilik for their lively discussions and tremendous support on our common journey.

My special thanks go to Arek, who has been the irreplaceable source of fun and sun. I am truly fascinated to find the chance to work together in our projects, although not sure if our white board would say the same. Thank you for your endless help, support, patient, and light. Thank you for always being there.

Finally, I would like to give my deepest thanks to my favourite people; Iko, Vasfi and Selin who have always been the biggest luck and strength in my life wherever they are. Values thought by them have been my guidance and their sui generis personalities have become a continuous source of inspiration. I am grateful for their patience, love, care, and unconditional support.